I.A.D Innovative Aerospace Design	End Term Report	Ref.: MAE 4350-001-2016 Date: 23. Jan. 2017 Page: 1 of 124 Pages Status: In Progress

Designing a Light Twin-Engine GA Aircraft				
Signatures:				
	Name:	**Signature:**	**Dept.:**	**Date:**
Author:	Jonathan Carrera Travis Webb Michael Gibson Nazmus Sakib Boot Nguyen Abram Suarez	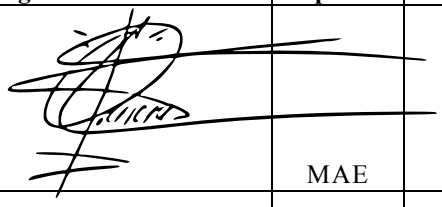	MAE	1/23/2017
Seen:	Dr. Smith		MAE	

Summary:

As a company we take enormous pride in our work. We seek to meet the needs of our customers while ensuring safety. We stand behind our work to guarantee a quality product that exceeds our costumer's expectations. For this particular project, our costumer, Dr. Dudley Smith, has requested a twin-engine aircraft that meets specified criteria (delineated within the document). This midterm report goes into detail as to how the conceptual sizing of the aircraft was determined. It is important to note these quantities obtained here, such as aircraft geometry, performance parameters, etc. are *preliminary* design milestones (delimitated in the second portion of this report) derived from previously determined *conceptual* starting point (delineated in the first portion of this report) by which the final *detailed* design portion of this project will be based. Iterations will occur as the project matures; therefore, these values will be subject to change in the upcoming stages of design.

Distribution:		
Institution:	**Dept.:**	**Name:**
The University of Texas at Arlington	MAE	Dr. Smith

Work Disclosure Statement

The work we performed to document the results presented in this report was performed by us, or it is otherwise acknowledged.

Date: 1/23/2017

Signature: 

Contents

List of Figures

PART I

PART II

List of Tables

PART I

PART II

Nomenclature

a = Speed of sound
a_0 = Section lift curve slope of a 2D wing
a_t = 3D lift curve slope of a horizontal tail
a_w = 3D lift curve slope of a wing
a,b,c,d = Regression line constants
AR = Aspect ratio
ARH = Aspect Ratio of Horizontal Tail
ARV = Aspect Ratio of Vertical Tail
ARw = Aspect Ratio of Main Wing
b = Wing Span [ft]
bht = Wing Span of Horizontal Tail
bvt = Wing Span of Vertical Tail
bhp = Brake Horsepower
c_p = Specific fuel consumption, [lbs./hp/hr.]
C = Main Wing Chord
C_D = Drag Coefficient
C_D = Drag Coefficient
C_{D0l} = Zero-Lift Drag Coefficient
C_{Do} = Zero lift drag coefficient
C_{Do} = Zero lift drag coefficient
cg = Center of Gravity
CGR = Climb gradient, [rad]
$CGRP$ = Climb gradient parameter, [rad]
C_L = Lift Coefficient
C_{Lmax} = Coefficient of Lift clean
C_{LmaxL} = Coefficient of Lift at Landing
C_{Lmaxr} = Coefficient of Lift at the root of the wing
C_{Lmaxt} = Coefficient of Lift at Tip of Wing
C_{LmaxTO} = Coefficient of Lift at Takeoff
$C_{l\beta}$ = Dihedral effect
C_P = Power Coefficient
C_Q = Torque Coefficient
C_T = Thrust Coefficient
$C_{n\beta_f}$ = Change in aerodynamic yawing moment coefficient with sideslip angle of the fuselage
$C_{n\beta_v}$ = Change in aerodynamic yawing moment coefficient with sideslip angle of the vertical tail
$C_{n\beta_w}$ = Change in aerodynamic yawing moment coefficient with sideslip angle of the wing
$C_{n\delta_r}$ = Change in yawing moment with respect to rudder deflection
$C_{y\beta_v}$ = Change in the aerodynamic side force coefficient with respect to sideslip angle
$C_{L\alpha}$ = Change in lift coefficient with respect to angle of attack
$C_{n\beta}$ = Aerodynamic yawing moment coefficient change with sideslip angle
$(dC_N/d\alpha)_{N_{P_{Tc=0}}}$ = Change in normal force coefficient with respect to the angle of attack
$\left(\frac{dC_m}{dC_L}\right)_P$ = Change in pitching moment coefficient with respect to the lift coefficient for the propeller
$\left(\frac{dC_m}{dC_L}\right)_{fus}$ = Change in pitching moment coefficient with respect to the lift coefficient for the fuselage

$\left(\frac{dC_m}{dC_L}\right)_{wing}$ = Change in pitching moment coefficient with respect to the lift coefficient for the wing
$\frac{dC_m}{dC_L}$ = Total change in pitching moment coefficient with respect to the the lift coefficient
$\frac{dT_c}{dC_L}$ = Change in thrust coefficient with respect to the lift coefficient
D = Diameter [ft]
D = Drag, [lbs.]
D_p = Propeller diameter, [ft.]
E = Endurance, [hours]
f = Equivalent parasite area, [ft^2]
F = Weight sensitivity parameter, [lbs.]
FAR = Federal Air Regulation
h = Altitude, [ft]
h = Altitude, [ft.]
HP = Horsepower
I_p = Power index, [(hp/ft$^{2)1/3}$]
J = Advance Ratio
K_N = Empirically determined factor
K_{R1} = Reynold's number correlation factor
K_f = Fuselage stability coefficient
l_p = Distance to the center of the propeller from the center of the fuselage
L_f = Length of the fuselage
L = Lift, [lbs.]
L, ht = Length of Aerodynamic Center of Horizontal Tail
L, vt = Length of Aerodynamic Center for the Vertical Tail
L/D = Lift-to-drag ratio
L/D = Lift-to-drag ratio
M = Mach Number
M_{ff} = Mission Fuel Fraction, [end weight/ begin weight]
MGC = Mean Geometric Chord
n = Propeller Ω [rps]
N = Number of propellers
N = Number of engines
$N_{t_{crit}}$ = Critical one engine out yawing moment
N_0 = Stick fixed neutral point
N_{0wind} = Neutral point for propeller windmilling
N_D = Drag induced yawing moment
ΔN_0 = Forward shift of the neutral point due to critical powered flight
nm = Nautical mile, [6,076 ft.]
P = Power [HP/550 ft-pound per sec]
P = Power, [hp]
q = Dynamic Pressure [psf]
$\bar{q}_{mc}$ = Dynamic pressure [psf]
Q = Torque [lb-ft]
R = Range, [nm]
RC = Rate of climb, [fpm, fps]
RCP = Rate of climb parameter, [hp/lbs.]
s = Distance (used in takeoff and landing Equations)
S_{wet} = Wetted Area
S = Wing Area [ft^2]

Sh	=	Historical Horizontal Tail Area
ShT	=	Area of Horizontal Tail
S_P	=	Propeller disk area
S_c	=	Canard tail surface area
Svh	=	Historical Vertical Tail Area
SvT	=	Vertical Tail Area
Sw	=	Wing Area
Swh	=	Historical Wing Area
T	=	Thrust [lb]
t/c	=	Thickness ratio in relation of the chord
thp	=	Total Horsepower
TOP_{23}	=	FAR 23 Take-off parameter
$TSFC$	=	Thrust Specific Fuel Consumption [lbm/hr/lb]
V	=	True air speed
$\bar{V}$	=	Tail volume coefficient
V_{mc}	=	Velocity at minimum control
V_{cr}	=	Cruise velocity, [mph, fps, kts.]
V_{cr}	=	Cruise velocity, [mph, fps, kts.]
Vht	=	Volume Coefficient of Horizontal Tail
Vvt	=	Volume Coefficient of Vertical Tail
W	=	Weight [lb]
W_{CREW}	=	Weight of the crew, [lbs.]
W_E	=	Empty weight, [lbs.]
W_F	=	Fuel weight, [lbs.]
W_{FEQ}	=	Fixed equipment weight, [lbs.]
W_{Fres}	=	Reserved fuel quantity, [lbs.]
W_{Fused}	=	Actual fuel used, [lbs.]
W_{ME}	=	Manufactures empty weight, [lbs.]
W_{OE}	=	Operating empty weight, [lbs.]
W_{PL}	=	Weight of payload, [lbs.]
W_{tfo}	=	Trapped fuel and oil in engine, [lbs.]
W_{TO}	=	Takeoff weight, [lbs.]
W_{UL}	=	Useful load, [lbs.]
W	=	Total Weight of Aircraft
Xh	=	Chord of Horizontal Tail
Xv	=	Chord of Vertical Tail
w_f	=	Fuselage width
y_t	=	Lateral thrust moment arm
z_f	=	Vertical height of the fuselage at the root chord
z_v	=	The z-axis distance from the *cg* to the vertical tail aerodynamic center

π = 3.1415
ρ = Air density, [slugs/ft^3]
σ = Density ratio
μ_G = Ground friction
η_p = Propeller efficiency
$\delta_{\epsilon 0}$ = Elevator deflection required at zero lift
$\delta_{\epsilon max}$ = Maximum elevator deflection
δ_r = Rudder deflection
η_t = Horizontal tail efficiency
Δ = Angle of sweep, Change in-.
α_0 = Zero lift Angle of Attack [rad]
β = Pitch Angle
θ = Angle of Attack [rad]
ρ = Density [slug/ft^3]
σ = Solidity
Φ = Induced Angle [rad]
$d\beta/d\alpha$ = Change in sideslip with respect to angle of attack
$d\varepsilon/d\alpha$ = Change in downwash with respect to angle of attack
β = Mach number correction

I. Introduction

The following report summarizes the procedures delineated in Parts I and II (*Preliminary Sizing Airplanes* & *Preliminary Configuration Design and Integration of the Propulsion System*, respectively) of Jan Roskam's Airplane Design series. These procedures will be implemented to design an aircraft of the desired type as requested by our costumer, Dr. Dudley Smith. Systematic preliminary sizing of a Light-Economical-General-Aviation-Trainer -Twin Aircraft will be shown in the first portion of this report along with FAR-23 (Federal Air Regulations) in order to ensure a safe and reliable product that is built to federal standards. A refinement of performance parameters will be delineated on the second portion of this report. Initially, assumptions will be made about the aircraft based on empirical data from similar aircraft. The first will be to find the weight estimation based on empirical data and mission conditions. After that, using known assumptions, the effect that other variables have on the takeoff weight such as payload weight and empty weight will be calculated (otherwise known as Sensitivity Gradients). Then, a relationship between power loading and wing loading, a graph will be showing the trends between the stall speed sizing, takeoff sizing, landing field sizing, FAR requirements, and cruise speed as power loading and wing loading vary with each other to determine the defining criteria between all the given conditions (this will conclude the first portion of this report). For the latter portion of this report, historical data will once again be utilized to size the empennage, locate the center of gravity, and find the placement of the undercarriage. Other parameters will be analyzed and established such as drag polars, propeller and engine specifications, refined weights and balance, first pass at static stability and performance parameters to ensure these meet our configuration and FA regulations. Shortcomings will be then presented at the end with proposed variations to our configuration along with a conclusion.

II. Part I

Sizing Procedure Overview

The following list provides the order in which the conceptual parameters were determined. Due to the complexity of such task it is important to being with a parameter that will latter help yield other important parameters, hence the order of flow. This will become apparent to the reader progresses through the document.

1) Specifications
2) Takeoff Weight, W_{TO}
3) Sensitivity Gradients
4) Wing Loading, Power Loading, Drag Polars, (W/S, P/W, $C_l^{3/2}/C_d$)
5) Cruise Speed

All of these parameters will then be matched together to present constrains to determine the best approach to continue preliminary design.

Specifications

The costume has listed the specifications that the aircraft must meet as seen in **Table 1-1**. These requirements are crucial for the first iteration preliminary sizing.

Table 1-1 Design Requirements

Light Economical Twin Aircraft			
Requirement		**Value**	**Unit**
Seating Capacity		4	Persons
Useful load		950	lb.
Baggage Allowance		176	lb.
Baggage Volume		23	Ft^3
Cabin Interior Width		48	in.
Cabin Height		36	in.
Maximum dry tank range		725	nm.
V_{SL0}	<=	48	knots.
V_{MC}	<	V_S	
Service Ceiling	>=	15,000	ft.
V_{CR} **@ 75% Power**	>=	140	knots.
Single Engine ROC @ SLS		250	fpm

The specifications for this aircraft fall under the light-twin-engine aircraft type. The Beech Duchess, as seen in **Fig. 1-1**, is an adequate model to obtain reasonable initial parameters. As mentioned above, most initial parameters are derived of selected based on historical data. It is important to make sure that the data that is collected corresponds to the specified family of aircraft. Assumptions will be made through out this document, it is important for the reader to be sure to understand these assumptions.

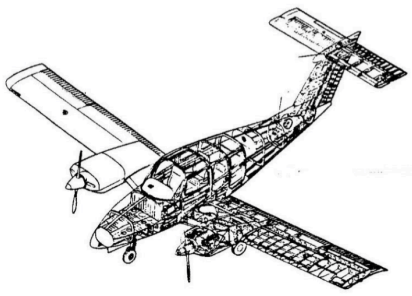

Figure 1 - 1 Beech Douches

Preliminary Weight Calculations

Finding the takeoff weight of the aircraft, W_{TO}, is essential to determining other preceding parameters. However, some parameters must

be defined before being able to determine a reasonable takeoff weight value. **Eqn. (1)** defines what useful load is.

$$W_{UL} = W_F + W_{PL} + W_{CREW} \tag{1}$$

Weight of the fuel, W_F, plus weight of the payload, W_{PL} is classified as useful load, where the term "useful" indicates "interchangeability." Meaning, fuel can be interchanged for payload and vise versa. However, for this analysis, the weight of the crew will also be categorized as useful load.

Presented in the specification the useful load, W_{UL}, is given to be 950 lbs. An average weight of 175 lbs. per passenger plus 30 lbs. of luggage per passenger will be assumed. The weight of the payload, W_{PL}, comes out to be 820 lbs. for the specified capacity in table 1. Solving **Eqn. (1)** for the weight of the mission fuel, W_F, yields an amount of 130 lbs. or 21.6 gallons. This tentative fuel weight is not enough to accomplish the range of 725 nm that is desired. Iteration must be done on the weight of the payload. Cabin capacity will be lowered to a maximum of two passengers and one crewmember making the *payload weight* 615 lbs. for our first pass and consequently making more room to increase the amount of fuel. Solving **Eqn. (1)** for the weight of the fuel with our new W_{PL} yields a mission-fuel weight, W_F, of 335 lbs. of 55.7 gallons of fuel availability.

It is important to note that the weight of the mission fuel is the sum of the actual fuel used for the mission, W_{Fused}, and a reserve quantity, W_{Fres}, which is only a fraction of the mission fuel. This reserved fuel is included as a precaution in case of needed additional loiter time or in case of needed additional range requirements to reach an alternate airport.

$$W_F = W_{Fused} + W_{Fres} \tag{2}$$

There is another weight category named the "operating empty weight," W_{OE}, which consists of the empty weight of the aircraft, trapped fuel and oil (unusable fuel and oil), and weight of the crew.

$$W_{OE} = W_E + W_{tfo} + W_{CREW} \tag{3}$$

Here, W_{CREW} is equal to zero since we have chosen to categorize the weight of the crew as 'useful'. The total takeoff weight, W_{TO}, is conveniently expressed as the summation of both the operating empty weight and the useful load.

$$W_{TO} = W_{UL} + W_{OE} \tag{4}$$

Since the payload weight has been determined, the weight of the mission fuel can be established. Even though the *availability* for fuel was very superficially determined, the *Fuel Fraction* method by Roskam will be employed for a more thorough determination of this mission fuel. Roskam says, "in this method the airplane mission is broken down into a number of mission phases. The fuel used during each phase is found from a simple calculation or estimated on the basis of experience." These phases are numbered and have an initial and final weight of the aircraft associated with each phase arranged in a fraction where the final weight is compared to the initial weight, hence the name 'fuel fractions'. These phases are organized in such fashion: 1) Engine Star & Warm Up, 2) Taxi, 3) Take-Off, 4) Climb and Acceleration, 5) Cruise, 6) Loiter, 7) Descent, 8) Landing-Taxi-Shutdown. Fig. 3 shows a diagram of our mission. Roskam suggests a value for each one of these phases as seen in Table 1-2. Yet, two very important fuel fractions are not so easily determined (phases 5 and 6, Cruise and Loiter, respectively) and require further calculation.

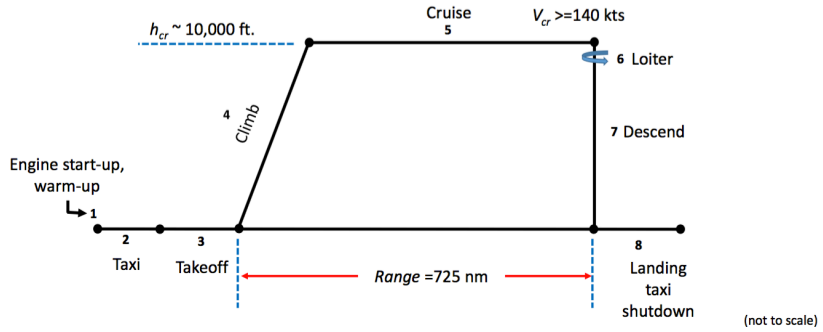

Figure 1 - 2 Mission Definition

However, for simplicity, we will assume a fuel fraction of 1 for phase 6, meaning; we will not consider any fuel usage for loitering and simply focus on our cruise fuel fraction, W5/W4. This fuel fraction can be estimated from the Breguet's range Eqn., which is represented as follows for propeller-driven aircraft.

$$R_{cr} = 375\left(\frac{\eta_p}{C_p}\right)_{cr}\left(\frac{L}{D}\right)_{cr}\ln\left(\frac{W_4}{W_5}\right) \tag{5}$$

Were R_{cr} is in statute miles. **Eqn. (5)** makes use of the Lift-to-Drag Ratio and the ratio between propeller efficiency and specific fuel consumption. These values are selected from historical data provided by Roskam, as seen in Table 1-2.

Table 1- 2 Suggested Fuel-Fractions for Several Mission Phases [1]

Mission Phase No. / Airplane Type:	Engine Start, Warm-up 1	Taxi 2	Take-off 3	Climb 4	Descent 7	Landing Taxi, Shutdown 8
1. Homebuilt	0.998	0.998	0.998	0.995	0.995	0.995
2. Single Engine	0.995	0.997	0.998	0.992	0.993	0.993
3. Twin Engine	0.992	0.996	0.996	0.990	0.992	0.992
4. Agricultural	0.996	0.995	0.996	0.998	0.999	0.998
5. Business Jets	0.990	0.995	0.995	0.980	0.990	0.992
6. Regional TBP's	0.990	0.995	0.995	0.985	0.985	0.995
7. Transport Jets	0.990	0.990	0.995	0.980	0.990	0.992
8. Military Trainers	0.990	0.990	0.990	0.980	0.990	0.995
9. Fighters	0.990	0.990	0.990	0.96-0.90	0.990	0.995
10. Mil.Patrol, Bomb, Transport	0.990	0.990	0.995	0.980	0.990	0.992
11. Flying Boats, Amphibious, Float Airplanes	0.992	0.990	0.996	0.985	0.990	0.990
12. Supersonic Cruise	0.990	0.995	0.995	0.92-0.87	0.985	0.992

Notes: 1. The numbers in this table are based on experience or on judgment.
2. There is no substitute for common sense! If and when common sense so dictates, the reader should substitute other values for the fractions suggested in this table.

Table 1- 3 Suggested Values For L/D, c_j, eta$_p$, c_p For Several Mission Phases [1]

	Cruise				Loiter			
	L/D	c_j	c_p	η_p	L/D	c_j	c_p	η_p
Mission Phase No.(See Fig.2.1)		lbs/lbs/hr	lbs/hp/hr			lbs/lbs/hr	lbs/hp/hr	
		5				6		
Airplane Type								
1. Homebuilt	8-10*		0.6-0.8	0.7	10-12		0.5-0.7	0.6
2. Single Engine	8-10		0.5-0.7	0.8	10-12		0.5-0.7	0.7
3. Twin Engine	8-10		0.5-0.7	0.82	9-11		0.5-0.7	0.72
4. Agricultural	5-7		0.5-0.7	0.82	8-10		0.5-0.7	0.72
5. Business Jets	10-12	0.5-0.9			12-14	0.4-0.6		
6. Regional TBP's	11-13		0.4-0.6	0.85	14-16		0.5-0.7	0.77
7. Transport Jets	13-15	0.5-0.9			14-18	0.4-0.6		
8. Military Trainers	8-10	0.5-1.0	0.4-0.6	0.82	10-14	0.4-0.6	0.5-0.7	0.77
9. Fighters	4-7	0.6-1.4	0.5-0.7	0.82	6-9	0.6-0.8	0.5-0.7	0.77
10. Mil.Patrol, Bomb, Transport	13-15	0.5-0.9	0.4-0.7	0.82	14-18	0.4-0.6	0.5-0.7	0.77
11. Flying Boats, Amphibious, Float Airplanes	10-12	0.5-0.9	0.5-0.7	0.82	13-15	0.4-0.6	0.5-0.7	0.77
12. Supersonic Cruise	4-6	0.7-1.5			7-9	0.6-0.8		

Notes: 1. The numbers in this table represent ranges based on existing engines.
2. There is no substitute for common sense! If and when actual data are available, these should be used.
3. A good estimate for L/D can be made with the drag polar method of Sub-section 3.4.1.
* Homebuilts with smooth exteriors and/or high wing loadings can have L/D values which are considerably higher.

Like expressed in the footnotes bellow **Table 1-2**, these values are based on experience and/or judgment. Roskam encourages the reader to allow these values to be modified when common sense calls for it. Given our tremendous experience on this field over the years, we have chosen the Lift-to-Drag coefficient, *L/D* to be 11, the propeller efficiency, η_p to be 82% and the specific fuel consumption, c_p to be 0.5.

Table 1- 4 Initial Assumptions

	Value	Unit
Average weight per person	175	lb.
Average weight per baggage	30	lb.
Fuel weight	6	lb/gal
Lift-to-Drag coefficient, L/D	11	-
Propeller efficiency, η_p	.82	-
Specific fuel consumption	0.5	-

Substituting these values and the desired range value of 725 nm into **Eqn. (5)** and solving for the cruise fuel fraction, W_5/W_4 as seen in **Eqn. (6)** bellow will yield a value of 0.884.

$$\frac{W_5}{W_4} = e^{-\left(\frac{R_{cp}}{375*\left(\frac{\eta p}{C_p}\right)_{cr}\left(\frac{L}{D}\right)_{cr}}\right)} \tag{6}$$

Table 1-5 shows the Fuel Fractions used for our analysis, where M_{ff} is the *Mission Fuel Fraction*, which is the product of all the fuel fractions resulting in the final weight as it compares to the takeoff weight; in our case yielding a *Mission Fuel Fraction* of about 85%.

$$M_{ff} = \left(\frac{W_1}{W_{TO}}\right) \prod_{i=1}^{i=7} \left(\frac{W_{i+1}}{W_i}\right) \quad (7)$$

In other words, the aircraft will be about 15 % lighters when it lands then when it took off. This is only one component of the many needed to successfully determine a reasonable takeoff weight. The next immediate objective is to calculate an empty weight, W_E based on empirical mission data along with a tentative empty weight, W_{Etent}. These two will be compared with each other. Since both of these empty weights are a function of the takeoff weight (as it will be shown shortly) iterations must be done to the magnitude of the Takeoff weight, W_{TO} until the difference between these two empty weights is smaller than 1 lb.

Table 1- 5 Fuel-Fractions for the Mission Phases

Phases	Fuel Fractions	Historical Values
1 (Engine Start/ Warm Up)	W_1/W_TO	0.992
2 (Taxi)	W_2/W_1	0.996
3 (Takeoff)	W_3/W_2	0.996
4 (Climb To Cruise)	W_4/W_3	0.99
5 (Cruise)	*W_5/W_4*	*0.884*
6 (Loiter)	W_6/W_5	1
7 (Descend)	W_7/W_6	0.992
8 (Land/Taxi/ Shut Down)	W_8/W_7	0.992
Mff	***W_8/W_TO***	***0.848***

A few relationships must be expressed before the empty weight can be formulated, such as weight of the trapped fuel and oil. This is fuel and oil that is trapped within the engine and is not accessible. As expressed in **Eqn. (3)**, the trapped fuel and oil is categorize under the operating empty weight, W_{OE} and is defined to be about 5% of the total Takeoff weight.

$$W_{tfo} \approx (0.05)\, W_{TO} \quad (8)$$

Eqn. (2) is expressed bellow differently, where the *Mission Fuel Used, M_{Fused},* is *$(1\text{-}M_{ff})*W_{TO}$*, indicating that the mission fuel weight is also a function of the takeoff weight.

$$W_F = (1 - M_{ff}) W_{TOtent} + W_{Fres} \quad (9)$$

To simplify **Eqn. (9)** we will not take into account any residual fuel, at least not at this point in the design process. Consequently, $W_{Fres} = 0$

The payload weight (W_{PL}) and fuel weight (W_F) have been determined. By taking a guess at our takeoff weight a tentative value for the operating empty weight can be determined as seen in **Eqn. (10)**.

$$W_{OEtent} = W_{TOtent} - W_F - W_{PL} \quad (10)$$

We are now able to calculate the parameter of interest, which is the tentative empty weight, W_{Etent}.

$$W_{Etent} = W_{OEtent} - W_{tfo} - W_{CREW} \quad (11)$$

This tentative empty weight (W_{Etent}) must be compared to the empty weight derived from empirical data (W_E), as an optimal takeoff weight is chosen. **Table 1-6** delimitates weight data for various twin-engine propeller driven airplanes (primarily made out of aluminum). Using this table will give insight into a reasonable takeoff weight.

Table 1- 6 Weight Data for Twin Engine Propeller Driven [1]

No.	Type	Gross Take-off Weight, W_{TO} (lbs)	Empty Weight, W_E(lbs)	Maximum Landing Weight, W_{Land} (lbs)	Max. Internal Fuel Weight, W_{MIF}(lbs)
	BEECH				
1	Duchess 76	3,900	2,466	3,900	587
2	Baron 95-B55	5,100	3,236	5,100	587
3	Duke B60	6,775	4,423	6,775	834
4	King Air C90 (TBP)	9,650	5,765	9,168	2,515
	CESSNA				
5	Crusader T303	5,150	3,305	5,000	898
6	340A	5,990	3,948	5,990	1,192
7	402C Businessliner	6,850	4,077	6,850	1,250
8	414A Chancellor	6,750	4,368	6,750	1,250
9	421 Golden Eagle	7,450	4,668	7,450	1,250
10	Conquest I (TBP)	8,200	4,915	8,000	2,443
	PIPER				
11	Navajo	6,500	4,003	6,500	1,127
12	Chieftain	7,000	4,221	7,000	1,127
13	Aerostar 600A	5,500	3,737	5,500	1,018
14	Seminole PA-44-180	3,800	2,354	3,800	646
15	Seminole PA-44-180T	3,800	2,430	3,800	646
16	Cheyenne I (TBP)	8,700	4,910	8,700	2,017
17	Wing Derringer D-1	3,050	2,100	2,900	511
18	Partenavia P66C-160	2,183	1,322	2,183	251
19	Piaggio P166-DL3 (TBP)	9,480	5,732	8,377	1,850
20	Gulf-Am 840A (TBP)	10,325	6,629	10,325	2,784
21	Learfan 2100 (TBP)	7,350*	4,100	7,000	1,572
22	Rutan 40 Defiant	2,900*	1,610	2,900	528

* 21 and 22 are composite built airplanes

No. 17, the Wing Derringer as seen in **Fig. 1-3**, with a W_{TO} of 3,050 lbs. and a W_E of 2,100 lbs. is the closest to our concept aircraft. As noted, the aircrafts tabulated above were made out of aluminum construction. Since our concept will be composed of composite material, we can assume a safe reduction in weight of 10%. This yields a tentative take of weight of 2,745 lbs. This takeoff weight could be plugged into **Eqn. (9)** and obtain the weight of fuel that will allow for range requirement verification (but that is not our primary objective at this point). Up to this point, the tentative empty weight (W_{Etent}) has been calculated from **Eqn. (11)**. To determine the empty weight (W_E) based on empirical-historical data; **Fig. 1-4** must be utilized. This Fig. presents a linear correlation between the $\log_{10}$ (W_{TO}) and $\log_{10}$ (W_E). **Eqn. (12)** will be use to estimate the empty weight.

Figure 1 - 3 Wing Derringer (mid

Table 1- 7 Regression line Constants A and B of Equations (12) [1]

Airplane Type	A	B
1. Homebuilts		
Pers. fun and transportation	0.3411	0.9519
Scaled Fighters	0.5542	0.8654
Composites	0.8222	0.8050
2. Single Engine Propeller Driven	-0.1440	1.1162
3. Twin Engine Propeller Driven	0.0966	1.0298
Composites	0.1130	1.0403
4. Agricultural	-0.4398	1.1946
5. Business Jets	0.2678	0.9979
6. Regional TBP	0.3774	0.9647
7. Transport Jets	0.0833	1.0383
8. Military Trainers		
Jets	0.6632	0.8640
Turboprops	-1.4041	1.4660
Turboprops without No.2	0.1677	0.9978
Piston/Props	0.5627	0.8761
9. Fighters		
Jets(+ ext.load)	0.5091	0.9505
Jets(clean)	0.1362	1.0116
Turboprops(+ ext.load)	0.2705	0.9830
10. Mil. Patrol, Bomb and Transport		
Jets	-0.2009	1.1037
Turboprops	-0.4179	1.1446
11. Flying Boats, Amphibious and Float Airplanes	0.1703	1.0083
12. Supersonic Cruise	0.4221	0.9876

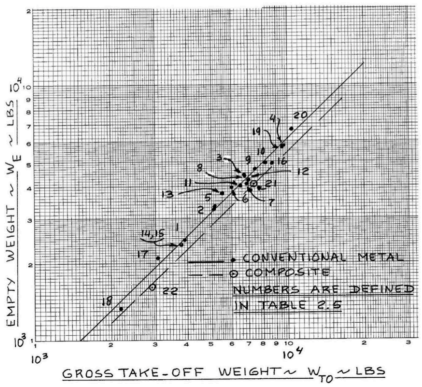

Figure 1 - 4 Weight Trends for Twin Engine Propeller Driven Airplanes [1]

Eqn. (12) is the empirical relationship seen in **Fig. 1-4** and Roskam provides its constants in **Table 1-7** for a twin-engine aircraft.

$$W_E = invlog_{10}\left\{\frac{log_{10}W_{TO} - A}{B}\right\} \tag{12}$$

Since composite materials will be used to construct this aircraft, the values of 0.1130 and 1.0403 will be chosen for A and B, respectively. Plugging in these values along with our tentative takeoff weight into **Eqn. (12)** will yield the empty weight. An excel spreadsheet program was created that allows to easily input a takeoff weight and iterate until the difference between W_{Etent} and W_E is less than 1 lb. The takeoff weight that yielded a difference of 0.011 lbs. was 2740 lbs. View **Table A1** (Appendix 1) to view the program with such iteration.

Sensitivity Gradients

It is important to reiterate the fact that the results obtained in the fuel-fraction method depend on the values selected from the historical data, especially those in the Breguet range and endurance Equations (Equations (5) and (6)). Several variables affect our takeoff weight. Payload Weight, W_P.

1. Empty Weight, W_E
2. Range, R
3. Endurance, E
4. Lift-to-drag ratio, L/D
5. Specific fuel consumption, c
6. Propeller efficiency, η_p

The effect of these variables on the resultant takeoff weight, W_{TO}, must be determined to identify the one with a greater influence in order to allocate efforts effectively to ensure that mission requirements can be achieved. Roskam provided the following Equations; the derivation of parameters will not be presented in this report. If the reader is interested in the derivation of these, it is encouraged to reference *Airplane Design Volume 1* by Roskam[1]

$$D = W_{PL} + W_{CREW} \tag{13}$$

$$C = \frac{W_E + D}{W_{TO}} \tag{14}$$

$$log_{10}W_{TO} = A + Blog_{10}(CW_{TO} - D) \tag{15}$$

Where the parameters A and B are from the regression from **Table 1**-7, and while C and D are from the mission analysis delineated in Roskam. D equals to 615 lbs. and C equals 0.798. According to Roskam, **Eqn. (15)** is another opportunity for a numerical solution to the iteration process discussed earlier.

The sensitivity to payload weight is expressed bellow

$$\frac{\partial W_{TO}}{\partial W_{PL}} = \frac{B\,W_{TO}}{D - C(1-B)W_{TO}} \tag{16}$$

The sensitivity to empty weight is expressed bellow

$$\frac{\partial W_{TO}}{\partial W_E} = \frac{B\,W_{TO}}{inv\,log_{10}(\frac{log_{10}W_{TO} - A}{B})} \tag{17}$$

The sensitivity to Range, Endurance, c_p, η_p, and L/D where y is the dummy variable

$$\frac{\partial W_{TO}}{\partial y} = \frac{B\,(W_{TO})^2 \frac{\partial C}{\partial y} - BW_{TO}\frac{\partial D}{\partial y}}{\{C(1-B)W_{TO} - D\}} \tag{18}$$

A few relationships will be needed to be defined before being able to evaluate **Eqn. (13)** for any of those parameters. We will not go through the derivation here; the reader is encouraged to reference Roskam. We will skip down to where F is defined bellow

$$F = \frac{-B(W_{TO})^2(1-M_{res})M_{ff}}{\{CW_{TO}(1-B) - D\}} \tag{19}$$

Were F is equal to 9,415 lbs. and M_{res} is the reserve fuel fraction in terms of the fuel used. Roskam derives this quantity, but for simplicity purposes, we are letting that equal to zero. The sensitivity of the takeoff weight range can be expressed as follows

$$\frac{\partial W_{TO}}{\partial R} = F\frac{\overline{\partial(R)}}{\partial y} \tag{20}$$

$$\frac{\partial W_{TO}}{\partial E} = F\frac{\overline{\partial(E)}}{\partial y} \tag{21}$$

We can make and interesting observation from the Eqn. bellow; range does not depend on velocity.

$$\frac{\partial W_{TO}}{\partial R} = \frac{Fc_p}{326\eta_p\frac{L}{D}} \tag{22}$$

$$\frac{\partial W_{TO}}{\partial c_p} = \frac{FR}{326\eta_p\frac{L}{D}} \tag{23}$$

$$\frac{\partial W_{TO}}{\partial \eta_p} = \frac{-FRc_p}{326(\eta_p)^2\frac{L}{D}} \tag{24}$$

Table 1- 8 Bellow lists the values of each one of these for our particular values.

Table 1- 8 Calculated Sensitivity Gradients

Partial Derivatives (SENSITIVITY GRADIENTS)						
	Airplane Growth	***[lb/lb]***	***[lb/lb/hp/hr]***	***[lbs.]***	***[lbs.]***	
d(Wto)/R	*d(Wto)/dy*	*d(Wto)/d(W_pL)*	*d(Wto)/d(cp)*	*d(Wto)/d(L/D)*	*d(Wto)/d(eta_prop)*	*d(Wto)/d(E)*
1.60	*4.05*	*4.05*	*2321.3*	*-105.51*	*-1415.42*	*1.82*

Nominal values for the sensitivity of takeoff weight to range from 4 to 6 lb./nm but because our aircraft is made out of composite and evaluation at max range, the derivative is smaller than normal. From table 5 it is apparent that the specific fuel consumption has the greatest influence on the takeoff weight and range has the least amount of influence on the takeoff weight. The power plant characteristics are of most importance. This conclusion will become evident as the report progresses.

Sizing

There are additional performance criteria that need to be meet such as stall speed, takeoff field distance, landing field distance, cruise speed / maximum speed, rate of climb when all engines are operating, rate of climb when one engine is inoperative, time-to-climb, maneuvering etc. Determining these values is done by strategically using common variables between them to make a plotted graph that will show which sizing criteria is most critical and the limits when choosing the dimensions of the wing. These are the common variables:

1) Main Wing Area, S
2) Thrust at takeoff, T_{TO}
3) Power at takeoff, P_{TO}
4) Maximum required lift coefficient, C_{Lmax}, with a clean configuration (flaps up)
5) Maximum required lift coefficient at takeoff, $C_{L,max,TO}$
6) Maximum required lift coefficient at landing, $C_{L,max,L}$
7) Wing Loading (W/S)
8) Thrust Loading (T/S)
9) Power Loading (W/P)

It is desirable to find a combination of the highest possible wing loading and the lowest possible thrust (or Power) that resides within the requirements. This will generally result in the lowest weight, therefore the lowest cost. It is important to also make sure to meet FAR Part 23 requirements on stall/cruise speeds for aircrafts of the same type. According to FAR Part 23 for aircraft with a takeoff weight, less than 6,000 lbs. must have a stall speed of no more than 61 kts, unless certain climb gradient criteria are met.

1. STALL SPEED SIZING

There are various configurations by which these parameters must be calculated; clean, takeoff (no flaps, just gear), landing with flaps (no gear) and landing with gears (flaps and gear). The configuration being considered will be clarified as Equations are presented and calculations made.

For stall speed,

$$V_s = \left[\frac{2(W/S)}{\rho C_{Lmax}}\right]^{1/2} \tag{25}$$

Were ρ is the density for sea level 0.002378 slugs/ft^3. We will keep in mind that the coefficient of lift is highly influenced by the wing and airfoil design, flap type and flap size and the location of the center of gravity. These are correlations will be considered further in the design process. For now we will resort to Roskam's data on typical values for maximum lift coefficient. Since our aircraft is than 6,000 lbs. at takeoff, we must have a stall speed less than 45 kts. at sea level conditions with full flaps, and power off. And for a clean configuration the stall speed must be less than 60 kts. from table 6 we will consider our coefficient of max lift at landing (C_{LmaxL}) to be equal to 2.0, and our general coefficient of lift (C_{Lmax}) to be equal to 1.6. **Eqn. (25)** is solved for the wing loading at the two required speeds. The lesser value will indicate the maximum wing loading limit.

Table 1- 9 Typical Values For Maximum Lift

Airplane Type	$C_{L_{max}}$	$C_{L_{max_{TO}}}$	$C_{L_{max_L}}$
1. Homebuilts	1.2 - 1.8	1.2 - 1.8	1.2 - 2.0*
2. Single Engine Propeller Driven	1.3 - 1.9	1.3 - 1.9	1.6 - 2.3
3. Twin Engine Propeller Driven	1.2 - 1.8	1.4 - 2.0	1.6 - 2.5
4. Agricultural	1.3 - 1.9	1.3 - 1.9	1.3 - 1.9
5. Business Jets	1.4 - 1.8	1.6 - 2.2	1.6 - 2.6
6. Regional TBP	1.5 - 1.9	1.7 - 2.1	1.9 - 3.3
7. Transport Jets	1.2 - 1.8	1.6 - 2.2	1.8 - 2.8
8. Military Trainers	1.2 - 1.8	1.4 - 2.0	1.6 - 2.2
9. Fighters	1.2 - 1.8	1.4 - 2.0	1.6 - 2.6
10. Mil. Patrol, Bomb and Transports	1.2 - 1.8	1.6 - 2.2	1.8 - 3.0
11. Flying Boats, Amphibious and Float Airplanes	1.2 - 1.8	1.6 - 2.2	1.8 - 3.4
12. Supersonic Cruise Airplanes	1.2 - 1.8	1.6 - 2.0	1.8 - 2.2

$$(W/S) = \frac{(V_s)^2 \rho C_{Lmax}}{2} \tag{26}$$

$$\left(\frac{W}{S}\right) = \frac{(48 * 1.688)^2 \rho (2.0)}{2} = 15.6 \tag{27}$$

$$\left(\frac{W}{S}\right) = \frac{(60 * 1.688)^2 \rho (1.6)}{2} = 19.51 \tag{28}$$

The limit has been set at a wing loading (W/S) of 15.6 psf. Dividing the determined takeoff weight by this wing loading will yield a wing area of 175.6 ft^2. Plotting this limitation on a power loading versus wing loading graph, the limiting wing loading looks as such.

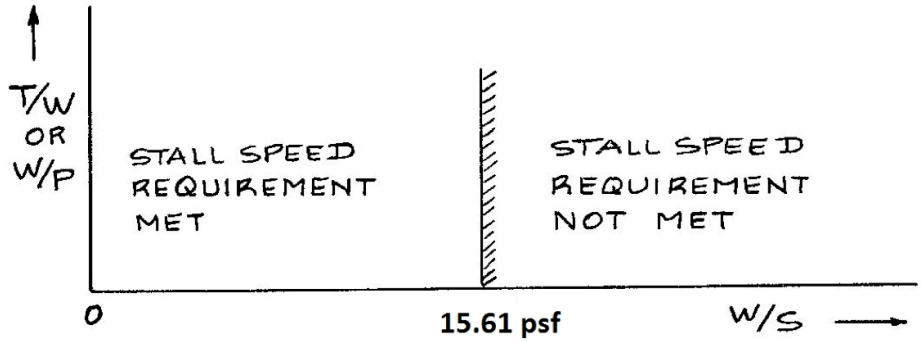

Figure 1 - 5 Example of Stall Speed Sizing

2. TAKEOFF DISTANCE REQUIREMENTS

The takeoff distance requirements will be considered next (s_{TOG}). This parameter is determined by the following factors: takeoff weight, takeoff speed of lift off speed (V_{TO}), Thrust/Weight at takeoff (T/W) or Weight/Power at takeoff (W/P) and the propeller characteristics, aerodynamic drag coefficient C_{DG} and ground friction (μ_G). FAR Part 23 guidelines are consulted in order to follow general aviation aircraft design specifications concerning the takeoff ground run (s_{TOG}). According to these specifications, the takeoff parameter (TOP_{23}) is proportional to the ground run as seen in **Eqn. (29)**.

$$TOP_{23} = \frac{(W/S)_{TO}(W/P)_{TO}}{\sigma C_{LmaxTO}} \qquad [lbs^2/ft^2hp] \tag{29}$$

The lift coefficient at takeoff, C_{LTO} is related to the maximum takeoff lift coefficient, (CL_{maxTO})

$$C_{LTO} = \frac{C_{LmaxTO}}{1.21} \tag{30}$$

This is due to a velocity gust margin of 10% being taken into account. **Fig. 1-6** shows the effect of TOP_{23} on the takeoff distance for a range of single and twin engine FAR Part 23 certified aircraft. The underlying assumption here is that most Part 23 aircraft are propeller driven. The reason for such scattered points has to do to the variation in takeoff procedures, the different characteristics of each aircraft studied and the rotation/lift off attitude (which is a function of control power, control feel, and the aircraft's inertia. It is noted within the Figure. that the total takeoff distance (S_{TO}) is 2/3rd longer compared to the ground run (S_{TOG}). The correlation line suggests the following relationship.

$$S_{TOG} = (4.9)TOP_{23} + (0.009)TOP_{23}{}^2 \tag{31}$$

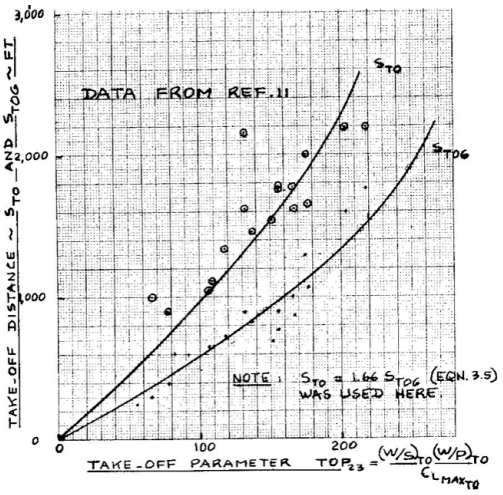

Figure 1 - 6 Effect of Takeoff Parameter on Takeoff Distance [1]

$$S_{TO} = (8.143)TOP_{23} + (0.0149)TOP_{23}{}^{2} \quad (32)$$

The takeoff criteria for this aircraft will be 1,500 ft. at an altitude of 5,000 ft. at standard day conditions (this altitude has been chosen to ensure that the aircraft can takeoff and land at any airport situated at an altitude of 5,000 ft.). 1,500 ft. (s_{to}) is plugged in to **Eqn. (31)** and it is solved for TOP_{23}. The value obtained is 145.5 lbs^2/ft^2hp. However, it is desired to create a tabulation of **Eqn. (29)**. In order to do these three parameters of interest must be isolated. Multiplying both sizes by sigma yields accomplishes this and yields a new value of TOP_{23} of 125.4 lbs^2/ft^2hp. The magnitude of the power loading $(W/P)_{TO}$ for a range of wing loadings $(W/S)_{TO}$ and takeoff maximum lift coefficients, (C_{LmaxTO}) will now be assessed. This will help the reader visualize the regions of wing loading and power loading for given values of C_{LmaxTO}. Since our limit of $(W/S)_{TO}$ is known to be 15.6 from **Eqn. (27)** and estimations for the takeoff C_{LmaxTO} from table 6 were determined, the power loading and thus our first guess at P_{TO} can be determined by interpolating these parameters. The data in table 6 came strictly from **Fig. 1-7**. The takeoff wing loading of 15.6 at a max takeoff coefficient of 1.4 were interpolated and tabulated as seen. For such configuration, we get a power loading of *13.7 lb./hp.* Dividing the takeoff weight by the power loading will yield the power needed for takeoff. The power needed for takeoff turns out to be 200 hp.

Table 1- 10 Determination of Power Loading

		CL_max_To					
		1.20	**1.40**	**1.60**	**2.00**	**2.40**	
(W/S)to	**10.0**	15.0	17.6	20.1	25.1	30.1	(W/P)to
	15.6	11.7	*13.7*	15.7	19.6	23.5	
	20.0	7.5	8.8	10.0	12.5	15.0	
	30.0	5.0	5.9	6.7	8.4	10.0	
	40.0	3.5	4.3	5.0	6.0	7.5	
	50.0	3.0	3.5	4.0	5.0	6.0	

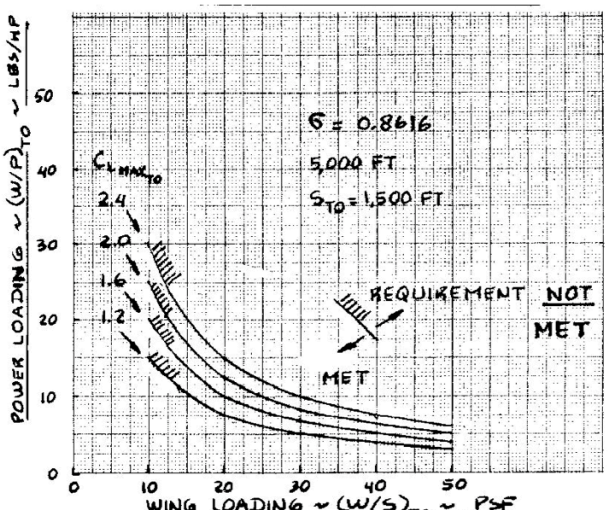

Figure 1 - 7 Effect of Takeoff Wing Loading and Maximum Takeoff Lift Coefficient on Takeoff Power Loading

The takeoff wing loading of 15.6 at a max takeoff coefficient of 1.4 were interpolated and tabulated as seen. For such configuration, we get a power loading of *13.7 lb./hp.* Dividing the takeoff weight by the power loading will yield the power needed for takeoff. The power needed for takeoff turns out to be 200 hp.

3. LANDING DISTANCE REQUIREMENTS

Landing distance requirements will be considered next. These landing distances parameters depend on the landing weight (W_L), approach speed (V_A), and deceleration method of the aircraft. **Fig. 1-8** shows the definitions of landing distances and velocities used in the FAR Part 23. The starting point will be historical values out of Roskam's typical values for landing weight to takeoff weight ratios as seen in **Table A2** (Appendix 2). For this airplane type 3 (twin-engine propeller driven) we are given a minimum W_L/W_{TO} of 0.88, an average W_L/W_{TO} of 0.99, and a maximum W_L/W_{TO} of 1.0. However, a W_L/W_{TO} of 0.95 will be chosen.

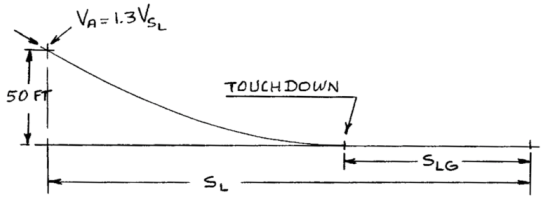

Figure 1 - 8 Definition of Landing Distances and Velocities used in FAR

The landing stall speed (V_{SL}) must now be determined. As seen in **Fig. 1-9** it is evident that the landing ground run (S_{LG}) is proportional to the square of the landing stall velocity (V_{SL}^2).

$$S_{LG} = 0.265\, V_{SL}^{\,2} \tag{33}$$

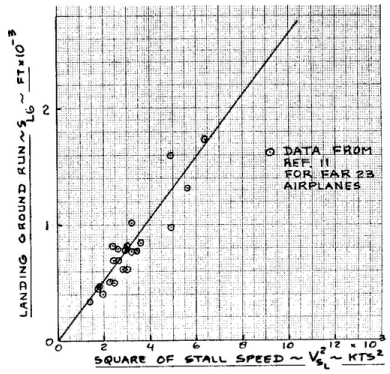

Figure 1 - 9 Effect of Square of Stall Speed on Landing Ground [1]

The correlation found in **Fig. 1-9** is nothing more than $S_L = 1.938 S_{LG}$. By combining these results, the landing ground run can be expressed in terms of landing stall velocity.

$$S_L = 0.5136\, V_{SL}^{\,2} \tag{34}$$

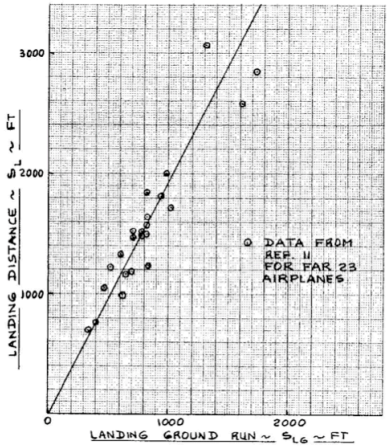

Figure 1 - 10 Correlation between Ground Run and Landing [1]

For this light twin landing filet length of 2,500 ft. will be defined at a 5,000 ft. altitude on a standard day where the density is equal to 0.002049 slugs/ft^3, yielding a landing stall velocity (V_{SL}) of 69.8 kts. and an approach velocity of 90.7 kts..

Recalling **Eqn. (25)** and solving for the wing loading substituting this V_{SL} yields the allowable wing loadings to meet a landing distance requirement. These can be seen in **Fig. A1** in the Appendix.

4. CLIMBING REQUIREMENTS

The climb requirements will now be considered. For this step, an estimate of our aircraft's drag must be obtained to estimate the power required.

$$C_d = C_{Do} + \frac{{C_L}^2}{\pi ARe} \tag{35}$$

The zero-lift drag or parasite drag (C_{Do}) can be expressed as $C_{Do} = f / S$, were f if the flat-plate drag as depicted in **Fig. A2**. This equivalent flat-plate drag area can be related to the wetted area (area of the aircraft that would be in contact with water if submerged), S_{wet}. Using empirical data, the flat plate drag can be established from the wetted area. **Fig. 1-11** shows the correlation between the equivalent flat-plate drag of the aircraft versus the wetted area. Where the coefficient of skin friction (c_f) drives the values of a and b of **Eqn. (36)**

$$log_{10}(f) = a + b\ log_{10}(S_{wet}) \tag{36}$$

For a given coefficient of skin friction (c_f) the quantities for a and b are tabulated in **Fig. A3**. By examining the configurations in the database, one can select a reasonable estimate for these values. In order to estimate the drag a method to predict realistic values for the wetted area (S_{wet}), must be employed. It is evident that the ability to predict a realistic value for the wetted area (S_{wet}) is what allows for the estimation of the drag. Fortunately, enough Roskam provides **Fig. 1-12**, which states that the wetted area correlates well with the aircraft takeoff weight, typically following the two-thirds scaling law. **Fig. 1-12** allows us to make a reasonable prediction as to what the wetted area of an airplane will be without knowing what the airplane looks like. The line regression coefficients for **Eqn. (37)** are presented in **Table A4** in the Appendix. For this twin-engine propeller driven aircraft the values of 0.8635 and 0.5632 for c and d are obtained, respectively.

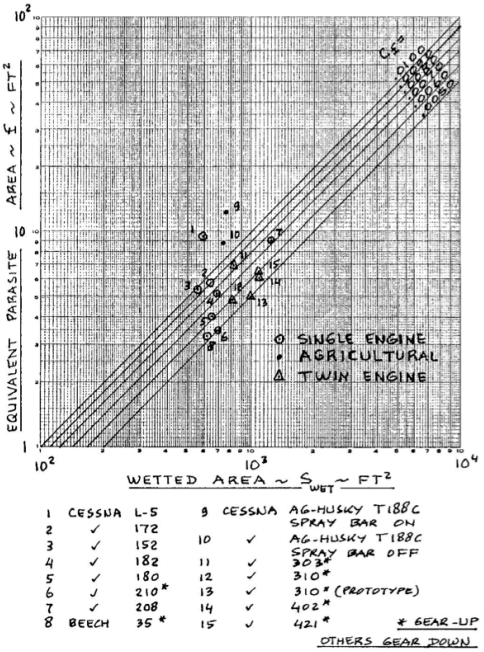

Figure 1 - 11 Effect of Equivalent Skin Friction on Parasite and Wetted Area [1]

$$log_{10}(S_{wet}) = c + d\ log_{10}(W_{TO}) \tag{37}$$

Eqn. (37) yielded a wetted area of about 630 ft^2. In order to estimate the flat plate drag, the wetted area, as a function of takeoff gross weight and type must first be determined. Then empirical data must be examined and a skin friction coefficient (c_f) that best represents our configuration must be selected. This skin coefficient is determined by the streamlining designed into the airplane and its smoothness. It is important to note that the scatter in the Fig.s is mainly due to differences in wing loadings, nacelle design and cabin sizes. Even so, most airplanes fall in the ten percent band making this a very good first time pass. We have selected our skin friction coefficient to be 0.007, which yields a flat plate drag of 4.41, and a zero lift drag (C_{Do}) of 0.025. Since an estimate for the takeoff weight was already obtained previously, the drag polar (as seen in **Eqn. (35)**) for the clean airplane can be determined. "For takeoff and for landing, the effects of flaps and of the landing gear need to be accounted

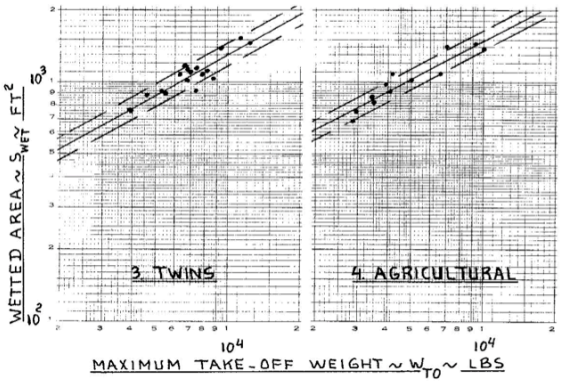

Figure 1 - 12 Correlation between Wetted Area and Takeoff Weight [1]

for. The additional zero-lift drag coefficients due to flaps and due to landing gear are strongly dependent on the size and type of these items (Roskam, 121)[1]."

The drag polar with estimates of changes due to various configurations (clean, takeoff flaps, landing flaps, landing gear) and their associated Oswald's 'e' have been calculated. An aspect ratio (AR) of 7 has been assumed in our calculations. **Table A5** in the appendix provides some first estimates for ΔC_{Do} and 'e' for different configurations.

Table 1-11 shows the values calculated for the drag polar ($C_L^{3/2}/C_D$)

Table 1- 11Coefficients of Drag and Drag Polar Results

Configuration	C_D	C_{Do}	$1/\pi ARe$	e	C_L	$C_L^{3/2}/C_D$
CLEAN	0.133	0.0251	0.05478	0.83	1.4	12.50
TAKE-OFF	0.143	0.0351	0.05478	0.83	1.4	11.62
LANDING	0.287	0.0851	0.06223	0.73	1.8	8.42
LANDING (f&g)	0.312	0.1101	0.06230	0.73	1.8	7.74

Calculating the drag polar is crucial due to the fact that when $C_L^{3/2}/C_D$ is maximum the power required is the least, making the specific power the greatest. At the velocity where this occurs is when the specific power is the greatest and respectively when the highest rate of climb can be achieved. These values will be used to calculate the FAR requirements discussed later in this report.

5. CRUISE SPEED REQUIREMENTS

The sizing cruise speed requirements will now be considered. A relationship between the wing loading and the power loading must be derived. The cruise speed (*Vcr*) will be calculated first using **Eqn. (38)**.

$$V_{CR} = \left[\frac{\left(\frac{W}{S}\right)}{\left(\frac{W}{P}\right)} \left(\frac{\sigma C_{Do}}{\eta_P} \right) \right]^{\frac{1}{3}} \tag{38}$$

Here, the cruise velocity is proportional to the power index[2] (*Ip*).

$$I_P = \left[\frac{\left(\frac{W}{S}\right)}{\sigma \left(\frac{W}{P}\right)} \right]^{\frac{1}{3}} \tag{39}$$

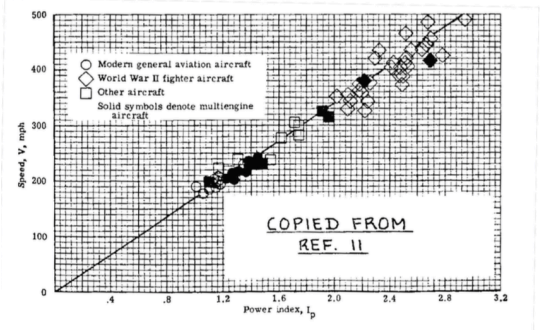

Figure 1 - 13 Correlation of Airplane Speed with Power Index for Retractable Gear, Cantilevered Wing Configurations[1]

The cruise criterion was set at 140 kts.. This aircraft was chosen to cruise at approximately 7,500 ft. and in the neighborhood of 75-80% power. Retractable gear is desired and consequently **Fig. 1-13** can be utilized. **Equations (38)** and **(39)** were constructed to utilize velocity in miles per hour. So a conversion must be made from 140 kts. to miles per hour. 161.28 miles per hour is the velocity that will be inputted to these Equations. Utilizing **Fig. 1-13** to determine the power index (*Ip*) and utilizing the density ratio at 7,500 ft. we can write a relationship between the power loading and the wing loading as seen in **Eqn. (40)**.

$$\left(\frac{W}{P}\right) = \frac{1}{\sigma(I_P)^3}\left(\frac{W}{S}\right) \tag{40}$$

Were I_p was found to be 0.88 and a value of 0.7983 for σ was used. **Eqn. (40)** then becomes a proportionality Eqn. were the wing loading is proportional to the power loading by a factor of 1.8382. This relationship is depicted in **Fig. 1-17**.

Matching all Size Requirements

A series of relationships have been established. The combination of these parameters will allow the most optimal design point to be chosen that will yield the lightest and consequently the cheapest aircraft. The next Fig.s will show all the requirements separately.

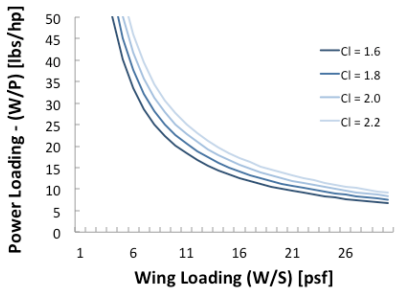

Figure 1 - 14 Allowable Wing Loading to Meet a Landing Distance Requirements

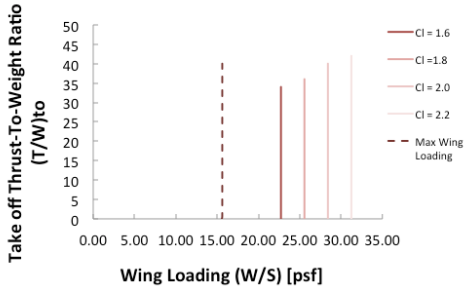

Figure 1 - 15 Effect of the Takeoff Wing Loading and Maximum Landing Lift Coefficient on the Takeoff Power Loading

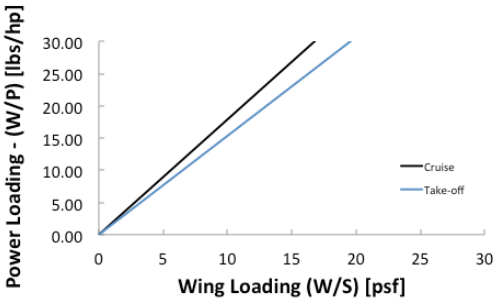

Figure 1 - 16 Allowable Values of Wing Loading and Thrust-to-Wing Ratio to Meet a Given Cruise Speed

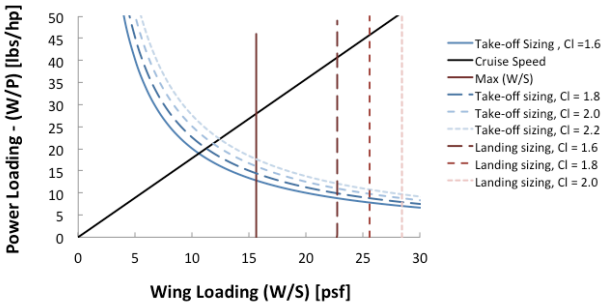

Figure 1 - 17 Matching Sizing Requirements

FAR 23.65 AEO Rate of Climb

For rate of climb for all engines operating for this type of aircraft, FAR 23.65 is the guidelines, these guidelines are as follows.

1. Minimum climb rate at sea level of 300 feet per minute.
2. Not more than maximum continuous power on all engines
3. Landing gear retracted
4. Flaps in the takeoff position
5. Cowl flaps as required for proper engine cooling

Once those conditions are met the Equations set out in the requirements are given and using the known variables a relation between the power loading and the wing loading can now be determined. The Equations given are as follows.

$$RC = 33000 * RCP \tag{41}$$

$$RCP = \left[\frac{\eta_p}{\left(\frac{W}{P}\right)} - \left[\frac{\left(\frac{W}{S}\right)^{\frac{1}{2}}}{19*\left(\frac{C_L^{\frac{3}{2}}}{C_D}\right)\sigma^{\frac{1}{2}}}\right]\right] \tag{42}$$

Using those Equations as well as the assumptions previously stated as well as the coefficient of lift and drag coinciding with the guidelines, the final power loading vs. wing loading graph would look like the following Fig..

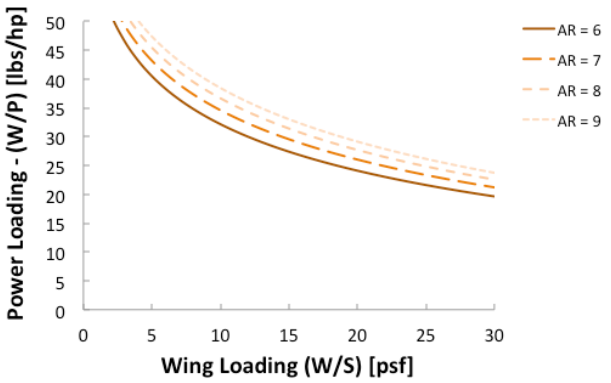

Figure 1 - 18 FAR 23.65 Rate of Climb (AEO)

These where evaluated at a coefficient of lift, C_L, of 1.6 while the aspect ratio was varied. While this graph alone has a set maximum power loading to wing loading all the FAR requirements graphs need to be discussed and put all together to ding the defining FAR requirement and then integrated those values with the values of the other graphs to discover the main defining criteria.

FAR 23.65 AEO Climb Gradient

This is the system for the regulation climb gradient, which is assumed to be at least 1:12. From here with the assumptions known and the Equations given below a relationship between the power loading and the wing loading can be determined. This is with CGR = climb gradient and CGRP = climb gradient parameter.

$$CGRP = \frac{\left(CGR + \left(\frac{1}{\frac{C_L}{C_D}}\right)\right)}{C_L{}^{\frac{1}{2}}} \tag{43}$$

$$\frac{W}{P} = \frac{\left(\frac{18.97 * (\eta_p}{CGRP}\right)}{\left(\frac{W}{S}\right)^{\frac{1}{2}}} \tag{44}$$

Recall that values of from **Table 1- 11** were used to calculate these requirements.

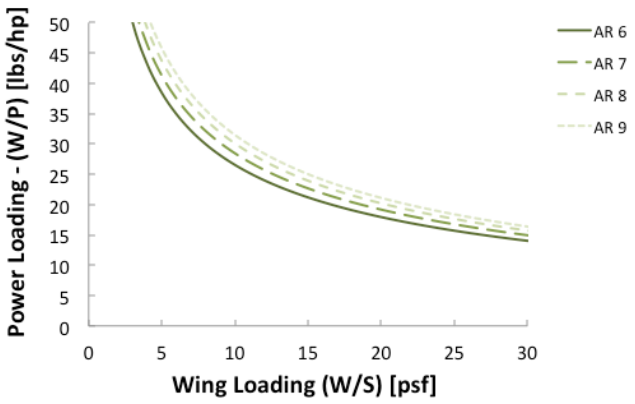

Figure 1 - 19 FAR 23.65 Climb Gradient (AEO)

FAR 23.67 OEI Rate of Climb

With one engine out and the FAR requirement showing

1. For multiengine (reciprocating engines) airplanes with W_{TO} < 6,000 and with V_{S0} < 61 knots the requirement is that the steady climb rate at 5,000 ft. altitude *must be determined.*
2. Critical engine inoperative and its propeller in minimum drag position
3. Remaining engines at no more than maximum continuous power
4. Landing gear retracted
5. Cowl flaps as required for proper engine cooling
6. Wing flaps in the most favorable position

With this the OEI, the rate of climb was given as 250 feet per minute in the design requirements **(Table 1-1)**. **Equations (41-42)** are employed once more and rearrange to express the power loading as a function of wing loading. Drag polar values from **Table 1- 11** were utilized here for the specified configuration listed above.

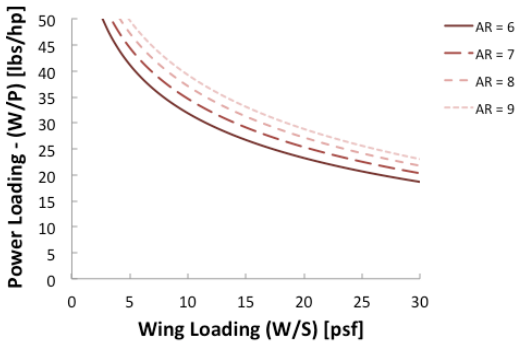

Figure 1 - 20 FAR 23.67 Rate of Climb (OEI)

The variation with aspect ratios is shown. As expected, the change will increase power loading and therefore decrease the size of the engine needed to operate the aircraft.

FAR 23. 77 AEO Climb Gradient

Now FAR 23.77 AEO CGR is the same as FAR 23.65 AEO CGR however it accounts for landing conditions, along with a steady climb angle being a minimum of 1:30. Using **Equations (43-44)** we obtain the following Fig..

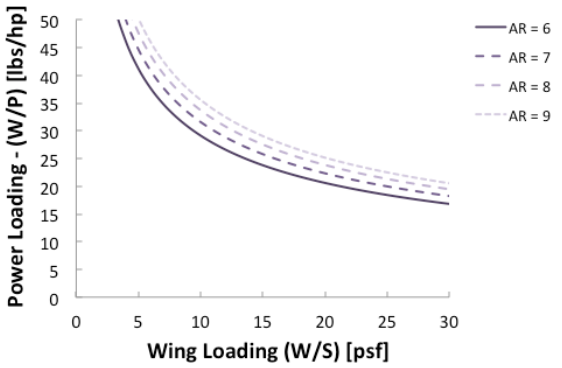

Figure 1 - 21 FAR 23.67 Rate of Climb (OEI)

The variation with aspect ratios is shown. **Fig.s 1-18** through **1-21** will now be superimposed taking only the curves from each FAR requirement with an aspect ratio of 7 since that is the aspect ratio of this aircraft.

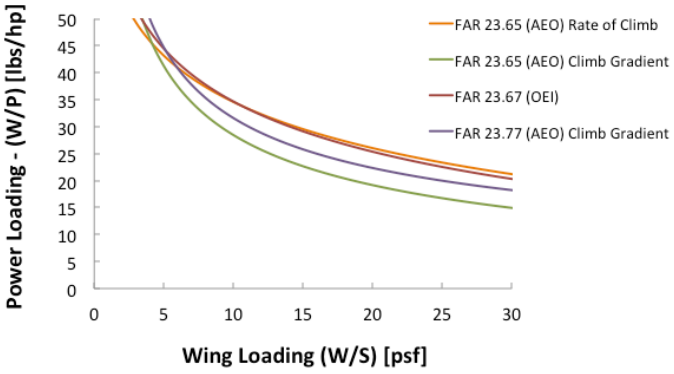

Figure 1 - 22 Matching FAR 23 Requirements

Fig. 1-22 shows that bellow a wing loading of 4 FAR 23.65's rate of climb requirement dictates the limit, and for wing loadings grader and equal to 5 are dictated by FAR 23.65's climb gradient. Remember all of these were determined for a coefficient of lift, C_L of 1.6.

It is desired to match all of these results and select a design point with the highest power loading (W/P) and highest wing loading (W/S). Higher power loading will yield the smallest engine that will meet these requirements. Higher wing loading will yield the less drag created on the wing and therefore lead to better fuel efficiencies.

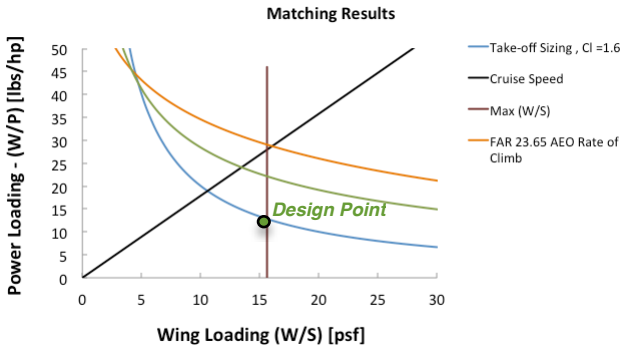

Figure 1 - 23 Matching FAR 23 and Sizing Requirements

It is important to note that our design point must be on or left of the Max (W/S) vertical line and under the lower most function. In this case being the takeoff-sizing requirement at a C_L of 1.6. This will ensure that every single one of the limiting requirements is met. In this case, the optimal design point is at a wing loading of 15.6 lbs./ft^2 and at a power loading of 14 lb./HP.

So in conclusion, for the desired range to be achieved, even though the aircraft can hold four passengers with luggage, it can only be achieved when there are three passengers and luggage. In regards to the sensitivity, the payload weight will change at a greater factor per lb. change than the empty weight, both changing at a greater pace than the range. Yet, the specific fuel consumption will have the greatest effect on the takeoff weight. Finally in regards to the power loading and wing loading sizing, the factors that determine this are the cruise speed and the landing sizing and maybe FAR 23.77 given the right changes within the other criteria. With all this info, a set of data to recreate this process should be able to be accomplished given a new set of design criteria.

III. Part 2

Empennage Sizing and Disposition and for Control Surface Sizing and Disposition

To begin the I.A.D 4350 aircraft design, historical data needs to be analyzed in order to identify a reasonable range sizing parameters for the vertical tail, horizontal tail, and main wing. The analyze began by looking through Dr. Jan Roskam Volume II that gave multiple twin engine propeller driven airplanes data for the horizontal tail and elevator as well as rudder and aileron data as seen in **Fig.2-1** and **Fig A3** in the appendix**.**

Type	Wing Area S ft^2	Wing mgc $\bar{c}$ ft	Wing Airfoil root/tip NACA*	Hor. Tail Area S_h ft^2	S_e/S_h	x_h ft	$\bar{V}_h$	Elevator Chord root/tip fr.c_h
CESSNA								
310R	179	4.77	23018/23009	54.3	0.41	14.9	0.95	.42/.39
402B	196	4.77	23018/23009	60.7	0.29	16.5	1.07	.41/.39
414A	226	4.73	23018/23009	60.7	0.27	16.4	0.93	.37/.38
T303	189	4.9	23017/23012	48.1	0.42	14.9	0.78	.41/.44
PIPER								
PA-31P	229	5.79	$63_3$415/$63_3$212	68.7	0.44	16.2	0.84	.41/.51
PA-44-180T	184	4.34	NA	23.4	1.0	15.7	0.46	stabilator
Chieftain	229	6.00	63_3A415/63_3A212	61.4	0.38	16.1	0.72	0.38
Cheyenne I	229	5.69	63_3A415/63_3A212	70.5	0.40	15.7	0.85	.40/.41
Cheyen. III	293	7.33	63_3A415/63_3A212	61.8	0.39	23.7	0.68	.35/.44
BEECH								
Duchess	181	5.08	63_3A415	39.4	0.35	15.6	0.67	0.40
Duke B60	213	6.60	23016.5/23010.5	62.0	0.27	14.5	0.64	0.39
Lear Fan								
2100	163	4.36	NA	55.0	0.23	13.1	1.01	.36/.31
Rockwell								
Comdr 700	200	5.28	NA	55.4	0.37	19.7	1.03	0.37
Piaggio								
P166-DL3	286	6.06	230 series	51.6	0.27	17.2	0.51	.40/.50
EMB-121	296	6.62	NA	62.9	0.43	20.3	0.65	.39/.46

* Unless otherwise indicated

Figure 2 - 1 Twin Engine Propeller Driven Airplane: Horizontal Tail Volume and Elevator Data

Furthermore, this data was input in Excel and the average was calculated to find an estimate of lengths, volumes, and areas of the main wing, horizontal tail, and vertical tail. All averages can be seen in Table 2-1 and 2-2 **for the structure components and controls that was organize into its respective area.**

Table 2 - 1 Historical Data on Main Wings, Horizontal and Vertical Tails [2]

STRUCTURES									
AIRCRAFT	MAIN WING			HORIZONTAL TAIL			VERTICAL TAIL		
	AREA	MGC	SPAN	Volume Coeff	Area	Distance from mgc to mgc	Volume Coeff	Area	Distance from mgc to mgc
Cessna 310 R	179	4.77	36.9	0.95	54.3	14.9	0.063	26.1	15.9
Cessna 402 B	196	4.77	39.9	1.07	60.7	16.5	0.08	37.9	16.5
Cessna 414 A	226	4.73	44.1	0.93	60.7	16.4	0.071	41.3	17
T303	189	4.9	39	0.78	48.1	14.9	0.052	23.2	16.5
Conquest I	225	-	44.1	-	-	-	0.071	41.3	17.1
PA - 31P	229	5.79	40.7	0.84	68.7	16.2	0.056	30.1	17.2
PA- 44-180T	184	4.34	38.6	0.46	23.4	15.7	0.044	21.5	14.4
Chieftain	229	6	40.7	0.72	61.4	16.1	0.055	29.5	17.3
Cheyenne I	229	5.69	42.7	0.85	70.5	15.7	0.045	26.5	16.5
Cheyenne III	293	7.33	47.7	0.68	61.8	23.7	0.065	43.6	20.8
Duchess	181	5.08	38	0.67	39.4	15.6	0.053	25.6	14.2
Duke B60	213	6.6	39.3	0.64	62	14.5	0.06	28.8	17.4
2100	163	4.36	39.3	1.01	55	13.1	0.097	44.4	14
Commander 700	200	5.28	42.5	1.03	55.4	19.7	0.096	39.9	20.5
P166-DL3	286	6.06	48.2	0.51	51.6	17.2	0.041	30.7	18.3
EMB-21	296	6.62	46.4	0.65	62.9	20.3	0.055	42.6	17.8
	S	C	b	Vh	Sh	Xh	Vv	Sv	Xv
Average	219.875	5.488	41.75625	0.786	55.73	16.7	0.06275	33.3125	16.9625

Table 2 - 2 Historical Data on Main Wings, Horizontal and Vertical Tails [2]

CONTROLS							
AIRCRAFT	MAIN WING			HORIZONTAL TAIL		Vertical Wing	
	Wing Airfoil		Aileron to Wing Area	Elevator to Horizontal Area	Elevatro Chord	Rudder to Vertial Area	Rudder Chord
	Root	Tip	Sa/S	Se/Sh	root/tip	Sr/Sv	root/tip
Cessna 310 R	23018	23009	0.064	0.41	.42/.39	0.45	.48/.41
Cessna 402 B	23018	23009	0.058	0.29	.41/.39	0.47	.48/.40
Cessna 414 A	23018	23009	0.061	0.27	.37/.38	0.38	.49/.37
T303	23017	23012	0.087	0.42	.41/.44	0.44	.46/.39
Conquest I	-	-	0.06			0.38	.47/.34
PA - 31P	63-s-415	63-1-212	0.056	0.44	.41/.51	0.38	.37/.42
PA- 44-180T	-	-	0.077	1	STABILATOR	0.37	.30/.50
Chieftain	63-2-A415	63-1-A212	0.06	0.38	0.38	0.4	.40/.38
Cheyenne I	63-2-A415	63-1-A212	0.057	0.4	.40/.41	0.4	.37/.42
Cheyenne III	63-2-A415	63-1-A212	0.046	0.39	.35/.44	0.46	0.33
Duchess	63-2-A415		0.059	0.35	0.4	0.29	.34/.42
Duke B60	23016.5	23010.5	0.054	0.27	0.39	0.43	.44/.46
2100	-	-	0.044	0.23	.36/.31	0.17	.32/.34
Commander 700	-	-	0.087	0.37	0.37	0.38	.37/.38
P166-DL3	230 Seriese		0.073	0.27	.40/.50	0.43	.38/.43
EMB-21	-	-	0.052	0.43	.39.46	0.45	.42/.41
Average	-		0.062	0.39	-	0.39	-

The sizing for the preliminary design of the main wing was already calculated to be 175 ft^2. Furthermore, it was decided to use an aspect ratio (AR) of 7 from historical data. Moreover, using these values the wingspan of the main wing was calculated to be 35.05 ft. and can be seen in **Eqn. (45)**. In addition, the wing mean geometric chord (MCG) was also calculated by dividing the wing area by the wingspan and can be seen in **Eqn. (46)**. Both calculated answers seemed reasonable for our aircraft since they were closed to the historical data average calculated in **Table 2-2**. Also, the horizontal tail area and vertical area where calculated by first finding the relationship ratio of main wing with horizontal tail and showed to be 25.3% of the main wing seen in **Eqn. (47)**. Furthermore, the vertical had the same process and was found to be 15.1% of the main wing through historical data seen in **Eqn. (48)**. Moreover, taking the historical data of the distance from the mean geometric chord of the wing and the MGC of the horizontal tail than getting the ratio of the horizontal by main and multiplying it by the calculated chord of our aircraft the lengths of the aerodynamic center of the horizontal was found and can be seen in **Eqn. (49)**. The same process was made for the lengths of the aerodynamic center of the vertical tail seen in **Eqn. (50)**.

$$b = \sqrt{Sw \times ARw} \tag{45}$$

$$MGC = \frac{Sw}{b} \tag{46}$$

$$ShT = \frac{Sh}{Swh} \times Sw \tag{47}$$

$$SvT = \frac{Sv}{Swh} \times Sw \tag{48}$$

$$L, ht = \frac{Xh}{C} \times C \tag{49}$$

$$L, vt = \frac{Xv}{b} \times b \tag{50}$$

Furthermore, to continue the sizing of I.A.D 4350 aircraft the aspect ratio of the horizontal tail and aspect ratio of the vertical tail was estimated to be 4 and 1.46 respectively by using historical data seen in **Table 2-3**.

Table 2 - 3 Historical Data for Empennage

Aircraft			AVERAGE (ft)	AVERAGE (in)	CESSENA 310	CESSENA 402 B	CESSENA T 303	PA 44-180 T	ROCKWELL C 700
HT	Area (ft^2)	S ht	45.40	6536.97	7350.61	7127.75	5663.41	3412.136	9130.94
	Span (ft)	b ht	14.49	173.91	196.22	184.7	160.68	123.56	204.41
	Aspect Ratio	AR ht	4.73	4.73	5.24	4.79	4.56	4.47	4.58
VT	Area (ft^2)	S vt	25.09	3612.59	3410.41	4310.29	2906.15	2480.76	4955.33
	Span (ft)	b vt	6.53	78.33	81.47	80.01	75.81	57.82	96.53
	Aspect Ratio	AR vt	1.73	1.73	1.95	1.49	1.98	1.35	1.88

To continue, wing spans of the horizontal tail and the vertical tail was determined by using the predicted horizontal aspect ratio and vertical aspect ratio and multiplying them with their respective wing areas than square rooting the values as seen in **Eqn. (51)** and **(52)**.

$$bht = \sqrt{Sht \times ARH} \tag{51}$$

$$bvt = \sqrt{Svt \times ARV} \tag{52}$$

Therefore, the ratio between the horizontal area and the main area was calculated as well as the ratio between the vertical tail and the main wing area to further calculate the volume coefficients of both horizontal and vertical tails. Furthermore, the ratios of the lengths of the aerodynamic center divided by the chord was also calculated. Using these values the volume coefficient for the horizontal and vertical tail were calculated as seen in **Eqn. (53)** and **(54).**

$$Vht = \frac{Sht}{Sw} \times \frac{Lht}{c} \tag{53}$$

$$Vvt = \frac{Svt}{Sw} \times \frac{Lvt}{b} \tag{54}$$

All of these values and calculations can be seen in **Table 2-4**,

Table 2 - 4 Empennage Calculated Data

For our Aircraft			
Wing Area, ft^2	Sw	175.5	
Wing MGC, ft	C	5.01	
Wing Loading, lbs./ft^2	W/S	15.60	
Main Wing Span, ft	b	35.05	
Horizontal Tail Area, ft^2	S - hT	44.48	Sw*25.3%
Vertical Tail Area, ft^2	s - vT	26.59	Sw*15.1%
Lengths of ADC , ft	l - ht	15.24	(Xh/C*C)
Lengths of ADC , ft	l - vt	14.24	(Xv/b*b)
Horizontal Tail Span ,ft	b - ht	13.3	
Vertical Tail Span, ft	b - vt	6.23	
Wing Aspect Ratio	ARplane	7	
Horizontal Tail Aspect Ratio	ARH	4	
Vertical Aspect Ratio	ARV	1.46	
Sht/Sw	0.253447034		
Lht/c	3.043002915		
Vht	Sht/Sw lht/c	0.771	
Svt/Sw	0.151506538		
Lvt/b	0.406226613		
Vvt	Svt/Sw lvt/b	0.0615	

To continue, this data was also confirmed by analytically measuring the size of five different aircraft with scale drawings that can be seen in **Fig 2-2**.

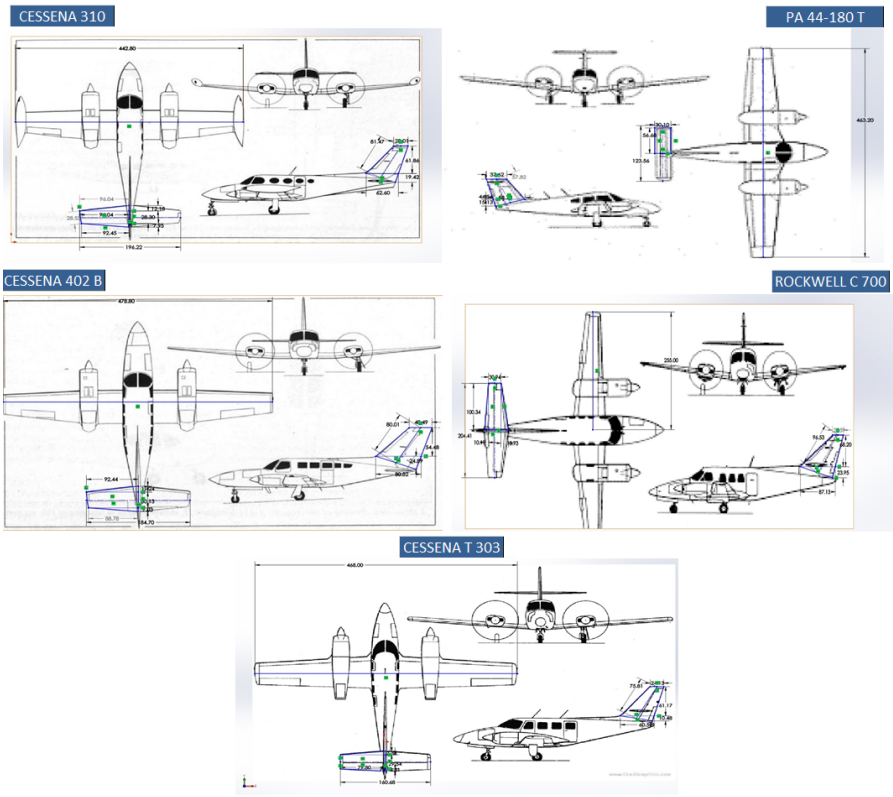

Figure 2 - 2 Aircraft use to Estimate Empennage

Ergonomics and Preliminary Drawings

To continue the analysis the aircraft fuselage was needed to be size to further our preliminary design. Some of the ergonomics and sizing was given in the mission requirements that set the fuselage width to 4 ft. Furthermore the minimum height of our fuselage from the top of the seat was given as 3ft. To continue, data for the fifth to ninety-five percentile ergonomics was acquire to further size the inside of the fuselage. Using the 5^{th} to 95^{th} percentile data it was determined that the length of the fuselage was going to be 9 ft. as seen in **Fig 2-3**. Moreover, leg room, seat height, seat inclination, controls size, arm length, torso height, head size, etc. where taken into account to construct the fuselage in inside and can be appreciated in **Fig 2-3**. Also the baggage was taken into account in the preliminary sizing of the fuselage since the volume of the luggage storage was given in the mission requirements. The minimum view needed for the pilots was determined to be 15 degrees downward where the pilot could still see the tip up the nose without any obstruction and a 20 degrees angle upward can also illustrated in **Fig 2-3**.

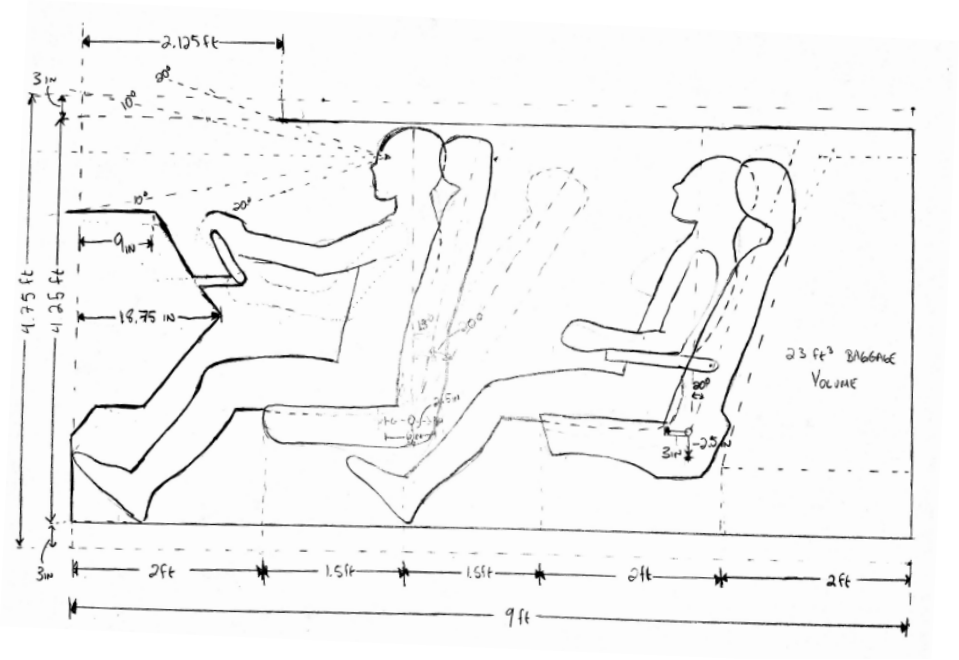

Figure 2 - 3 Ergonomics Side View of the Aircraft Design

Furthermore, the top view of the cockpit was also drawn to scale to further advance I.A.D 4350 aircraft sizing. It was required that the aircraft needed to have a capacity of four people using the 5th to 95th percentile data the average width of the human body hip was taken into account when seats where placed. Furthermore, from historical data it was determined that the material thickness was going to add 3 inches on each side. The cockpit was design in a way to allow comfort for the passengers but also try to minimize the length and width as much as possible to reduce unneeded weight. The top View of the preliminary cockpit design can be appreciated in **Fig 2-4**.

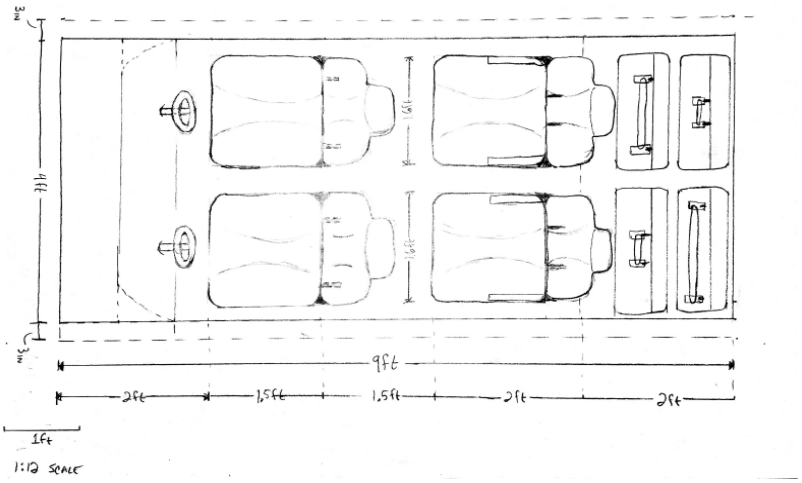

Figure 2 - 4 Ergonomics Top View of the Aircraft Design

Once the fuselage was sized the complete top, front, and side views of the entire aircraft were drawn to size taking an inch as a foot. Using the historical data analysis the length, width, and area of the aircraft were taken into account when drawing the model. Furthermore, in the preliminary drawing it was decided that the aircraft was going to have a constant slope between the top of the fuselage and the tip of the nose. This was concluded to be best for the design because of decrease in drag with constant slope and flow in the laminar boundary layer. Furthermore, having a constant slope increased the visibility of the pilot and met the requirements of 15 degrees downward visibility. Furthermore, the design process started with implementing mid-wing design since it lied between the features of high-wing and configurations and low-wing configurations. This idea quickly plunder since the wing spar was needed to be cut or the wing would have been needed pass through the fuselage that occupies space of the fuselage. Furthermore, using historical data it was noted that mid-wings where heavier, due to the necessity to reinforce the fuselage to sustain the wings. Also, it was found that mid-wings where more expensive than high and low-wings. Therefore, it was decided that a high wing was best suited for the design and the aerodynamic engineer will give further explanation.

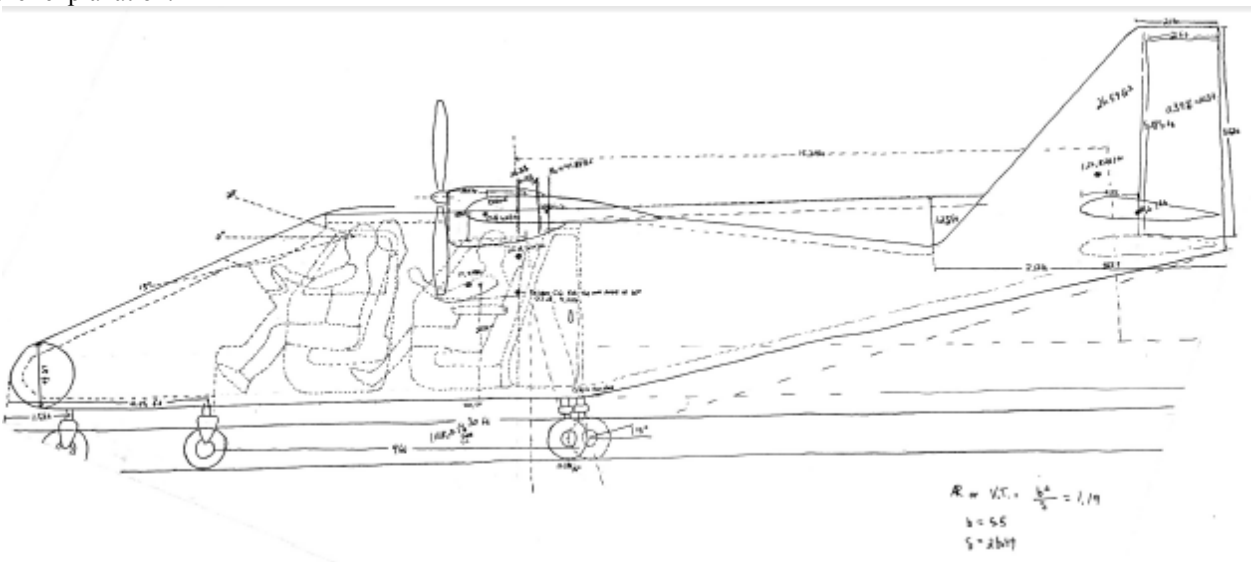

Figure 2 - 5 Side View of Aircraft Design

Furthermore, as seen in **Fig 2-5** the first drawing did not have enough structure in the tail for the horizontal tail to be placed and supported this is why the fuselage negative angle to tail was inverted to create more structure space for the horizontal wing support. Moreover, the gear also influenced the height of the empennage with respect to the ground since 15-16 degrees set by C_{Lmax} are needed as historical data states and will be further discussed in the gear placement section. To continue, the top view and front view were also drawn to scale of 1 foot = ½ inch as seen in **Fig 2-6**. Some of the constrains set by historical data and FAA regulations is that the propellers have to be at a minimum distance of 6 inches from the fuselage which also sets a minimum distance the engine was placed with respect to the wing. Furthermore, controls where estimated by historical data to be 25-35% for the main-wing flaps, 20-25% for the ailerons, and 30 % for the elevators. The quarter chord can be seen in the top view as well as the gear placement that will further be discussed.

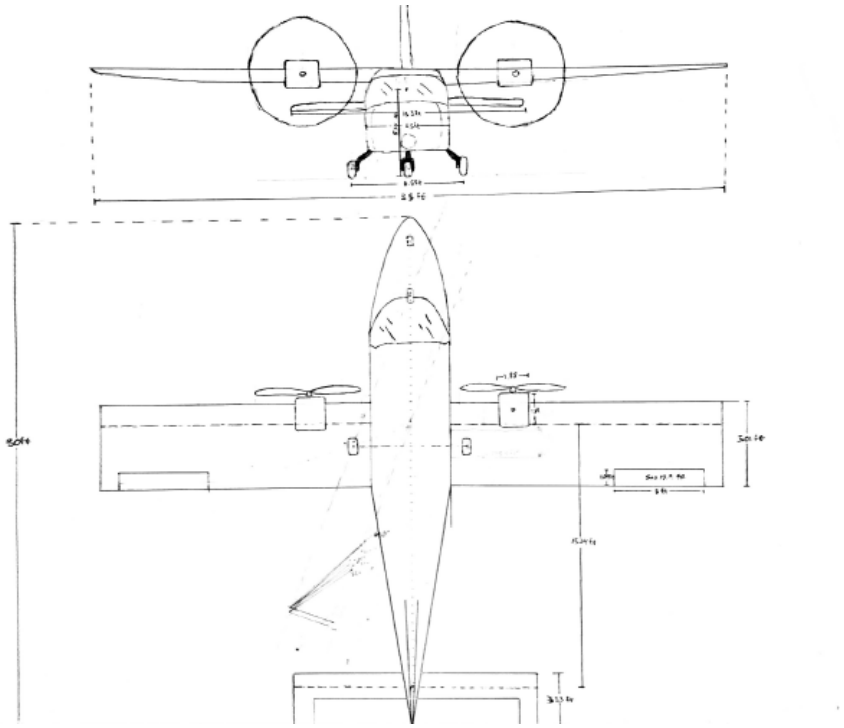

Figure 2 - 6 Preliminary Front and Top View of Aircraft

These hand drawing were transferred into AutoCAD, a drafting software, for better precision and quality.

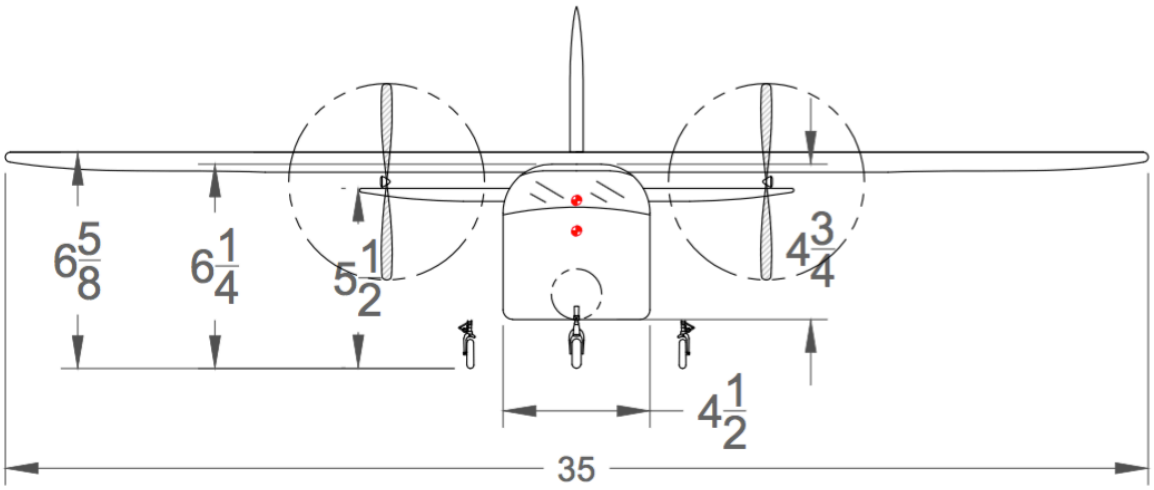

Figure 2 - 7 Preliminary AutoCAD Front View of Aircraft

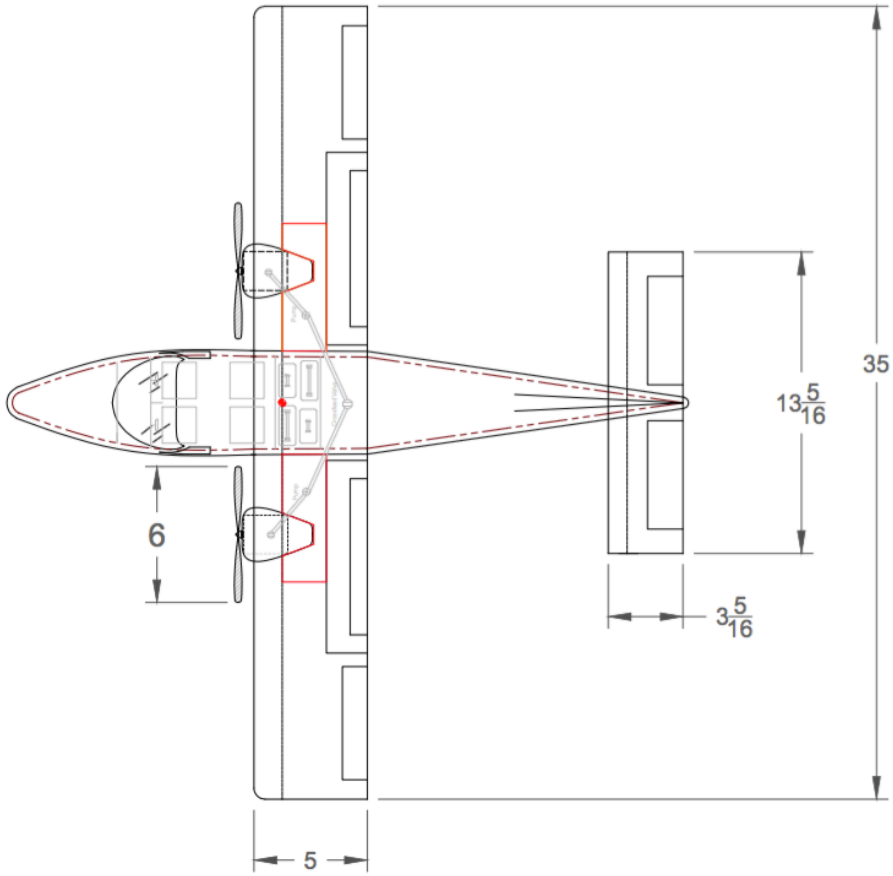

Figure 2 - 8 AutoCAD Top View of Aircraft

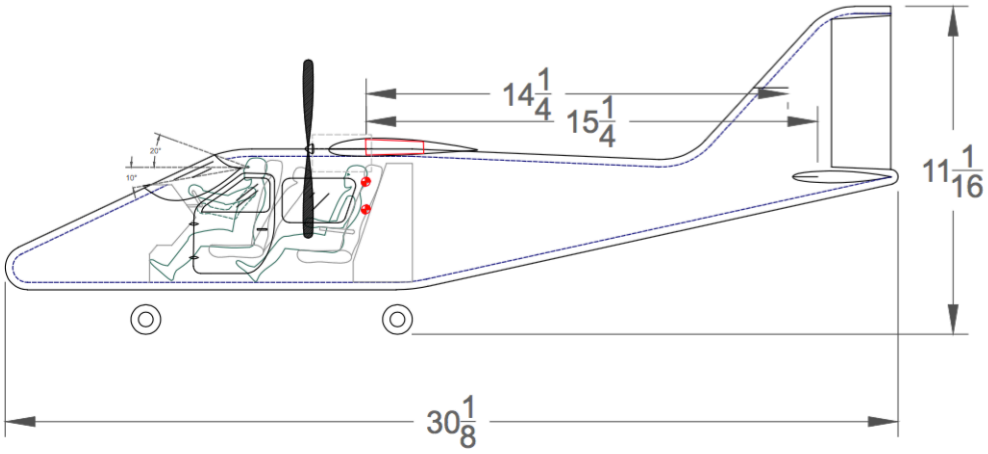

Figure 2 - 9 AutoCAD Side View of Aircraft

Neutral Point Calculations

The neutral point of the aircraft is one of the most important parameters when it comes about the longitudinal static stability of the aircraft. Since the aircraft has to be economical, adequate static stability should be present so as to minimize the presence of advanced control systems. The longitudinal stability theory is first developed for a simplified case of an airplane in gliding flight with controls locked (stick fixed) and propellers wind milling. The theories thus obtained can be expanded later on to account for the effects of power and free control.

Neutral point (stick fixed): The stick fixed Neutral point is obtained from the final stability Eqn. written for the airplane in gliding flight with fixed controls and no propeller. The Eqn. is:

$$\frac{dC_m}{dC_L} = \frac{x_a}{c} + \left(\frac{dC_m}{dC_L}\right)_{\substack{Fus \\ Nac}} - \frac{a_t}{a_w}\bar{V}\eta_t\left(1 - \frac{d\epsilon}{d\alpha}\right) \tag{55}$$

The above Eqn. and its step-by-step derivation are taken from Perkins and Hage textbook[16] as it provides a detailed description to finding the neutral points. In the above equation the first term is the wing contribution, the second term is the fuselage and nacelles contribution and the last term is the contribution of the horizontal tail. The wing contribution in the stability Eqn. can be written as:

$$\left(\frac{dC_m}{dC_L}\right)_{Wing} = x_{cg} - x_{ac} \tag{56}$$

This Eqn. indicates that for every percent of the m.a.c that the *cg* is moved aft, $(\frac{dC_m}{dC_L})_{wing}$ will increase positively by one percent. When the airplane is neutrally stable, $\left(\frac{dC_m}{dC_L}\right)$ is equal to zero. This is because at the neutral point the pitching moment generated by the lift coefficient becomes zero. Using this relation and the above two Equations the stick fixed neutral point with no propeller is obtained. This neutral point gives the most aft location at which the *cg* of the aircraft can be placed before making the aircraft unstable. Since stability is desired in the aircraft, this neutral point (N_0) puts a limit on the aircrafts permissible *cg* level. The neutral point is also very convenient to obtain, because once the neutral point is known, stability at other *cg* locations can be obtained with good accuracy.

$$N_0 = x_{cg(dC_m/dC_L=0)} = x_{ac} - \left(\frac{dC_m}{dC_L}\right)_{\substack{Fus \\ Nac}} + \frac{a_t}{a_w}\bar{V}\eta_t\left(1 - \frac{d\epsilon}{d\alpha}\right) \tag{57}$$

All the terms in the above Equations are known either directly or by derivations. The wing and the tail lift curve slopes are similar and can be obtained from **Eqn. (59)**. The contributions of the horizontal tail surface to the airplane stability are seriously affected by the downwash from the wing due to wing vortex system and thus it was necessary to evaluate the value. The change in downwash with respect to angle of attack ($d\varepsilon/d\alpha$) is obtained from the following Eqn.:

$$\frac{d\epsilon}{d\alpha} = \frac{114.6}{\pi A}a_w \tag{58}$$

$$a_w = \frac{a_0}{1 + \frac{57.3ra_0}{\pi A}} \tag{59}$$

$a_0 = 0.1096$ is the section lift curve slope for a 2D wing which is used here as the first estimate. Obtaining the value of a_w gives $d\varepsilon/d\alpha$. Tail volume coefficient ($\bar{V}$) is obtained from **Eqn. (60)**, which is a function of the horizontal tail area. For a preliminary estimate, the efficiency of the horizontal tail has been assumed to be: $\eta_{ht} = 1$. Putting the exact values in **Eqn. (57)** the tail contribution is calculated.

$$\frac{S_t}{S}\frac{l_t}{c} = \bar{V} \tag{60}$$

The contribution of the fuselage and nacelles to the static longitudinal stability of the airplane are always destabilizing and are large in magnitude. The theory accounting for the effects of the fuselage and nacelle on the airplane stability is really complex and doesn't fit into the criteria of the preliminary estimation. An easier but less accurate method is thus used which is given in the following Eqn.:

$$\left(\frac{dC_m}{dC_L}\right)_{\substack{Fus \\ or\ Nac}} = \frac{K_f w_f^2 L_f}{S_w c a_w} \tag{61}$$

The empirical factor (K_f) is developed from experimental evidence and is read form the graph. All other values in **Eqn. (55)** are obtained already and are described in the nomenclature section. The position of the quarter chord in percent body length is obtained from the preliminary CAD models. For normal fuselage arrangement, this method is fairly accurate, but for abnormal fuselage or nacelle arrangements, the method is not accurate and alternate methods should be used. However, this method is accurate enough for a preliminary estimate. Knowing the fuselage effect on the aircraft stability the stick fixed neutral point is calculated from **Eqn. (57)**.

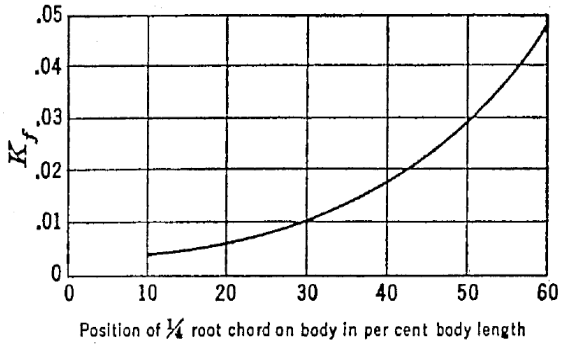

Figure 2 - 10 Fuselage Stability Coefficients[8]

Neutral point (Stick fixed, propeller wind milling): In the previous discussion power effects were not taken into account while calculating the neutral point of the aircraft. If propellers are attached the stability contribution due to propeller is also added to the initial stability Eqn.. The contribution of the running propeller to the aircraft's equilibrium can be broken down into two main effects. The first of these is the direct propeller contribution, due to forces created by the propeller itself. The second includes indirect effects which arise from the slipstream of the propeller and its interaction with the wing and the tail. The stability contribution of these direct propeller forces is given below:

$$\frac{dC_{mp}}{dC_L} = \frac{dT_c}{dC_L}\frac{2D^2}{S_w}\frac{h}{c}N + \frac{dC_{N_p}}{dC_L}\frac{l_p}{S_w}\frac{S_p}{c}N \tag{62}$$

At wind milling condition, the propellers are not producing any forward thrust. But the normal force contribution on static stability is considerably large even when the propellers are wind milling ($T_c = 0$). At windmilling condition, only two of the propeller contributions to stability remain. One of these is the direct contribution of the normal force, and the other is the effect of downwash from the propeller on the horizontal tail. The stability contribution of propeller normal force is given as:

$$\left(\frac{dC_m}{dC_L}\right)_{N_p} = \frac{\left(\frac{dC_N}{d\alpha}\right)_p \left(1 + \frac{d\epsilon}{d\alpha}\right) l_p S_p}{S_w c a_w} \tag{63}$$

The Eqn. is modified when ($T_c = 0$) and **Eqn. (64)** is obtained.

$$\left(\frac{dC_m}{dC_L}\right)_{N_{pTc=0}} = \frac{(dC_N/d\alpha)_{pT=0}(1 + d\epsilon/d\alpha) l_p S_p \, N}{S_w c a_w} \tag{64}$$

Where, $(dC_N/d\alpha)_{N_{P_{Tc=0}}} = .00165$, this number is obtained from the propeller data for two-bladed propeller tabulated in Ref. 2 only for a first estimate. The effect of the propeller downwash on the horizontal tail is obtained from the following Eqn.:

$$\left(\frac{dC_m}{dC_L}\right)_{\epsilon_{pT=0}} = \frac{a_t}{a_w} \frac{\bar{V}\eta_t}{.07} \left(\frac{dC_N}{d\alpha}\right)_{pT=0} \frac{d\beta}{d\alpha} \tag{65}$$

All the values in the above Eqn. are known except $d\beta/d\alpha$, which is obtained from **Fig. 2-11**. The desired propeller configuration for the economical light twin indicates that curve b should be used from **Fig. 2-11**. The necessary geometric values are approximated with a reasonable accuracy from the preliminary CAD model. Obtaining the value of $d\beta/d\alpha$ from **Fig. 2-11** made way for the calculation of the effect of the propeller downwash on the horizontal tail. The final static longitudinal Eqn. for the aircraft in flaps-up, gliding with propellers wind milling is expressed in **Eqn. (66)** and the stick fixed, propeller wind milling neutral point is given in **Eqn. (67)**.

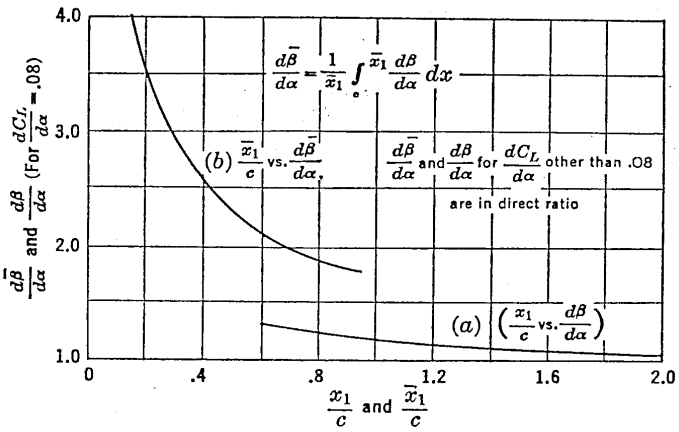

Figure 2 - 11 Chart for Computing Upwash[8]

$$\frac{dC_m}{dC_L} = \frac{x_a}{c} + \left(\frac{dC_m}{dC_L}\right)_{\substack{Fus \\ Nac}} - \frac{a_t}{a_w} \bar{V}\eta_t (1 - d\epsilon/d\alpha) + N \frac{(dC_N/d\alpha)_{pT=0} \, d\beta/d\alpha \, l_p S_p}{S_w c a_w} + \frac{a_t}{a_w} \frac{\bar{V}\eta_t}{.07} \left(\frac{dC_N}{d\alpha}\right)_{pT=0} \frac{d\beta}{d\alpha} \tag{66}$$

$$N_{0\text{Wind}} = x_{ac} - \left(\frac{dC_m}{dC_L}\right)_{\substack{Fus \\ Nac}} + \frac{a_t}{a_w} \bar{V}\eta_t \left(1 - \frac{d\epsilon}{d\alpha}\right) - N \frac{(dC_N/d\alpha)_{pT=0} \, d\beta/d\alpha \, l_p S_p}{S_w c a_w} - \frac{a_t}{a_w} \frac{\bar{V}\eta_t}{.07} \frac{d\beta}{d\alpha} \left(\frac{dC_N}{d\alpha}\right)_{pT=0} \tag{67}$$

Comparing **Equations (57)** and **(67)** it is observed that the second Eqn. has everything of the first Eqn. with two subtracted values which puts the windmilling neutral point in front of the stick fixed neutral point and serves as another constraint on the *cg* movement of the aircraft.

Neutral point (Stick fixed, critical power on flight): When the propellers are producing thrust, the neutral point shifts even forward from the wind milling neutral point. The value has been fixed from empirically determined table and serves as a good first estimate. The shift is $\Delta N_0 = -.08$ for a twin-engine cargo aircraft.

Forward *cg* limit: Just as the neutral point serve as the aft most *cg* limit of an aircraft, there is also a forward *cg* limit which restricts the forward movement of the *cg* The most forward permissible *cg* limit comes from the elevator theory: the elevator must always be capable of bringing the aircraft into equilibrium at the maximum lift coefficient attainable by the airplane. As the *cg* moves forward, the airplane becomes more stable and more up elevator is required to trim out the C_{Lmax}. Ultimately there exists a point at which the elevator will be just powerful enough to attain equilibrium at the maximum lift coefficient. If the airplane is flown when balanced at any *cg* ahead of this, maximum lift will not be obtained with full up elevator. This ultimate point is the forward most location of the *cg* given by the following Eqn.:

$$\left(\frac{dC_m}{dC_L}\right)_{\max} = (\delta_{e_0} - \delta_{e_{\max}}) \frac{C_{m\delta}}{C_{L_{\max}}} \tag{68}$$

The above Eqn. gives the critical forward *cg* for propeller wind milling because the airplane is usually more stable at wind milling than at high power. **Eqn. (68)** indicates how far the forward c.g can be moved from the aft wind milling neutral point.

Forward c.g. limit with ground effects: From the above discussion it is seen that the magnitude of the elevator control power limits the amount of static longitudinal stability allowable and thereby limits the forward c.g. position. This development was carried out under the assumption that the airplane was being flown at a high altitude to be free from the confining effects of the ground. Presence of ground has a large effect on the equilibrium and stability because of the effects of the ground on the induced flow field from the wing. The major effect of the ground is to reduce the downwash of the tail. Thereby increasing the tail angle of attack positively, requiring more up elevator to maintain equilibrium at the same lift coefficient. The reduction in downwash also increases the slope of the wing and tail lift curves. As the limitation on the airplane's forward c.g. is the requirement that gull up elevator will just trim out at C_{Lmax}, it is apparent from this discussion that the critical condition on elevator will be to trim out C_{Lmax} in presence of ground. This requirement would put a more severe constraint on the forward c.g limit. A very approximate method for allowing for the effects of the ground on the elevator angle require to trim out C_{Lmax} is to assume that all the effects can be approximated by assuming that downwash at the tail with ground effect is just half of that in free flight. Under these assumptions the change in elevator angle due to ground effect becomes simply:

$$\Delta\delta_{eg} = \frac{\Delta\varepsilon}{\tau} \tag{69}$$

$$\text{Where, } \Delta\varepsilon = -\frac{C_L}{\pi AR} \times 57.3 \tag{70}$$

Giving,

$$\Delta\delta_{eg} = -\frac{C_L}{\pi AR\tau} \times 57.3 \tag{71}$$

Plugging in the numbers gave a value of $\Delta N'_{0,forward} = .14246$. This means that the forward c.g. location would move aft 14.246% of the wing chord from the forward c.g. location.

Neutral point (Stick Free): One way the pilot feels the static longitudinal stability of the airplane is through the variation of the elevator angle and, thereby, the control position, with change in air speed. This variation is a function of the stability criterion, and was referred to as the stick fixed static longitudinal stability. Another way the pilot feels the static longitudinal stability is through the stick force required to change the speed of the airplane from a given trim condition. The magnitude of the stick force required to change the speed from any given trim condition cannot be related directly to the stability criterion with fixed elevators developed previously, but can be shown to be closely related to a new criterion with control left free to float with the wind. This type of longitudinal stability is commonly referred to as the stick free stability. It is observed that the stick free conditions impose on a heavier restriction on the usable range of the c.g. which will be apparent later at the end. The equation of static longitudinal stability, stick free, props off can be written as:

$$\left(\frac{dC_m}{dC_L}\right)_{\text{Free}} = \frac{x_a}{c} + \left(\frac{dC_m}{dC_L}\right)_{\substack{Fus\\Nac}} - \frac{a_t}{a_w}\bar{V}\eta_t\left(1-\frac{d\epsilon}{d\alpha}\right)\left(1-\frac{C_{h_\alpha}}{C_{h_\delta}}\tau\right) \tag{72}$$

Similarly the stick free stability for props windmilling is given as:

$$\left(\frac{dC_m}{dC_L}\right)_{\text{Free}} = \frac{x_a}{c} + \left(\frac{dC_m}{dC_L}\right)_{\substack{Fus\\Nac}} - \frac{a_t}{a_w}\bar{V}\eta_t\left(1-\frac{d\epsilon}{d\alpha}\right)\left(1-\frac{C_{h_\alpha}}{C_{h_\delta}}\tau\right) + \frac{N(dC_N/d\alpha)_{pT=0}\,(d\beta/d\alpha)l_p S_p}{S_w c a_w} + \frac{a_t}{a_w}\frac{\bar{V}\eta_t}{.07}\left(\frac{d\beta}{d\alpha}\right)\left(\frac{dC_N}{d\alpha}\right)_{pT=0} \tag{73}$$

Comparing **Eqns. (72) and (73)** with **Eqns. (55) and (66)** it is seen that the effect of freeing the elevator enters the tail term as the multiplying factor $\left(1-\tau\frac{C_{h\alpha}}{C_{h\delta}}\right)$. For an aiplane equipped with an elevator having no change in the hinge moment with angle of attack ($C_{h\alpha}=0$) **Eqns. (72) and (73)** becomes exactly like **Eqns. (55) and (66)** respectively. The stick free neutral point for the propeller off condition can be obtained from **Eqn. (72) as:**

$$N_0{}' = x_{ac} - \left(\frac{dC_m}{dC_L}\right)_{\substack{Fus\\Nac}} + \frac{a_t}{a_w}\bar{V}\eta_t\left(1-\frac{d\epsilon}{d\alpha}\right)\left(1-\frac{C_{h_\alpha}}{C_{h_\delta}}\tau\right) \tag{74}$$

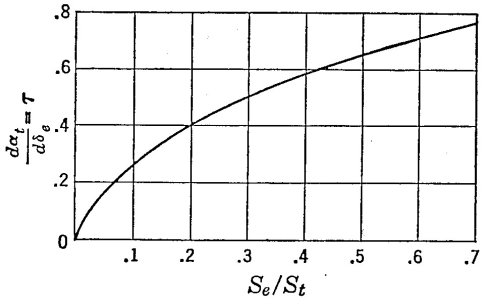

Figure 2 - 12 Elevator Effectiveness[8]

The elevator effectiveness term, τ, is obtained from **Fig. 2-12**. The hinge moment parameters are actually three-dimensional hinge moment parameters related to the two dimensional hinge moment parameters by lifting line theory as:

$C_{h\alpha} = c_{h\alpha}\frac{a}{a_0}$ and $C_{h\delta} = c_{h\delta} + \tau(C_{h\alpha} - c_{h\alpha})$.

The horizontal tail airfoil was chosen to be NACA-0012 which is geometrically similar to NACA-0009. So as a first estimate, the two dimensional hinge moment coefficients ($c_{h\delta}, c_{h\alpha}$) were estimated from the NACA-0009 hinge moment parameter data as described in **Fig. 2-13**.

Combining the results obtained from the above segments a graph is plotted with different c.g. locations. The graph is portrayed in **Fig. 2-14**. As seen from the Fig., the stick fixed neutral point is at 42% of the m.a.c. and is the aft most

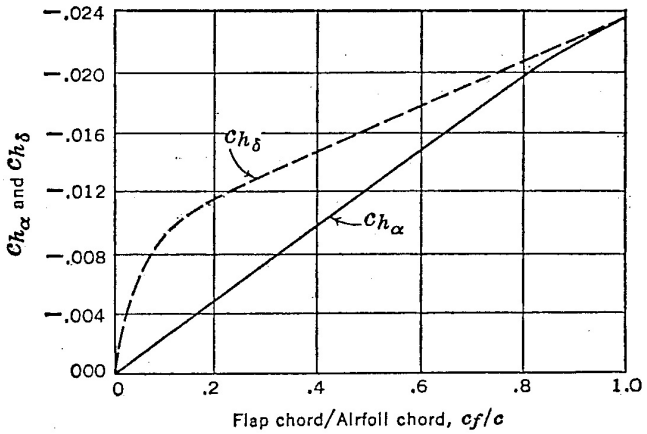

Figure 2 - 13 Section Hinge Moment Parameter for NACA-0009 Airfoil

c.g. location of the aircraft. The wind milling neutral point is slightly less that the stick fixed neutral point because of the presence of negative terms in the Eqn. it is at about 33% of the m.a.c. The critical power on flight neutral point is at 41% of the m.a.c and the most forward c.g. limit is at 11% of the m.a.c. The stick free neutral point for a windmilling flight is at 35%. The forwad c.g. limit with ground effect is at 19%. So the usable c.g. range with 10% static margin is 19 – 25% for all flight conditions.

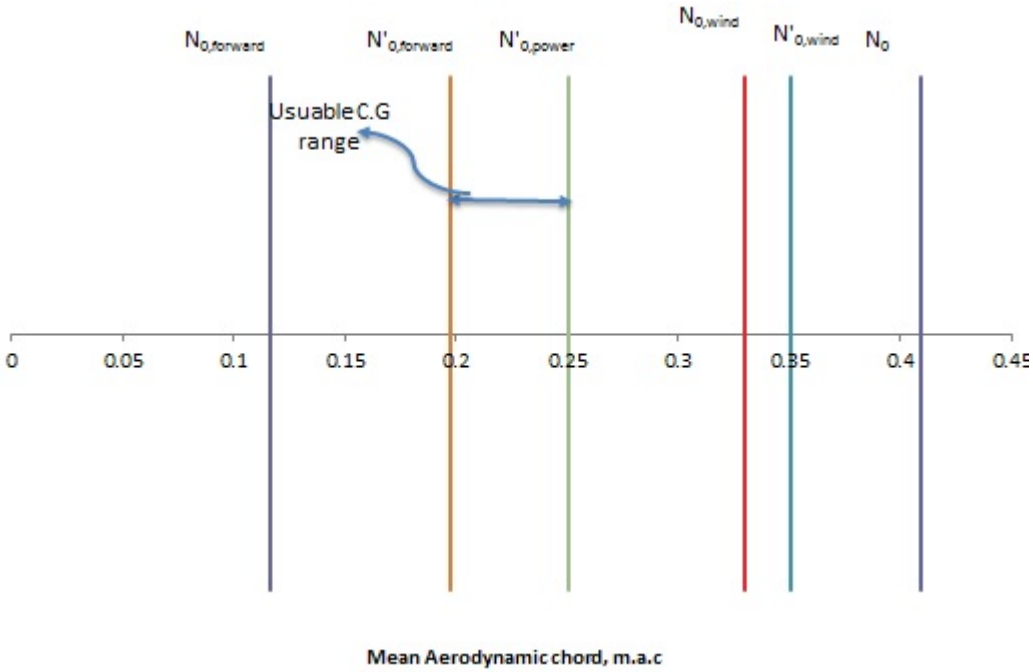

Figure 2 - 14 C.G. Locations of the Aircraft

Weights/Weight Components and Center of Gravity

In order to get a rough estimate of weight components, weight data from Roskam Volume II were average by using none dimensional data for different type of aircraft as well as dimensional data as seen in **Table A6** (in

appendix). This data was needed to compare values with historical data as well as determining the center of gravity of the I.A.D 4350 aircraft. To calculate the center of gravity the weight of the aircraft was needed to be refined.

Moreover, the Fundamentals of Aircraft and Airship Design Volume I from Leland M. Nicolai and Grant E. Carichner were used to determine the refined weights. For the main wing Eqn. 20.69 from Fundamentals of Aircraft and Airship Design Volume 1 was used to calculate the weight of the main wing as seen in **Eqn. (69)**. Where the takeoff weight was in pounds, ultimate load factor (1.5 x limit load factor), where AR is the main wing aspect ratio, ignoring wing quarter chord sweep since sweep has not been decided for the preliminary design, wing area in square feet, wing taper ratio, maximum wing thickness ratio taken as 0.12, and velocity as 140 knots which gave a main wing weight about 365.8 lb.

Wing,

$$\mathrm{Wt} = 96.948\left[\left(\frac{W_{\mathrm{TO}}\,N}{10^5}\right)^{0.65}\left(\frac{\mathrm{AR}}{\cos\Lambda_{1/4}}\right)^{0.57}\left(\frac{S_w}{100}\right)^{0.61}\left(\frac{1+\lambda}{2t/c}\right)^{0.36}\left(1+\frac{V_e}{500}\right)^{0.5}\right]^{0.993} \quad (20.69) \tag{69}$$

Furthermore, the horizontal tail was also calculated using **Eqn. (70)** by using the horizontal tail area, distance form wing one-fourth mac to tail one fourth mac, horizontal tail span in feet, and horizontal tail maximum thickness in inches that gave a horizontal weight of 62.13 lb.

Horizontal Tail,

$$\mathrm{Wt} = 127\left[\left(\frac{W_{\mathrm{TO}}\,N}{10^5}\right)^{0.87}\left(\frac{S_H}{100}\right)^{1.2}\left(\frac{\ell_T}{10}\right)^{0.483}\left(\frac{b_H}{t_{\mathrm{HR}}}\right)^{0.5}\right]^{0.458} \tag{70}$$

Moreover the vertical tail weight was also calculated by using the vertical tail area in square feet, vertical tail span in feet, and critical tail maximum root thickness in inches as seen in **Eqn. (71)** and given a value of 5. 7

Vertical Tail,

$$\mathrm{Wt} = 98.5\left[\left(\frac{W_{\mathrm{TO}}\,N}{10^5}\right)^{0.87}\left(\frac{S_V}{100}\right)^{1.2}\left(\frac{b_V}{t_{\mathrm{VR}}}\right)^{0.5}\right] \tag{71}$$

To continue, the gear weight was also calculated to be 208.5 lb. with **Eqn. (72)** by using the length of main landing gear strut in inches, landing weight that is weight takeoff minus 60% fuel, and ultimate loading factor at landing weight.

Landing Gear,

$$\mathrm{Wt} = 0.054\left(L_{\mathrm{LG}}\right)^{0.501}\left(W_{\mathrm{LAND}}N_{\mathrm{LAND}}\right)^{0.684} \tag{72}$$

Also, the propulsion-refined weight was estimated to be 653.01 lb. with **Eqn. (73)** by using bare engine weight and number of engines.

Propulsion,

$$\mathrm{Wt} = 2.575\left(W_{\mathrm{ENG}}\right)^{0.922} N_E \tag{73}$$

The Fuel system was also taken into account and was calculated to be 75.35 lb. that included the total fuel in gallons, percentage of fuel tanks integrated at 100%, and number of separate fuel tanks 2 and can be seen in **Eqn. (74)**.

Fuel System,

$$\mathrm{Wt} = 2.49\left(F_G\right)^{0.6}\left(\frac{1}{1+\mathrm{Int}}\right)^{0.3}\left(N_T\right)^{0.2}\left(N_E\right)^{0.13} \tag{74}$$

The surface controls were calculated with **Eqn. (75) and (76)** using the takeoff weight and finding the controls for powered surface control systems and unpowered surface control systems that where calculated to be 275.33 lb.

Surface Controls,

$$\mathrm{Wt} = 1.08\left(W_{\mathrm{TO}}\right)^{0.7} \tag{75}$$

$$\mathrm{Wt} = 1.066\left(W_{\mathrm{TO}}\right)^{0.626} \tag{76}$$

The electrical system weight prediction relationship were expressed in terms of the total weight of the fuel system and the electronics system where the fuel system weight in pounds and the weight of installed electronics in pounds were taken to count as seen in **Eqn. (77)** and given a value of 121 lb.

Electrical System,

$$\mathrm{Wt} = 12.57\left(\frac{W_{\mathrm{FS}} + W_{\mathrm{TRON}}}{1000}\right)^{0.51} \tag{77}$$

Furnishings where also taken into account when refining the total weight of the aircraft. Where the number of crew seats and maximum dynamic pressure in pounds per square foot was taken to account as seen in **Eqn. (78)**. Furthermore, passenger seats were determined as well with weight allowance for miscellaneous furnishings to end at a total of 94.88 lb.

Furnishings,

$$\mathrm{Wt} = 34.5\left(N_{\mathrm{CR}}\right)\left(q\right)^{0.25} \tag{78}$$

Moreover, air conditioning and anti-icing estimated weights where also calculated by using **Eqn. (79)**. The number of passengers, number of crew, weight of installed electronics in pounds, and equivalent maximum Mach number at sea level were used to calculate the weight that gave 60.24 lb.

Air Conditioning and Anti-Icing,

$$\text{Wt} = 0.265\left(W_{\text{TO}}\right)^{0.52}\left(N_{\text{CR}} + N_{\text{PASS}}\right)^{0.68}\left(W_{\text{TRON}}\right)^{0.17}\left(M_E\right)^{0.08} \tag{79}$$

The electronics (avionics) were calculated using the bare avionics equipment weight (uninstalled) and using **Eqn. (80)**.

Electronics (Avionics),

$$W_{\text{TRON}} = 2.117\left(W_{\text{AU}}\right)^{0.933} \tag{80}$$

Finally, the fuselage was also calculated by taking the length of the fuselage in feet, the maximum width in feet, and the fuselage maximum depth in feet with **Eqn. (81)** and gave a value of 399.93 lb.

Fuselage,

$$\text{Wt} = 200\left[\left(\frac{W_{\text{TO}}\,N}{10^5}\right)^{0.286}\left(\frac{L}{10}\right)^{0.857}\left(\frac{W+D}{10}\right)\left(\frac{V_e}{100}\right)^{0.338}\right]^{1.1} \tag{81}$$

The fuel Weight was taken into account that was calculated to be 368.5 lb. and by adding all the weights it was determined that the takeoff weight of the I.A.D 4350 aircraft was 2766.31 lb.

To calculate the center of gravity for the entire aircraft a reference line was drawn in Error! Reference source not found. and the distance of each component with respect to the reference line was multiplied by its respected weight. All of the weights found in **Equations (69)** – **(81)** were multiplied with its respective distance to the reference line than added all together. After calculating the displacement in the x-axis and y-axis the total weight added was divided by the total weight of the aircraft that gave both the x-axis and y-axis coordinates for the center of gravity that can be seen in Error! Reference source not found. and **Eqn. (82)**.

$$cg \cdot W = df \cdot wf + de \cdot we + dp \cdot wp + \cdots \tag{82}$$

Landing Gear Sizing and Placement

Aircrafts have a variety of landing gear systems and the most common types used today are conventional, tricycle, and tandem. The conventional landing gear consists of two forward wheels by the aircraft center of gravity and a small third wheel on the tail. Furthermore, this design is easily pitch over if breaks are applied too soon and landing control becomes very difficult as well as takeoff. Moreover, tricycle landing gear has three wheels two main wheels and a nose wheel. The tricycle gear makes aircraft easier to handle on the ground, makes landing much safer, and decrease the chance for the aircraft to pitch forward. Finally, the tandem landing gear is used for very large aircraft and was not needed for the I.A.D 4350 design. These can be seen in **Fig. 2 - 13**. For the I.A.D 4350 it was decided to implement a tricycle landing arrangement.

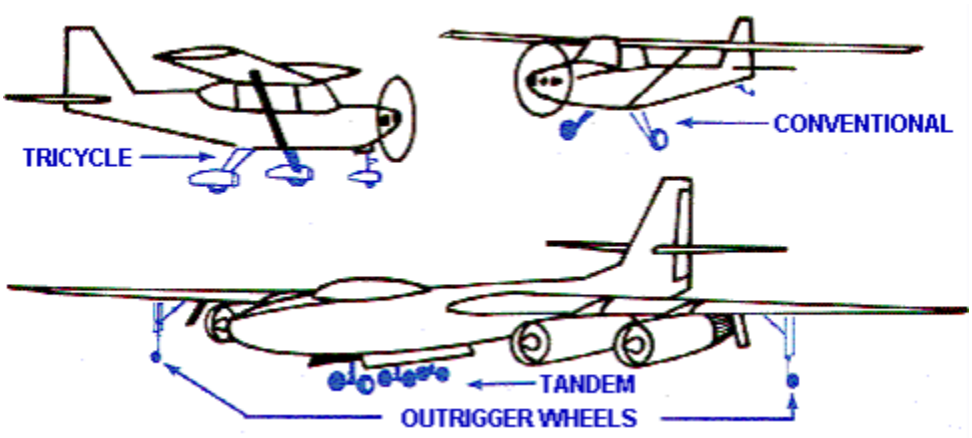

Figure 2 - 16 Landing Gear Arrangements[2]

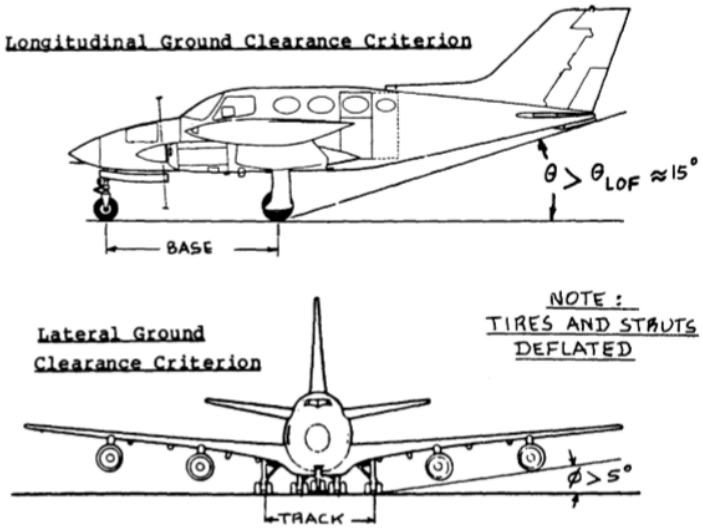

Figure 2 - 15 Longitudinal and Lateral Ground Clearance Criterion[2]

To continue the design process of the I.A.D 4350 aircraft the landing gear placement had to be calculated. There are two different criteria needing to be analyzed, the tip-over criteria, and the ground clearance criteria. Furthermore, for typical landing gear the aft most center of gravity is where the main landing gear must be placed. Also, the usual relationship between main gear and the most aft center of gravity for a tricycle gear is 15 degrees and can be seen in **Figure 2 - 9**. To prevent the aircraft from a tip-over scenario calculation of the tip-over angle where made in the top-view of the aircraft. Using the top-view scale drawing and creating two parallel lines between the center of gravity and the 15 degrees gear placement. Furthermore, a perpendicular line was drawn to connect both lines and the height from the ground to the center of gravity was also drawn to calculate the tip-over angel that was needed to be less than 55 degrees according to Dr. Roskam. The lateral and longitudinal ground clearance angles apply to tricycle gear. A 15-degree angle was needed from the ground to the edge of the tail for ground clearance. This can be illustrated in Fig. 14

To continue, at this stage of the preliminary design process retraction capability for the gears where consider for the I.A.D 4350 aircraft. It was determined to retract the front wheel forward and the two main wheels inward into the fuselage where a special compartment is going to be built. Retract gears where taken into account in the first place to reduce drag while the aircraft is at cruising altitude. Furthermore, this type of retract mechanism is illustrated in **Fig. 2-17** to clearly help understand the design.

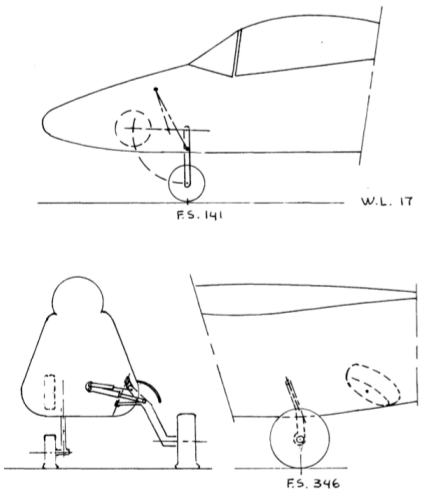

Figure 2 - 17 Landing Gear Retract Mechanism[2]

Primary Engine Choices

The engine choice first needs to come from the primary sizing requirements. Namely from a comparison between the wing loading and the power loading are needed to first find a required horsepower the engine needs to have. From that data and knowing that there are two engines the required horsepower from each engine is about 100 hp. Since propeller engines have been around since aircrafts have been flown, a new engine is not needed, as a number of engines that meet the 100 hp requirements are readily available to buy today. Knowing this the table below shows a number of aircraft that meet the requirements.

Table 2 - 5 Engine Choice

	Weight (lb)	HP	Cost	Fuel Consumption (gal/hr)	
Superior 100	*200*	*100*		*4.5*	*Experimental*
Rotax 912S	*168*	*100*	*18,000*	*7.26*	
Lycoming IO-233-LSA	*200*	*100*	*23000*	*5.25*	
Wilksch Airmotive Ltd. WAM-120	*220*	*120*	*23000*		

From these choices another requirement needs to be met that the engine is certified which rules out the superior 100 engine. And narrowing these choices even more the Rotax 912S engine has the least weight and cost for an increase in fuel consumption, while also having the more empirical performance data compared to the other engines

which is why this engine will be the primary focus for the engine performance calculations. From here and knowing the resources of the engine specification (Aero Propulsion Technologies, 2000) preliminary engine sizing can take place.

Engine Sizing

Engine data from the Rotax 912S is the most readily available with the engine CG already located, from this a MatLab code to find the overall CG with a propeller weight can be determined and is included in the Appendix.

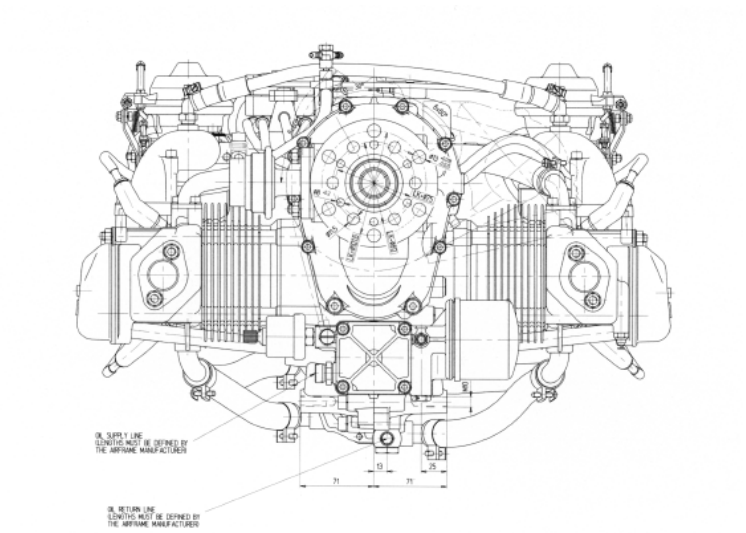

Figure 2 - 18 Rotax 912S Front View[11]

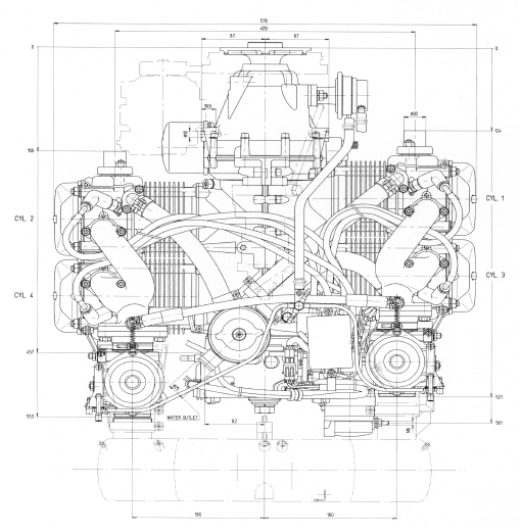

Figure 2 - 19 Rotax 912S Top View[11]

From there the CG data is transferred over to structures for overall aircraft CG calculations with a rough calculation being shown below.

Table 2 - 6 Engine CG Calculations

	ft	x,y,z (ft)
X CG	*0.905*	-
Y CG	*1*	-
Z CG	*0.843*	-
Engine Length	-	*1.84,1.88,1.29*

Propeller Sizing

For this part of the calculations a few assumptions must be made first. From a propeller database (Mt- Propeller, 2015) and knowing the max power is around 100 horsepower the propeller will have 2 blades. An average propeller for that configuration has a 6 ft. diameter. Today's propellers are normally carbon fiber, which would set the weight for that type at around 23.5 pounds. With an added hub of around 4.3 pounds that would make the total propeller weight at around 27.8 pounds, the culminated data shown below in the table.

Table 2 - 7 Propeller Sizing Data

	Number	Unit
Number of blades	2	
Propeller weight	23.5	lb.
Propeller weight with hub	27.8	lb.

With the Engine CG data and propeller CG data and using the MatLab code in the Appendix Codes shows the appropriate total CG for the engine. This total data is transferred over to the structures team to be used in calculations.

For a given propeller the engine horsepower produces too great of an rpm at 5800 rpm at max power. This would clearly cause a propeller stall, which would decrease the efficiency dramatically. This is solved by a transmission in the Rotax engine that decreases the engine rpm by a factor of 2.43 for a given engine horsepower.

Fuel Calculations

Now that the engine sizing has been acquired the fuel consumption and tank sizing can be found. The fuel consumption can be found empirically from the specifications from the Rotax engine data.

From this a MatLab code can be created to find the fuel consumption with engine rpm, which is included in the appendix.

From here tank sizing can be determined after a preliminary aircraft structure is created. The tank size is created from knowing what the fuel capacity of each engine from the leftover weight from the takeoff weight minus the empty weight plus the crew weight. With this and knowing the weight of the fuel is around 6 pounds per gallon around 25 gallons of fuel can be stored in each tank. With the aerodynamics team determining the airfoil size a fuel tank size can be calculated using the following MatLab code in the appendix.

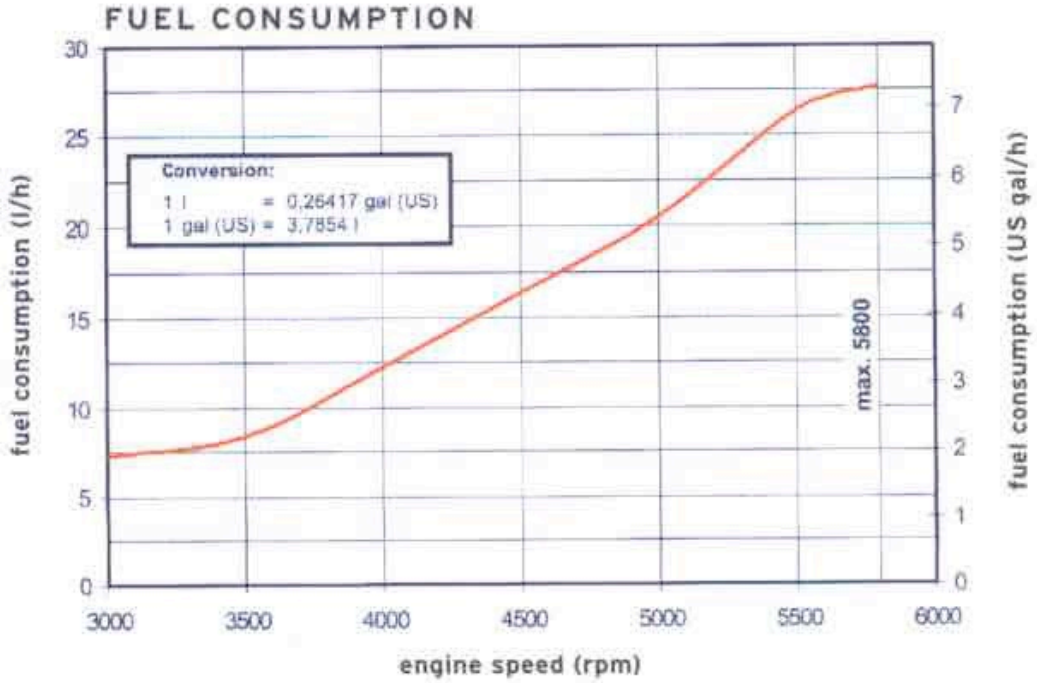

Figure 2 - 20 Fuel Consumption Empirical Data

From there and determining a high wing aircraft the fuel system can be determined to be a simple gravity feed into the engine with a pump to convert the fuel between tanks in case of an engine out condition, as shown in an example of this type of system

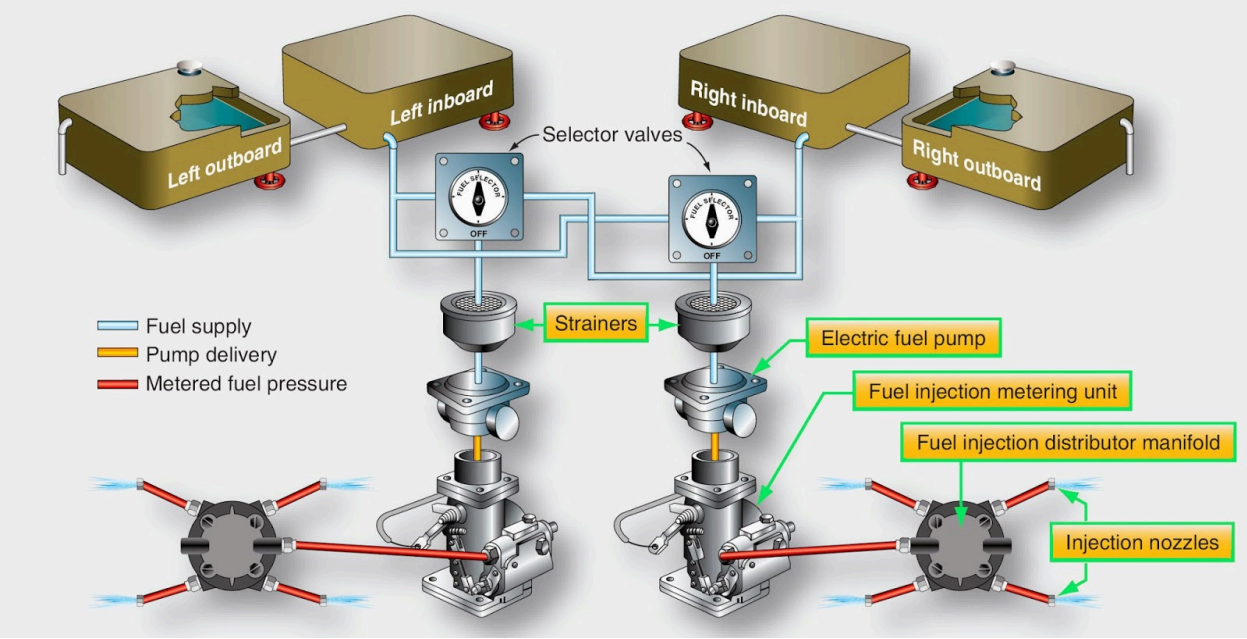

Figure 2 - 21 Fuel System Example

Now that a final weight has been determined estimate has been determined the final fuel weight limit can be calculated with it being 335 lbs. and knowing that the fuel used weighs about 6.3 lbs per gallon, the fuel limit can be determined as being 52.78 gal. with each fuel tank being able to hold a maximum of around 26 gal.

With the maximum fuel limit identified the fuel tank sizing can now be determined. Using a Matlab code based on the internal structure of the wing, it can be determined to be around 2.5 ft x .4 ft x 4.17 ft per fuel tank.

Flight Envelope

From the aircraft data, namely the efficiency factor, the zero lift coefficient of drag and the max coefficient of lift, a flight envelope for the given engine can be determined. This is determined with the following Eqn.. Reader is encouraged to reference **Eqn. (25)** in part 1 of this Report.

$$V = \sqrt{\frac{W}{.5*\rho*S*C_L}} \tag{83}$$

This is iterated to find the velocity at stall, minimum, and maximum to find the following table using the MatLab code shown in the appendix along with a graph that represents some given conditions.

Table 2 - 8 Flight Envelope Table

Altitude (ft)	Vstall (ft/s)	Vmin (ft/s)	Vmax (ft/s)
0	96.1567	66.0038	283.6879
1000	97.5835	68.0959	283.193
2000	99.0315	70.2633	282.6631
3000	100.5228	72.5434	282.0865
4000	102.0352	74.9069	281.4681
5000	103.5927	77.3966	280.7937
6000	105.1708	79.979	280.0691
7000	106.7956	82.7033	279.2768
8000	108.4691	85.5816	278.4082
9000	110.1628	88.5734	277.4709
10000	111.9066	91.7406	276.4399
11000	113.669	95.0365	275.3242
12000	115.4824	98.5339	274.092
13000	117.3486	102.2539	272.726
14000	119.2697	106.2215	271.2053
15000	121.2072	110.3784	269.5403

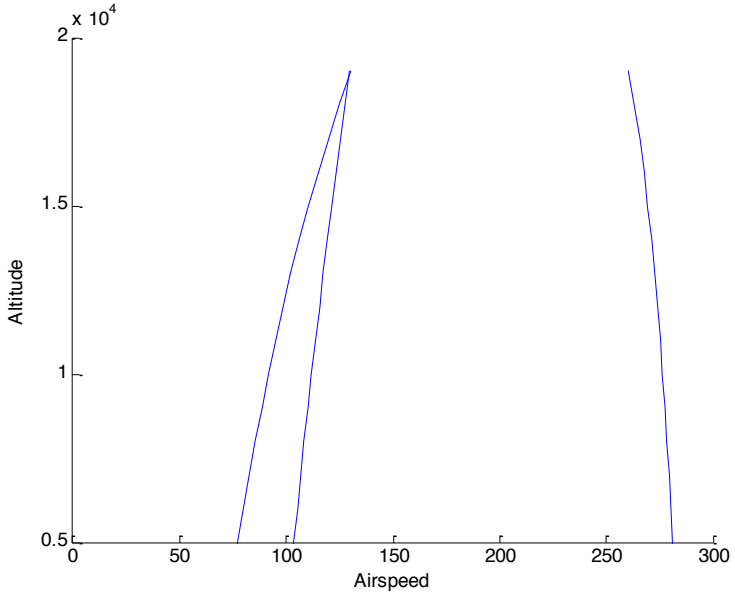

Figure 2 - 22 Flight Envelope at 60 kts.

This data is for one set condition and is subject to change as the mission changing and the code is open ended enough to meet every criteria.

Power Curves

Using the MatLab code in the appendix and the same conditions for the previous section, a power available and power required curve can be determined as altitude changes as shown below in the table and Figure.

Table 2 - 9 Thrust Available and Thrust Required Data at 60 kts.

Altitude	7500 ft				
Airspeed (ft/s)	Thrust (lb)	Drag (lb)	Airspeed (ft/s)	Thrust (lb)	Drag (lb)
40	429.3435	1505.756	180	429.3435	215.3079
50	429.3435	970.1203	190	429.3435	223.8575
60	429.3435	681.8229	200	429.3435	234.3884
70	429.3435	510.7655	210	429.3435	246.6945
80	429.3435	402.6045	220	429.3435	260.6155
90	429.3435	331.3785	230	429.3435	276.025
100	429.3435	283.4138	240	429.3435	292.8224
110	429.3435	250.9528	250	429.3435	310.927
120	429.3435	229.3283	260	429.3435	330.273
130	429.3435	215.5959	270	429.3435	350.8069
140	429.3435	207.8235	280	429.3435	372.4844
150	429.3435	204.7007	290	429.3435	395.2686
160	429.3435	205.3135	300	429.3435	419.1288
170	429.3435	209.0083			

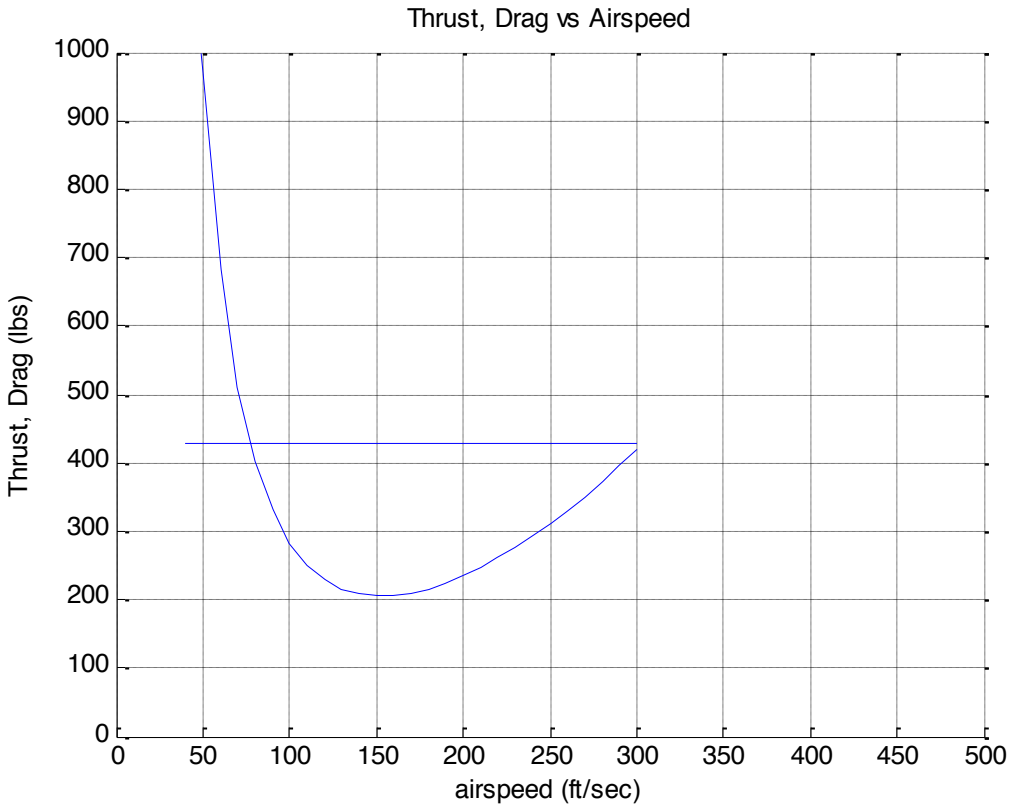

Figure 2 - 23 Thrust Required and Thrust Available Graphs Velocity at 60 kts.

This data has a series of graphs that show that power available decreases as altitude increases, as well as the curves changing for different mission criteria during the flight. Now these graphs and data are for a baseline engine setting that will change once more data has been compiled and should not be used as a final decision for the complete aircraft. The SFC can also be determined from the following Eqn..

$$SFC = \frac{\dot{m}_f}{P} \tag{84}$$

However this equation is does not take into account the propeller efficiency and will only be used as a baseline for a more integrated specific fuel consumption conclusion, which the SFC is the following for these three mission criteria.

Table 2 - 10 TSFC First Iteration

	fuel mass flow (lb/hr)	Power (HP)	SFC (lb/hp*hour)
Take-Off	45.27	100.6	.45
Climb	33.0174	90	.367
Cruise	22.54	75	.301

Propeller Blade Analysis

For the propeller blade it can be assumed that the propeller is a variable pitch propeller. This is due to the efficiency of the blades decrease in efficiency after a certain speed, which can be solved by a changing pitch during flight. This will cause the maximum propeller efficiency for a given drag. An Excel program has been developed that can calculate the thrust and power coefficient as well as the efficiency of the blade with respect to the advance ratio velocity over blade rps times blade diameter. Since the drag has not been calculated yet a set drag of 800 pounds has been chosen so the program will have an output as shown below.

Table 2 - 11 Blade Analysis Variable Pitch Settings

Altitude (ft)	7500							
Eng Pow %	75							
Graph Number	1	2	3	4	5	6	7	8
β	-1.733844515	4.965489	11.14689	17.74609	24.58444	31.55454	38.59371	45.69124
Velocity (knot)	0	20	40	60	80	100	120	140
Velocity (ft/s)	0	33.78	67.56	101.34	135.12	168.9	202.68	236.46
Drag (lb)	0	25.3778	101.511	228.4	406.045	634.446	913.602	1243.51
Cd0	0.026183514	0.026184	0.026184	0.026184	0.026184	0.026184	0.026184	0.026184
Cl	1.4	1.4	1.4	1.4	1.4	1.4	1.4	1.4
Cd	0.133568329	0.133568	0.133568	0.133568	0.133568	0.133568	0.133568	0.133568
Propeller Diameter (ft)	6	6	6	6	6	6	6	6

For the chosen variable pitch for each speed graphs for the thrust and power coefficients and efficiency can be found. But first a few conditions must be known, namely the twist data fit, the chord distance data, and the airfoil cl vs. cd data and the atmospheric data. These equations are listed below starting with the twist data fit.

$$\beta_T = 24.351 * (\frac{r}{R})^2 - 79.054 * \frac{r}{R} + 65.043 \tag{85}$$

The next Eqn. is the Cl vs. Cd fit

$$C_L = 6.27 * 10^{-3} * (C_D)^4 - 6.39 * 10^{-3} * (C_D)^3 + 5.85 * 10^{-3} * (C_D)^2 + 1.58 * 10^{-4} * C_D + 1.499 * 10^{-2} \tag{86}$$

The propeller chord distribution can be found a similar way empirically from the following Fig..

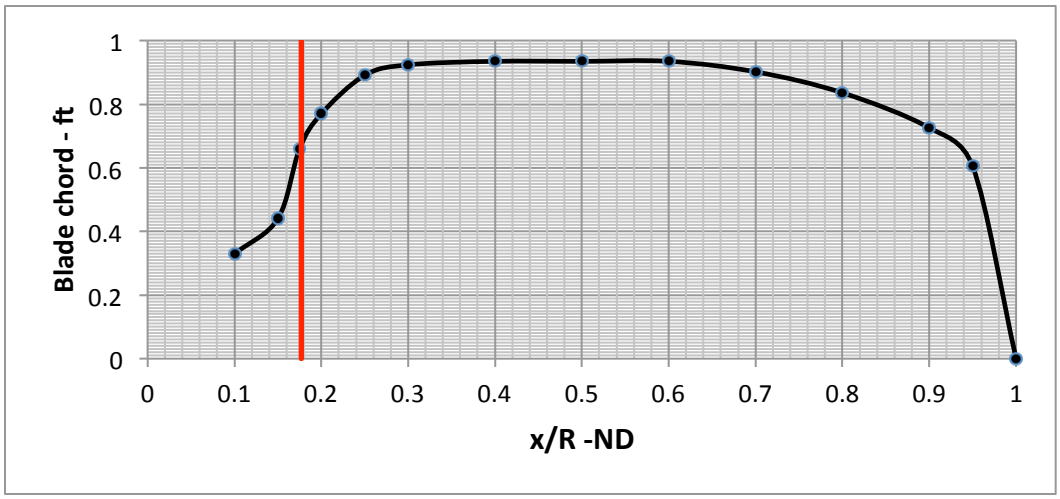

Figure 2 - 24 Chord Distribution

From this the propeller analysis equations can be used to find the total C_T, C_Q, C_P, and η_P which is found by integrating each part of the propeller. This first Eqn. is an addition to the twist with the variable pitch.

$$\beta = \beta_T + \beta_P \tag{87}$$

The next Eqn. is for the solidity of the propeller.

$$\sigma_r = \frac{(number\ of\ blades)*c}{\pi*(\frac{D}{2})} \tag{89}$$

For the next equations some constants must be established.

Table 2 - 12 Propeller Blade Constants

M_{dd}	.77
a_0	5.73

The next Equations are for an adjustment caused by a change in the compressibility of the air

$$M_{hell} = \frac{\sqrt{(\Omega*R*x)^2+V^2}}{a} \tag{90}$$

$$\frac{M_{hell}}{M_{dd}} = \frac{M_{hell}}{M_{dd}} \tag{91}$$

The next Equations are for geometry calculations for the propeller blades

$$\Phi = \tan^{-1}\frac{V}{\Omega*R*x} \tag{92}$$

$$\theta = \frac{\beta-\Phi}{1+\left(\frac{8*x*\sin\Phi)}{\sigma_r*a_0}\right)} \tag{93}$$

$$\Phi_0 = \Phi + \theta \tag{94}$$

$$\Phi_0 = \Phi + \theta \tag{95}$$

$$\alpha_0 = \beta - \Phi_0 \tag{96}$$

These Equations are used to find C_{l0}, λ_T, and λ_q.

$$C_{l0} = \alpha_0 * a_0 \tag{97}$$

$$\lambda_t = \left(\frac{\cos^2\theta}{\cos^2\Phi}\right) * (C_l \cos\Phi_0 - C_d \sin\Phi_0) \tag{98}$$

$$\lambda_q = \left(\frac{\cos^2\theta}{\cos^2\Phi}\right) * (C_l \cos\Phi_0 + C_d \sin\Phi_0) \tag{99}$$

And to find the derivative of C_t and C_q

$$\frac{dC_t}{dx} = 3.88 * x^2 * \sigma_r * \lambda_t \tag{100}$$

$$\frac{dC_q}{dx} = 1.94 * x^3 * \sigma_r * \lambda_q \tag{101}$$

Finally from this J, C_T, C_Q, C_P, η_{prop} Equations can be found

$$J = \frac{V}{n*D} \tag{102}$$

$$C_T = \sum_0^1 \frac{dC_t}{dx} \tag{103}$$

$$C_Q = \sum_0^1 \frac{dC_q}{dx} \tag{104}$$

$$C_P = 2 * \pi * C_q \tag{105}$$

$$\eta_p = \left(\frac{C_T}{C_P}\right) * J \tag{106}$$

All these Equations together and using a variable prop system the following graphs can be determined with each curve being equal to a varying pitch angle from the table beforehand.[10] (MIT, 2016)

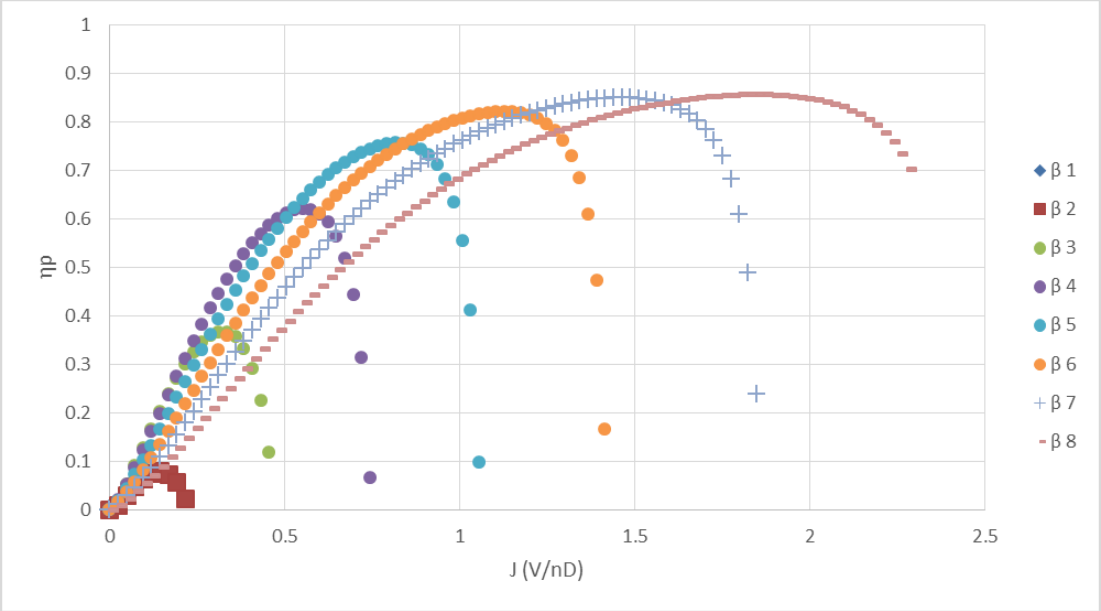

Figure 2 - 25 Propeller Efficiency vs. J

From this data the propeller efficiency for variable pitch prop is around .8-.85 for a pitch rate of above 20 degrees, as well as determine a curve fit graph for the efficiency taking into consideration that the pitch angle will change automatically to maintain a constant rpm.

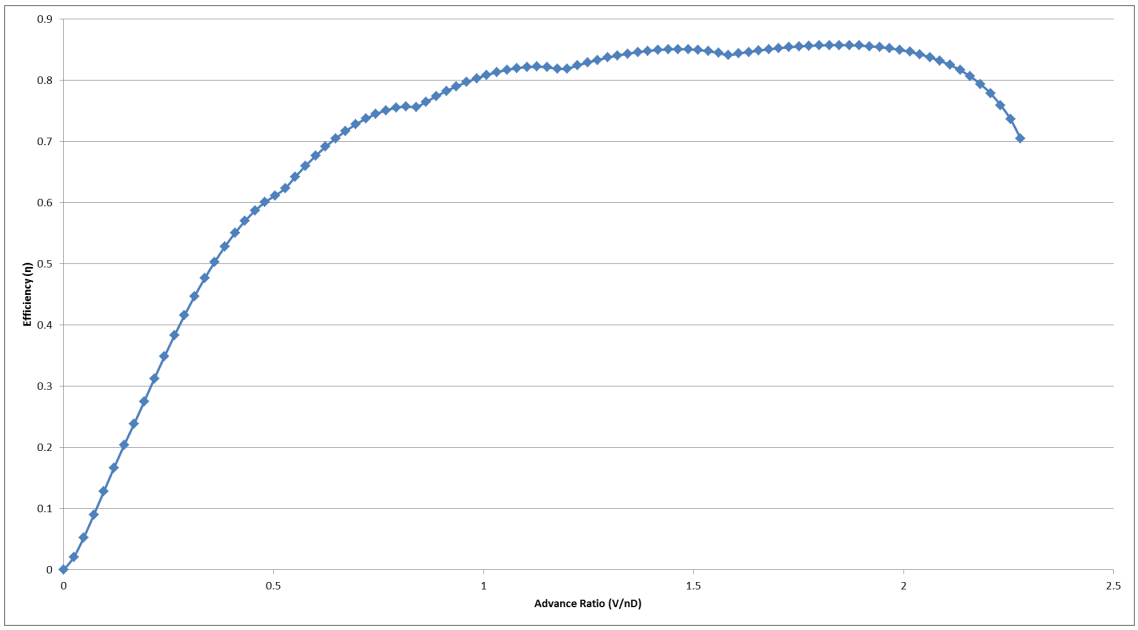

Figure 2 - 26 Propeller Efficiency vs. J Curve Fit

And this data is based on the coefficient of thrust and power as shown below.

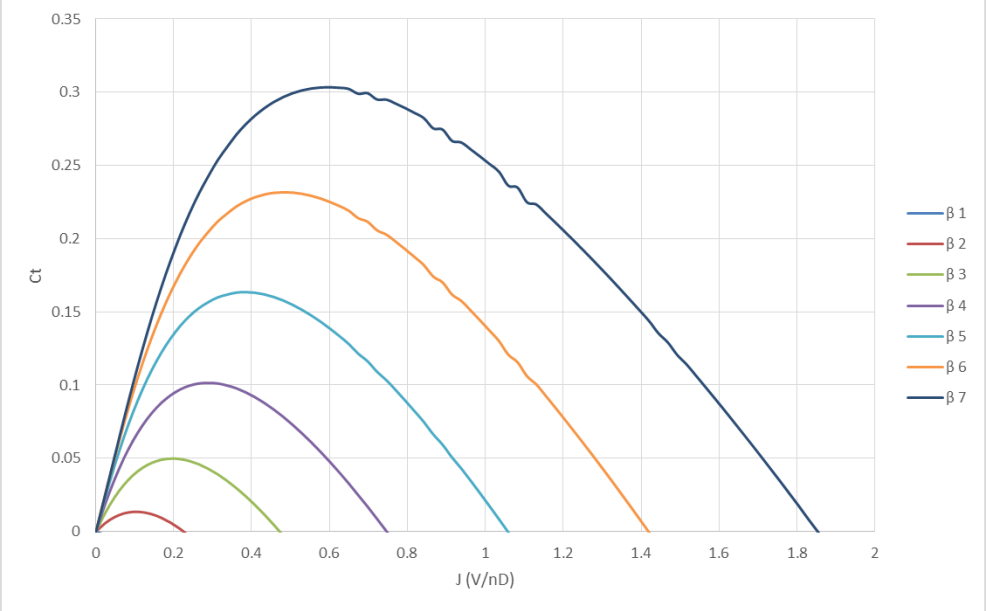

Figure 2 - 27 Thrust Coefficients vs. J

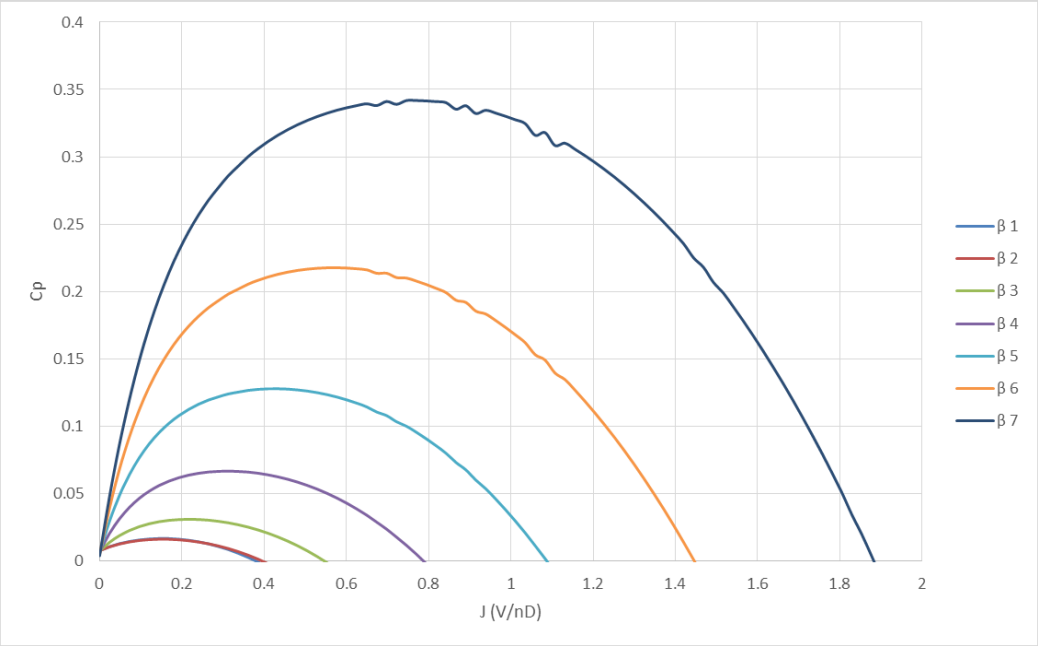

Figure 2 - 28 Power Coefficients vs. J

With these graphs the Equations for the forces can be found and are shown below. [10] (MIT, 2016)

$$Thrust = Drag \tag{107}$$

$$Torque = C_q * \left(\frac{RPM_{prop}}{60}\right)^2 * D^5 * \rho \tag{108}$$

$$Power = Torque * \frac{2*\pi*RPM_{prop}}{60} \tag{109}$$

$$bhp = \frac{Power}{550} \tag{110}$$

$$thp = bhp * \eta_p \tag{111}$$

$$P_{req} = .5 * \rho * V^3 * S * C_{D_0} + \left(\frac{W^2}{.5*\rho*V*S}\right)\left(\frac{1}{\pi*e*AR}\right) \tag{112}$$

As it can be seen an increase in speed will cause the propeller efficiency to go up, peak and then go down, however with a variable pitch propeller that maximum efficiency can be maintained throughout different speeds. While for the thrust and power coefficients as speed increases the coefficients decrease, however an increase in pitch cause a shift to increase the speed required for the decrease to happen.

With Equations 106-110, a power required vs. power available curve could be found with varying pitch angle, as shown below.

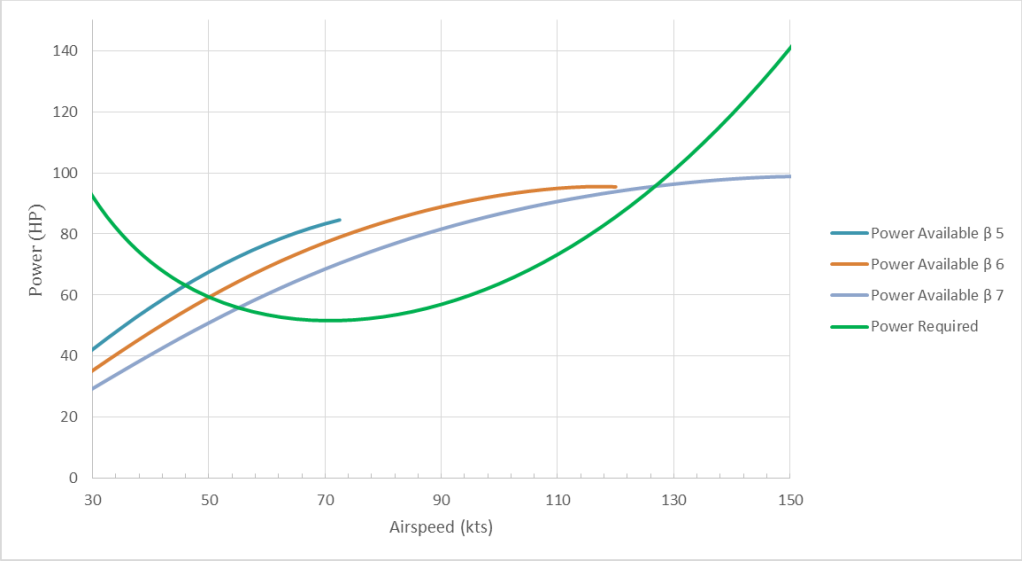

Figure 2 - 29 Power vs. Velocity

With a pitch angle to coincide with the drag at above stall speed being above the power required as shown below.

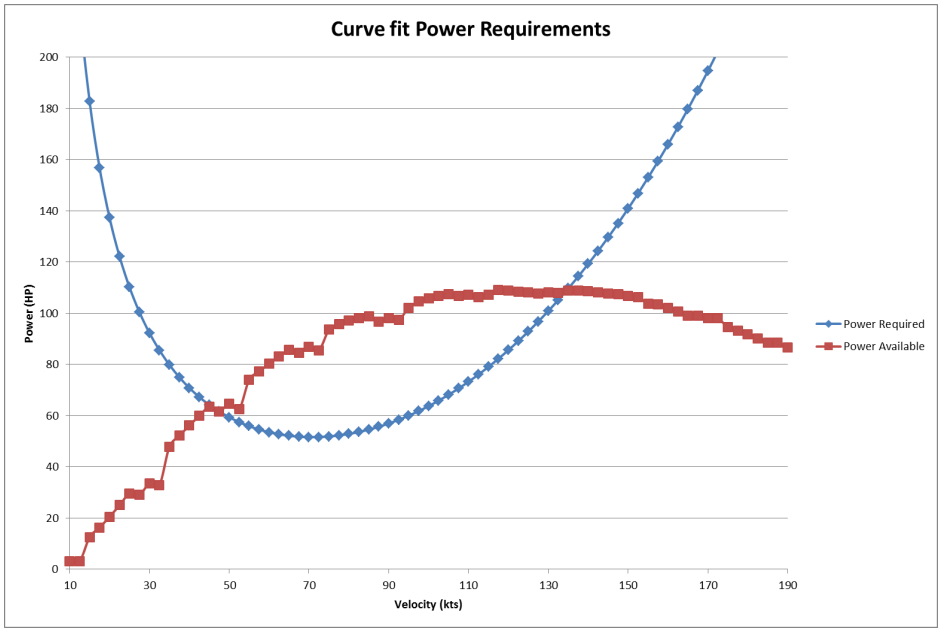

Figure 2 - 30 Power Available Variable Pitch 60 kts. vs. Power Required

This graph shows that for the best excess power as airspeed increases the pitch should increase with it. This is taking into account a set of variables shown below in the table, as well as having a higher power than the requires

Table 2 - 13 Power Required and Available Constants

Variable	Number	Unit
S	175.5	ft^2
Weight	2700	lb
CD0	0.02	
e	0.83	
AR	7	

Now finally in this section, know knowing the thrust horsepower and knowing it is a function of the efficiency and brake horsepower, and finally having the empirical data for the fuel consumption, a graph can be made up showing how brake specific fuel consumption changes with respect to the brake horse power.

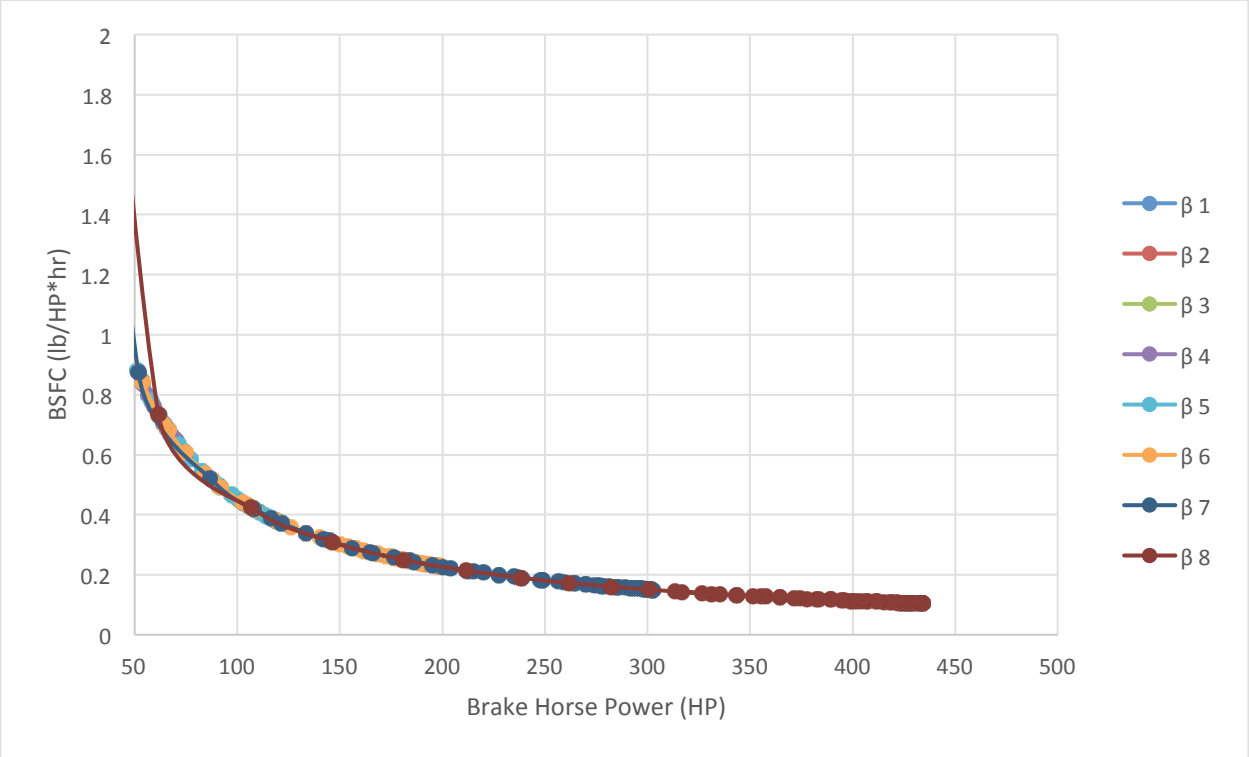

Figure 2 - 31 Brake Specific Horsepower @ Max Engine HP

From this figure, it can be seen that the higher the pitch angle is results in a higher brake horse power which in turn results in a much more efficient BSFC than at low speeds, however since this is related directly to the fuel consumption, while a higher engine speed will get better efficiency, doing that will ultimately increase the fuel consumption and decrease the efficiency of this value.

It should be known that these values are subject to change as the other teams provide more exact constants that are needed for the next iteration of the code

This data can be changed to fit to another variable like the rpm due to the fact that there are techniques to increase the horsepower while keeping the rpm intact, and the following figures show the brake specific fuel consumption, as well as the brake engine horsepower with respect to rpm.

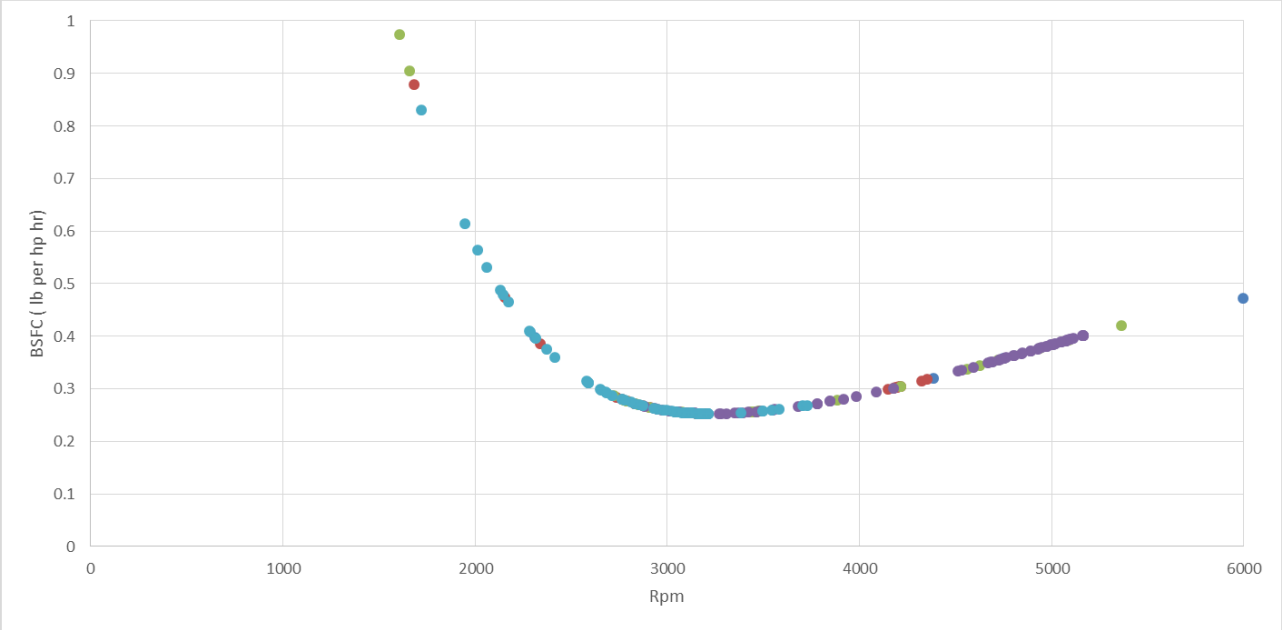

Figure 2 - 32 Break Specific Horsepower vs. Engine RPM

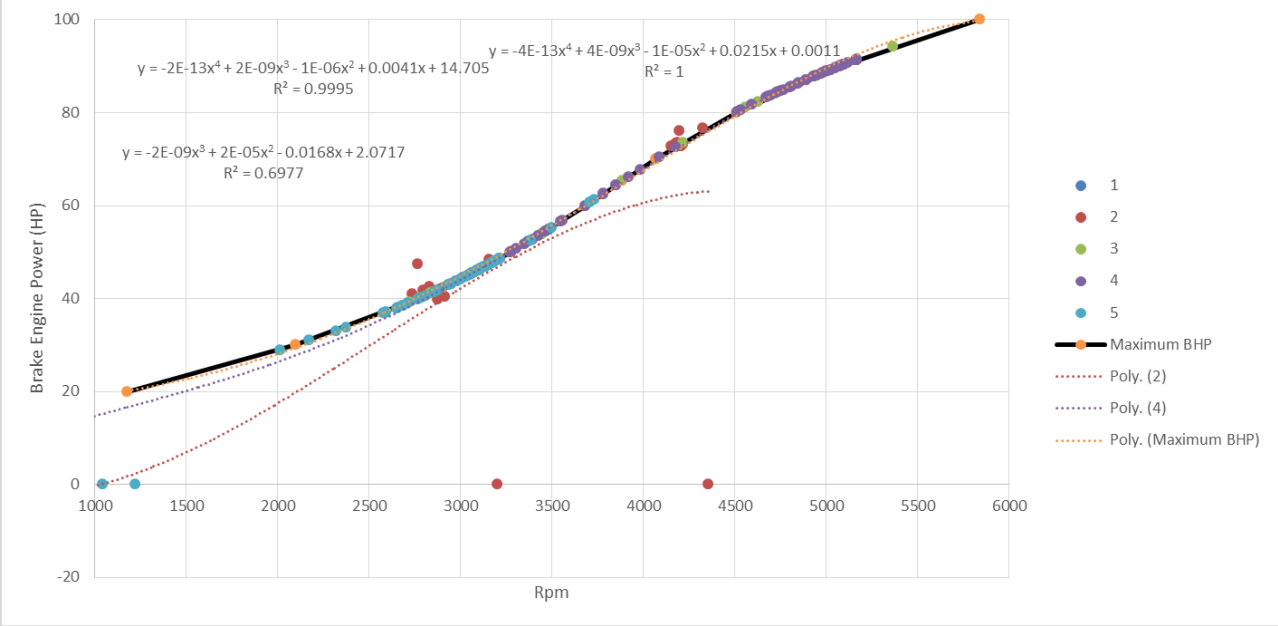

Figure 2 - 33 Break Engine Power vs. Engine RPM

Integration Analysis

Now that codes have been created to analysis the engine and propeller at a certain point, the next step is to iteration the codes through the entire mission profile to ensure that the selected configuration will work through the entire profile. Once that is completed if the configuration does not work at all mission points then the next step would be to go back and change certain aspects of the configuration and iterate again until a suitable configuration is found. Finally after that, once an engine configuration can be used at any mission profile to improve and narrow down the best possible way to use the engine to achieve the greatest results with the least amount of cost.

Final Fuel Tank Sizing

With the maximum fuel limit identified the fuel tank sizing can now be determined. Using a Matlab code based on the internal structure of the wing, it can be determined

Constraints

Now that all the values how been determined it can be clear to see that they do not meet the cruise velocity and speed required in the design condition, with the maximum velocity achievable at 75% power and 7500 ft altitude is 125 kts. So from here a new iteration must be done by changing the variables until the requirements can be met. This can be done in a view ways, first by lowering the weight to decrease the power required until a suitable weight can be determined. Second, by decreasing the drag coefficient to also decrease the power required. And finally, increasing the power of the engine by using a new engine to increase the power available or a new propeller geometry. However all these options have their own drawbacks with the options to lower the power required is almost impossible as the aircraft weight and drag have been lowered to their realistically minimum value and changing the engine will put a strain on the other groups as the engine would almost linearly increase in weight as the power went up and changing the propeller dimensions would change the placement of the engine to which both would throw off C.G. calculations for the other teams. So a new option has been determined, and that option is adding a supercharger to the engine to increase the power with minimal change with the rest of the system.

This fact can be shown with a constant power loading and the power increasing to achieve a cruise speed of 140kts at 7500 ft.

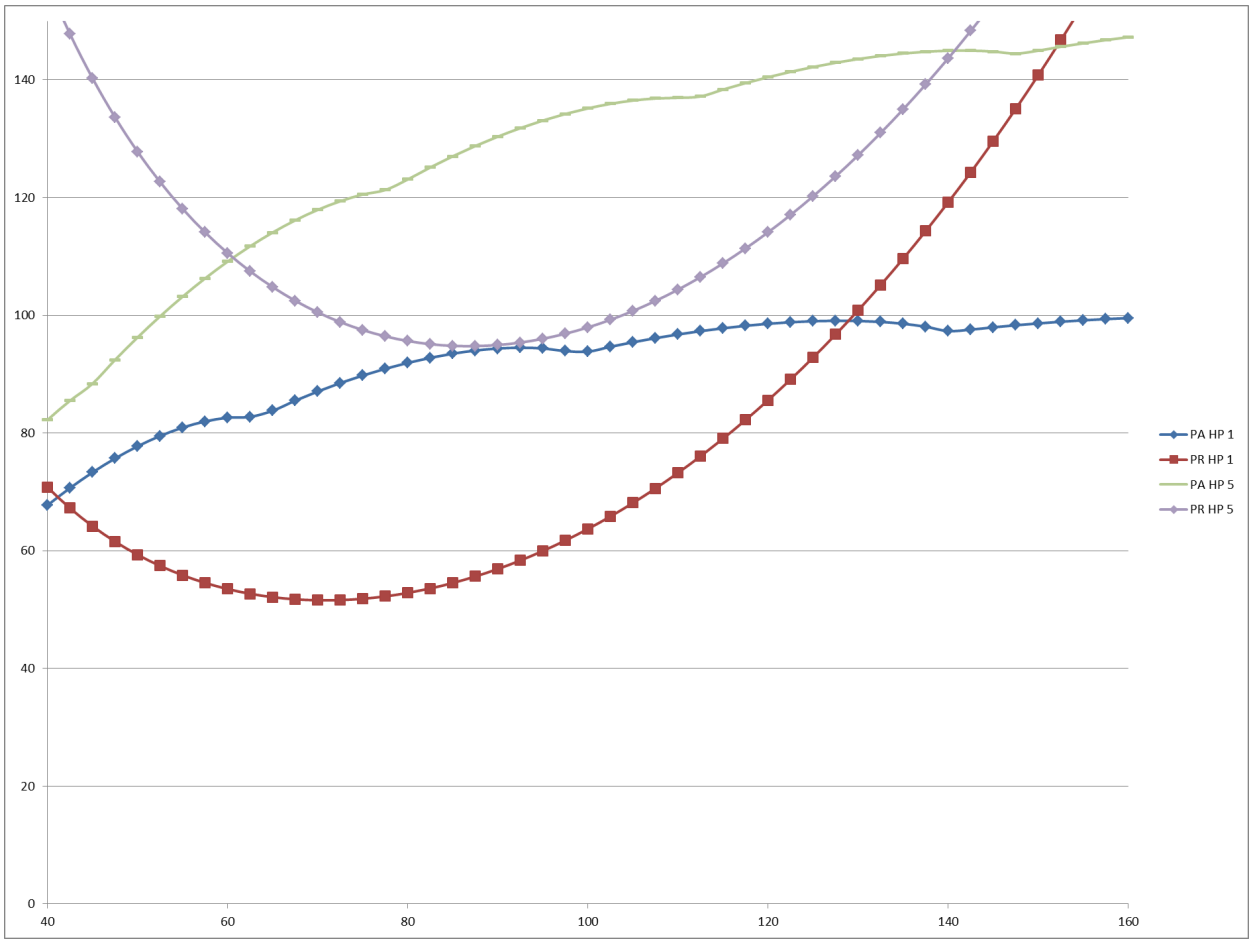

Figure 2 - 34 Power Available and Required for Constant Power Landing

As shown above the only way that currently an engine can work with a constant power loading increase is if the weight increases as well. With the max cruise speed and weight shown below.

Table 2 - 14 Power Required and Available Constants

HP	Vcr (kts)	Weight(lb)
200	127.5	2726
300	140	4171.5

As we can see the power available with weight of the aircraft is almost a linear function where an increase of 100 hp or 50 per engine and a weight increase of 1445.5 lb is required just to increase the maximum cruise velocity by 12.5 knots, which is not a good trade off.

Supercharger Add On

First off, to define a supercharger, it is an exterior add on compressor connected directly to the engine and powered by the engine to increase the air going into the engine and therefore increase the fuel combustion per second for the same RPM without the supercharger and ultimately achieve a higher power for the same rpm as before. So looking into the code, it can be determined that the main reason that the velocity needed cannot be

obtained is that the engine is ultimately just failing to breath at that required altitude. This is shown using the following equation.

$$BHP = BHP_{SL}\left(\frac{\delta}{\sqrt{\sigma'}}\right) \tag{112}$$

This equation ultimately the achievable power available by 23% at the cruise altitude which is a huge chunk of power coupled with the fact that power is also being lost by the propeller efficiency. Now, the propeller efficiency can't be changed and neither can the loss of percent power with altitude, however the amount of power being lost can be increased with a supercharger. With a supercharger providing a 25% boost to the engine these new graphs can be found at cruise velocity.

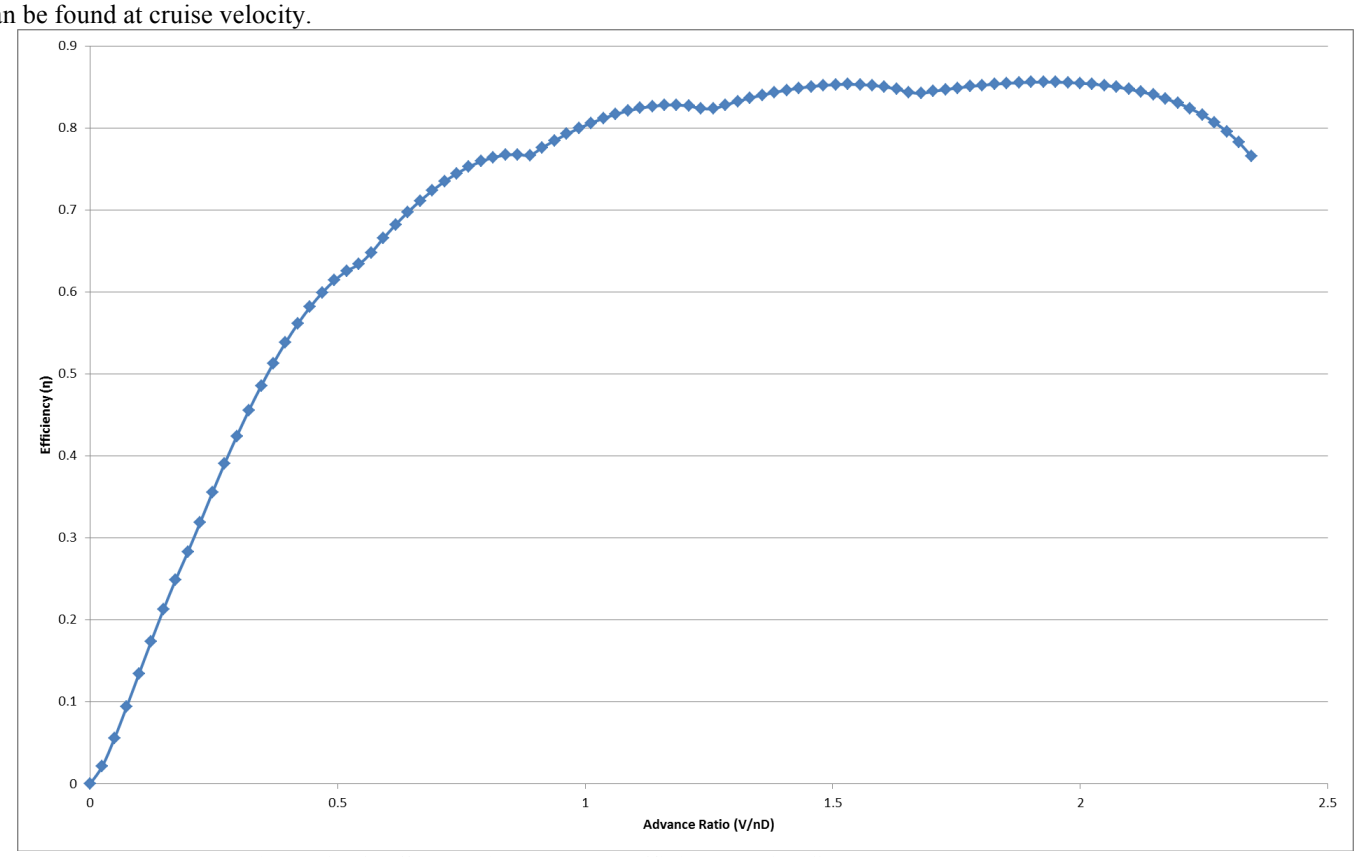

Figure 2 - 35 Curve Fit Propeller Efficiency With Supercharger

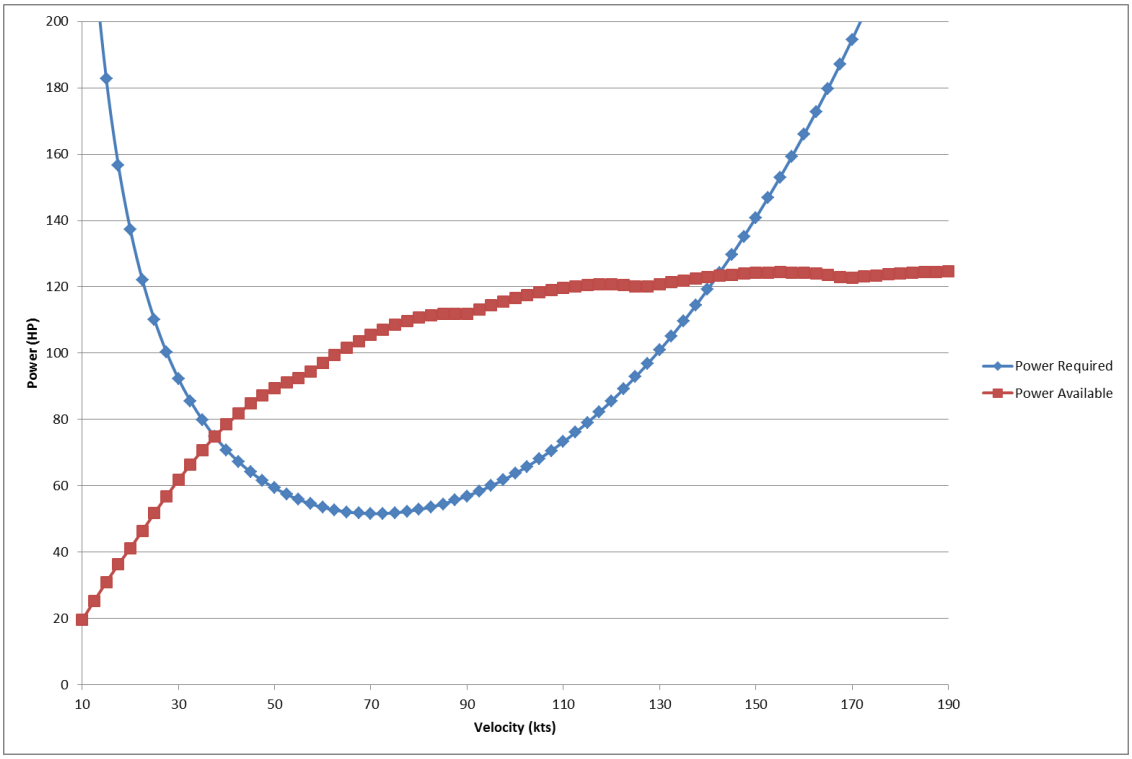

Figure 2 - 36 Power Available vs. Power Required With Supercharger

Table 2 - 15 Blade Analysis Variable Pitch Settings

	Maximum Cruise Velocity	Units
No Supercharger	125	kts
With Supercharger	141	kts

So as it can be shown, a supercharger can increase the power available into being a viable option with only limited drawbacks. The first being a small weight increase of around 10-20lbs per engine, the second being increased fuel consumption at lower speeds due to the increased fuel intake for a similar rpm. But the biggest one is an increase in the heating of the engine. However the engine in question can maintain a constant 90 hp so with a supercharger set to a 75% power at 90 hp per engine then the cooling system of the stock engine will be able to handle the new power output.

Other Conditions

Some other conditions aren't as vital for the design conditions, but still are just as crucial for flight, including the power available curves with one engine out, as well as the noise generated by the aircraft. The engine out conditions is shown below.

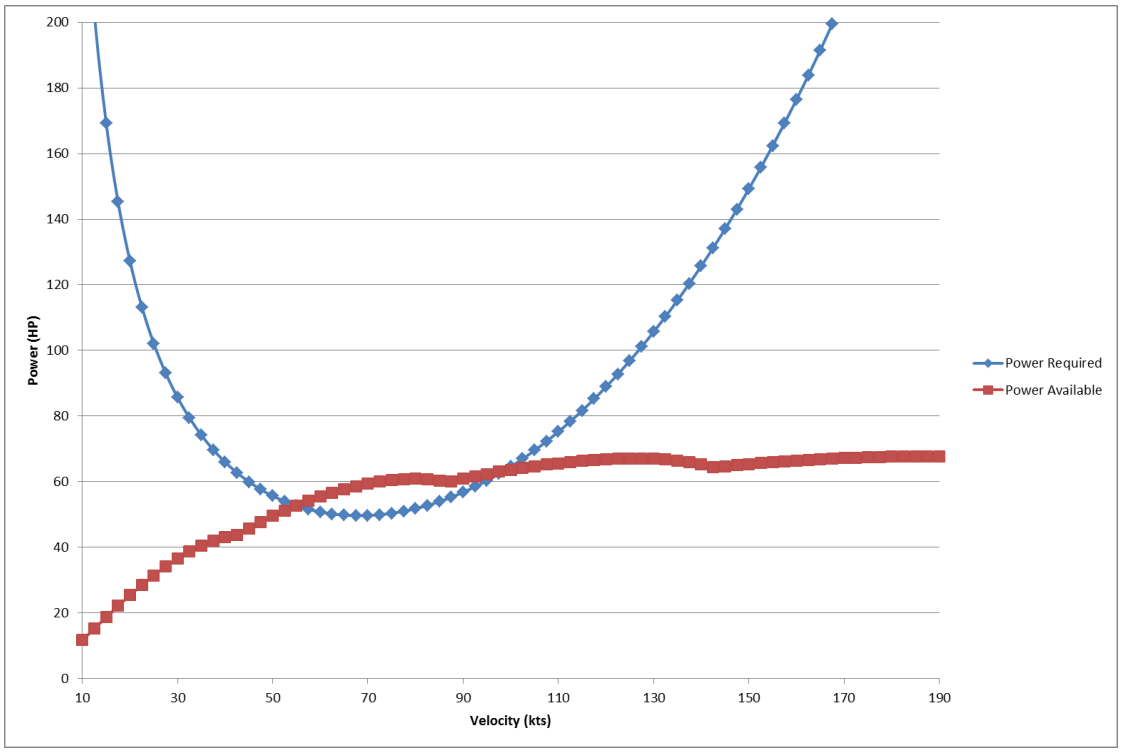

Figure 2 - 37 Power Available Vs. Power Required One Engine Out at 5000 ft. 75% Power

As shown when one engine out at the take-off altitude the min and max velocity are between 57.5-97.5 kts, as well as a max power available of 60 hp.

For the wing noise, that depends on the tip speed which is defined with the following equation.

$$V_{Tip} = \pi * n * D \tag{112}$$

And it is discovered that the max tip velocity in relation to Mach number is .69, which is well under a Mach number that will start causing vibrations and excess noise production, so in terms of permissible noise, this aircraft should be well under it.

Wing Plan form Design and Sizing and Locating Lateral Control Surfaces

The design of the wing did not go through many changes from the preliminary phase. This was because calculations can be kept simple for all different aspect of the aircraft. This allows for a fundamental knowledge, coding, and calculations that can all be a function of a feature on the aircraft. With this function, the best layout for the aircraft can be found by varying different features of the aircraft.

It was decided that a cantilever wing is to be used for this aircraft. This was done by using historical data from **Table 2 -13** Almost every twin engine propeller driven aircraft have a cantilever wing; this, and the fact that braced wings are much heavier, the cantilever wing was chosen.

Once the overall structural wing configuration has been chosen, it was then time to decide the overall wing/fuselage arrangement. A mid wing was out of the Eqn. for this aircraft because of the difficulty of having to reinforce the fuselage to sustain the wings. The choice was then down to a high wing or a low wing. **Table 2-14** provides the basic rating of how the different type of wing arrangements compared with each other. It can be seen

that the high wing has a lot better rating in almost every categories: interference drag, lateral stability, and visibility from cabin. Because the aircraft has a retractable landing gear, the last rating did not apply to it. Because of this, the obvious choice was to go with a high wing. These are basic comparison of the different wing placements, but a closer look at the advantages and disadvantages of a high wing will be discussed.

Type	Dihedral Angle, Γ_w, deg.	Incidence Angle, i_w, root/tip deg.	Aspect Ratio, A	Sweep Angle, $\Lambda_{c/4}$, deg.	Taper Ratio, λ_w	Max. Speed, V_{max}, kts	Wing Type
CESSNA							
310R	5	2.5/-.5	7.3	0	0.67	236	ctl/low
402B	5 (outer)	2/-.5	7.5	0 L.E.	0.67	227	ctl/low
414A	5	2.5/-.5	8.6	0 L.E.	0.60	232	ctl/low
T303	7	3/0	8.1	0 L.E.	0.71	216	ctl/low
PIPER							
PA-31P	6	1/-1.5	7.2	0	0.39	243	ctl/low
PA-44-180T	7.2	NA	8.1	0	0.63	196	ctl/low
Chieftain	5	1/-1.5	7.2	1.9	0.40	231	ctl/low
Cheyenne I	5	1.5/-1	7.4	0	0.37	249	ctl/low
Cheyenne III	5	1.5	7.8	0	0.31	296	ctl/low
BEECH							
Duchess 76	6.5	3/.6	8.0	0	0.80	194	ctl/low
Duke B60	6	4/0	7.2	0	0.32	246	ctl/low
Learfan 2100	4	1.5	9.5	0	0.45	369	ctl/low
Rockwell Commander							
700	7	NA	9.0	0	0.43	231	ctl/low
Piaggio P166-							
DL3	21.5/2.5*	2.7	7.3	7.5	0.35	215	ctl/gull
EMB-121	7	3	7.2	0.33	0.61	316	ctl/low

ctl = cantilever brcd = braced (strutted)
*21.5 inboard, 2.5 outboard on this gull wing configuration

Table 2 - 16 Historical Data for Twin Engine Propeller Driven Airplanes: Wind Geometric Data

	High wing	Mid Wing	Low Wing
Interference Drag	2	1	3
Lateral Stability	1	2	3
Visibility from Cabin*	1	2	3
Landing Gear Weight	3**	2	1

* strongly dependent on where the wing passes through the fuselage

** if the gear is retracted into the fuselage, gear weight is not necessarily a factor. In that case the landing gear often requires a 'bump fairing' which causes additional drag.

Table 2 - 17 Basic Comparison of Different Wing Placement [2]

High wing has many advantages that greatly benefit this aircraft for the mission given. Firstly, high wing aircraft are more laterally stable. Because this aircraft will be used for training, stability is very important. High wing increases the dihedral effect, $C_{l\beta}$, which is the amount of roll moment produced per degree of sideslip [1]. Secondly, high wing aircraft produce more lift than mid or low wing, this is due to the fact that high wing is attached to the top part of the fuselage. Thirdly, stall speed decreases because of the higher lift. Fourthly, the engines and propellers will less likely be damage by sand or debris because it is a lot higher up. Fifthly, the pilot will have a better view in lower-than horizon which is one of the requirements needed for this training aircraft. And lastly, the lower section of the fuselage will have a smoother aerodynamic shape because the wings will not be in the way.

With all these advantages come some disadvantages for aircrafts with high wings. Firstly, the aircraft will have more frontal area which leads to higher drag, but the higher lift will make up for it. Secondly, the take-off run distant will increase because the ground effect is lower. This does not really affect this aircraft because there are no specifications for this. Thirdly, the landing gear is longer and heavier for aircraft with high wings. This does not affect this aircraft because the gears are retractable into the fuselage, so the landing gear is no longer or heavier. Fourthly, the wing will produce higher induced drag, D_i, due to higher lift. As mention earlier, the lift will make up for the extra drag that is produced. Fifthly, the horizontal tail will be 20% larger and heavier than horizontal tail in low wing. This is because of the downwash of the high wing onto the tail. It was found, however, that the current horizontal tail used does not need to be bigger for this aircraft. And lastly, the aircraft has a weaker lateral control because of the high laterally dynamic stability. This is not a problem because stability is the main priority in the training aircraft.

As mentioned earlier, the current design of the aircraft is kept to the basic, so a fundamental coding of the aircraft can be created. Because of this, the current aircraft will have zero sweep with a wing thickness ratio, t/c, of 12%. Based on historical data, a thickness ratio of about 18% was used by many twin engine aircraft. But because this is a light twin engine, a smaller thickness ratio was selected to see if all the requirements can be met while also trying to lighter. The airfoil selected for the wing of the aircraft was NACA2412 while NACA0012 was used for the empennage. This aircraft have a taper ratio of .67. The dihedral angle of the wing is 2 degrees because it's a high wing, so it doesn't need as high of an angle as the aircrafts in historical data. The incidence angle of the wing is 2 degrees.

Verifying Clean Airplane C_{Lmax} and for Sizing High Lift Devices

This section will verify that the wing geometry selected is consistent with the required value of clean aircraft C_{Lmax} as well as the size of the high lift devices needed by this aircraft to meet the requirements for the C_{Lmax} at take-off and landing. The required C_{Lmax} is 1.528, C_{LmaxTO} is 1.528, and $C_{Lmax}L$ is 1.856.

It was first determine whether the wing planform can produce the required C_{Lmax} needed. For the current wing planform, the C_{Lmaxw} is assumed to be a trimmed value. It is safe to assume that the C_{LmaxW} is equal to 1.05 to 1.1 times the amount of C_{Lmax}, which accounts for the tail down load to trim on the wing. Because this aircraft has a l_h/c value of 4.015, a factor of 1.08 was assumed. **Eqn. (113)** was used to determine the estimated C_{Lmax} needed by the wing. This yielded a value of 1.650. Because this wing is not swept, this value does not change. **Eqn. (114)** was used to determine the C_{Lmax} produced by the wing. To determine the C_{Lmaxr} at the root and tip, a Reynolds number has to be found first. Reynolds number can be calculated by **Eqn. (115)**, where ρ is equal to 1.90E-03 slugs/ft^3, V= 256.1878 ft/sec for cruise speed, L= 6.061145 and 4.06067 ft for the chord of the wing at root and tip, respectively, and μ as 3.63E-7 lb*s/ft^2. This yielded a value of Re=8.12E6 and 5.44E6 for the root and tip of the wing, respectively. Using this Reynolds number and a t/c of 12%, the C_{Lmax} was found to be approximately 1.7602 and 1.705 for the root and the tip of the wing, spectively. Using Eqn. (2), plugging in .919 for the constant k_λ because of a taper value of .67, the C_{LmaxW} produced by the wing is 1.59. This is approximately 2% less than the required C_{Lmax} of the wing needed, so no change to the geometry of the wing is needed.

$$C_{Lmaxrequired} = 1.08 * C_{Lmax} \tag{113}$$

$$C_{L_{max_w}} = k_\lambda (C_{l_{max_r}} + C_{l_{max_t}})/2 \tag{114}$$

$$Re = \frac{\rho V L}{\mu} \tag{115}$$

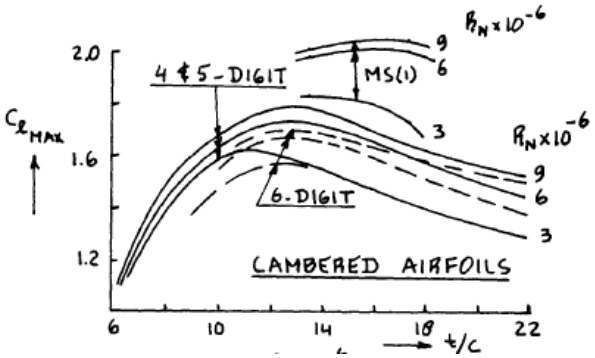

Flaps play a big part in the C_{Lmax} needed. The required incremental values of C_{Lmax} were calculated using Eq. (116) and (117). The factor 1.08 was used to account for additional trim penalties from the flaps. These values are calculated to be ΔC_{LmaxTO}=0 and ΔC_{LmaxL}=.3441. Because ΔC_{LmaxTO}=0, no flaps are needed at take-off. The flap lift increments at take-off is not very high, a single slotted flap can be used.

Figure 2 - 38 C_{Lmax} vs. t/c for Different Reynolds Number

$$\Delta C_{LmaxTO} = 1.08 * (C_{LmaxTO} - C_{Lmax}) \tag{116}$$

$$\Delta C_{LmaxL} = 1.08 * (C_{LmaxL} - C_{Lmax}) \tag{117}$$

The incremental section C_{Lmax} with the flaps down need to be calculated by using **Eqn. (118)**. This will determine whether the flaps meet the ΔC_{Lmax} needed for take-off and landing. K_λ is found using **Eqn. (119)** which accounts for the effect of sweep angle in the flaps down. Because this aircraft does not have a sweep angle, the angle is 0, yielding a K_λ value of .92. S_{WF} is the area of the flaps, as defined in Fig. 5. This in turn requires a ΔC_{lmaxL} of 1.0446. This is the approximate value of the ΔC_{lmax} needed for the flaps.

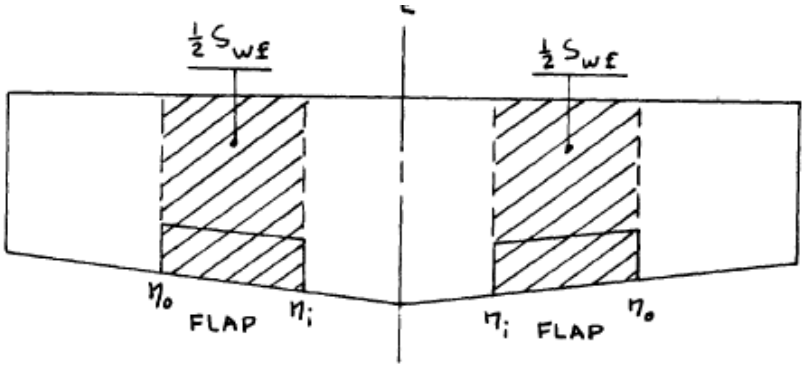

Figure 2 - 39 Definition of Area Flaps

$$\Delta C_{l_{max}} = \Delta C_{L_{max}} (S/S_{wf}) K_{\Lambda} \tag{118}$$

$$K_{\Lambda} = (1 - 0.08\cos^2 \Lambda_{c/4})\cos^{3/4} \Lambda_{c/4} \tag{119}$$

Once the approximate has been made, the require ΔC_L required which the flap must generate must be determined. Because sing slotted flaps were chosen for this aircraft, **Eqn. (120)** was used to calculate the ΔC_L. $\alpha_{\delta f}$ can be found using Fig. 5, where the assumed flap deflection for take-off is 15 degrees and the ratio of the flap to wing chord is .217. This yield a $\alpha_{\delta f}$ value of .5. $C_{L\alpha f}$ cis the flapped section lift curve slope and was found using **Eqn. (121)** $C_{L\alpha}$ is approximated as 2Π for small angle of attack. c'/c is given in **Eqn. (122)**. **Fig. 2-42** provides the geometric definition of c' and z_{fh} which z_{fh} is the hinge location. An educated guess of .1 was used for z_{fh}. These yield a c'/c value for take-off of 1.024 which then means that the $C_{L\alpha f}$ is equal to 6.435 for take-off. Then **Eqn. (122)** was used to find the actual ΔC_L needed which was found to be .842. ΔC_{LmaxTO} was then found to be .7834, using **Eqn. (123)**. It can be seen that this is closed to the assumed ΔC_{LmaxTO} found earlier for the geometry of the flaps.

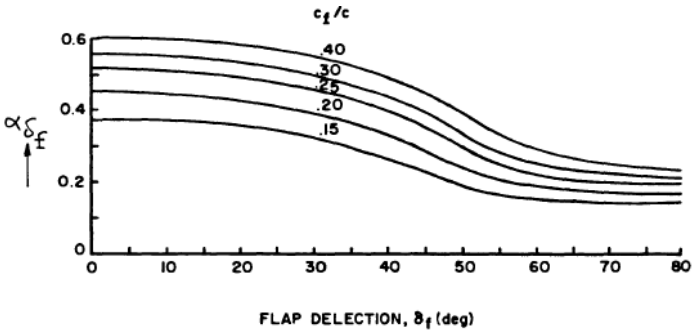

Figure 2 - 40 Section Lift Effectiveness Parameter for Single Slotted Flaps

For landing, the flap defection angle was assumed to be about 30 degrees, and from **Fig. 2 -40**, gives a $\alpha_{\delta f}$ value of .557. Using **Eqn. (122)**, c'/c for landing was found to be 1.033. And using **Eqn. (121)**, $C_{L\alpha f}$ was found to be 6.703. Using **Eqn. (121)**, ΔC_l was found to be 1.56. ΔC_{lmaxL} was found to be 1.56, using **Eqn. (122)**. This is more than the required ΔC_{lmaxL} needed to be produced by the flap.

It has been found that the flaps selected generate more ΔC_{Lmax} than needed. This means that the flaps meet the requirement and can even be scaled down a bit for lower drag.

$$\Delta C_l = C_{l_{\alpha_f}} \alpha_{\delta_f} \delta_f \tag{120}$$

$$C_{l_{\alpha_f}} = C_{l_\alpha} (c'/c) \tag{121}$$

$$c'/c = 1 + 2(z_{fh}/c)\tan(\delta_f/2) \tag{122}$$

$$\Delta C_l = (1/K)\Delta C_{l_{max}} \tag{123}$$

Stability and Control Analysis

Following the methods laid down by Dr. Roskam in his "Class I: Methods for Stability and Control Analysis" it is possible to rapidly determine whether or not the proposed configuration will have satisfactory stability and control characteristics. The method consists of several steps to validate the longitudinal static stability, the lateral static

stability and the minimum control speed with OEI. Other important stability and control characteristics such as take-off rotation, cross-wind controllability, trim through the *cg* range and a variety of dynamic stability considerations are not covered by this preliminary estimation.

Longitudinal static stability: A longitudinal X-plot for the aircraft is sufficient to determine the static stability of the aircraft. An example of the longitudinal X-plot is shown in **Fig. 2-41**.

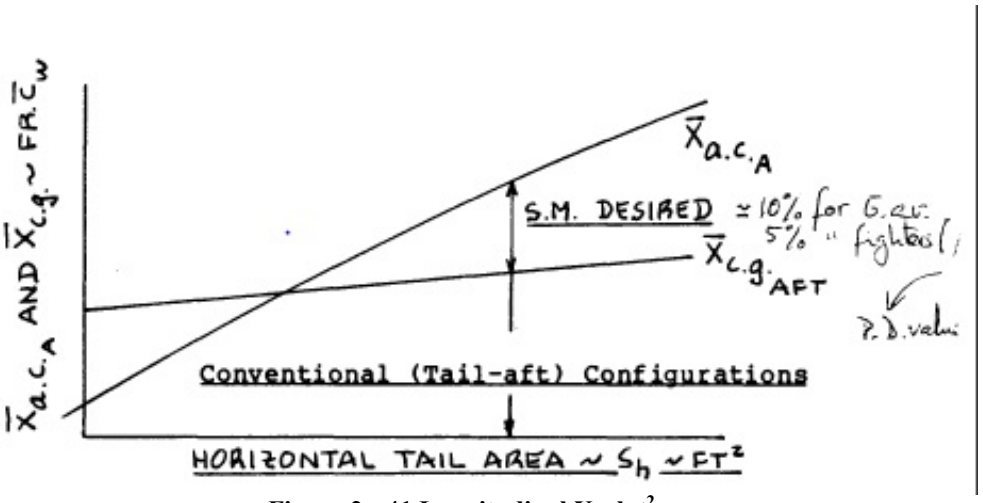

Figure 2 - 41 Longitudinal X-plot[2]

The *cg* leg represents the rate at which the *cg* moves aft or forward as a function of the horizontal tail or canard area. The a.c. leg represents the rate at which the a.c. moves aft or forward as a function of the horizontal tail or canard. The proposed aircraft horizontal tail design is conventional and does not include canard tail. So the canard part of the a.c. leg Eqn. is considered to be zero which will be apparent later during calculation. The a.c. leg is calculated using **Eqn. (124)**.

$$\bar{x}_{ac_A} = \left[\bar{x}_{ac_{wb}} + \left(C_{L\alpha_h}\left(1 - \frac{d\varepsilon_h}{d\alpha}\right)\frac{S_h}{S}\bar{x}_{ac_h} - C_{L\alpha_c}\left(1 + \frac{d\varepsilon_c}{d\alpha}\right)\frac{S_c}{S}\bar{x}_{ac_c}\right)/C_{L\alpha_{wb}}\right]/F \tag{124}$$

$$\text{Where, } F = \left[1 + \left(C_{L\alpha_h}\left(1 - \frac{d\varepsilon_h}{d\alpha}\right)\frac{S_h}{S} + C_{L\alpha_c}\left(1 + \frac{d\varepsilon_c}{d\alpha}\right)\frac{S_c}{S}\right)/C_{L\alpha_{wb}}\right] \tag{125}$$

The geometrical quantities in **Eqn. (124)** are shown in **Fig. 2-42**. Here, it is noted that the canard tail quantities are also included in the Eqn., however, since the conceptual aircraft is not canard the canard terms go to zero leaving a simplified Eqn.. The only unknown quantity in the above Eqn. are $C_{L\alpha_h}$ and $C_{L\alpha_{wb}}$ but they follow the same formula for calculation which is,

$$C_{L\alpha} = \frac{2\pi AR}{2+\sqrt{4+AR^2\beta^2(1+[tan^2\Delta/\beta^2])}} \tag{126}$$

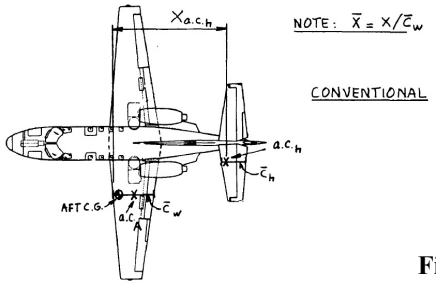

Figure 2 - 42 Geometric Quantities for A.C. Calculations[2]

Since the aircraft cruises at a subsonic speed (cruising speed is only $140\ kts$) the Mach correction term $\beta \approx 1$. The preliminary wing and horizontal tail designs are not swept to keep the calculations simple. So, $\Delta = 0°$. Using the above Eqn. $C_{L\alpha_h}$ and $C_{L\alpha_{wb}}$ can be calculated. Putting $S_c = 0$ and taking S_h as an independent variable the a.c. leg is obtained by

The ngton

sweeping through different values of S_h. The *cg* leg is calculated following conventional *cg* calculation methods. From the preliminary CAD model the *cg* location of each of the aircraft components are obtained. However, using Roskam's refined weight estimate methods the refined weights calculated are used instead of the weights obtained from the historical data. The refined weight estimate for the horizontal tail is a function of the horizontal tail area. As the tail area is swept at different values, the *cg* leg was formed. The refined weight estimate formula for the horizontal tail is given in **Eqn. (70)**. The X-plot of the conceptual aircraft is given in **Fig. 2 -43.**

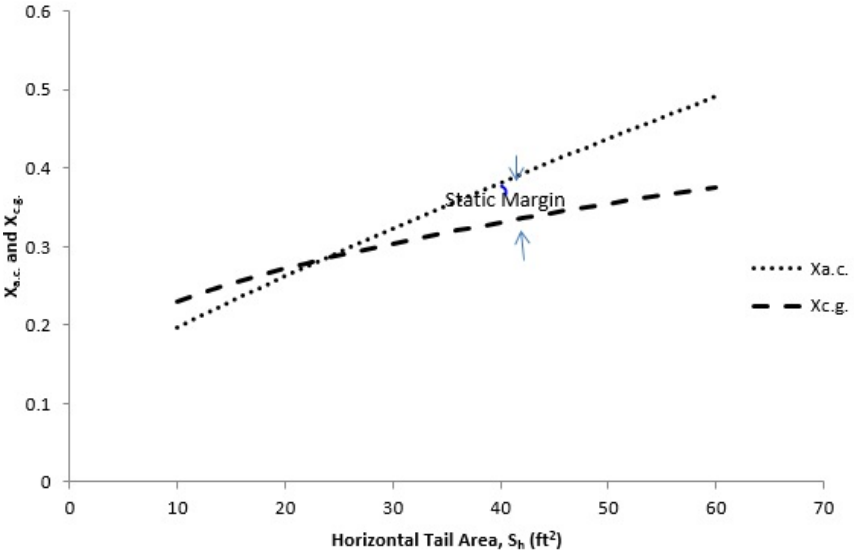

Figure 2 - 43 Longitudinal X-Plot of the Aircraft

From the above Fig. it is seen that the aircraft is stable at the primary assumed horizontal tail area $S_h = 44.48\ ft^2$ with a static margin of 5%. The conceptual aircraft is a light weight, economical and trainer aircraft pointing towards the fact that it should not rely on a feedback augmentation system. As a result, the aircraft has to be inherently stable. Since the aircraft is a twin engine GA type aircraft the specified static margin is 10%. To get 10% static margin the horizontal tail area should be increased to $48\ ft^2$. So the weight and balance calculations were reviewed and necessary adjustments were made. It was found out that the vertical tail weight calculation was wrong and after adding the right input value, longitudinal x-plot calculation was refined and **Fig. 2-44** had been obtained.

Lateral directional stability: Similar to the longitudinal static stability another X-plot has to be made for the lateral stability of the aircraft. In the longitudinal static stability, the horizontal tail size was the most important factor. Similarly, in lateral directional stability the vertical tail is the most important component. The $C_{n\beta}$ leg of the X-plot has to be calculated and plotted for several horizontal tail areas. The required formula is:

$$C_{n\beta} = C_{n\beta_w} + C_{n\beta_f} + C_{n\beta_v} \tag{127}$$

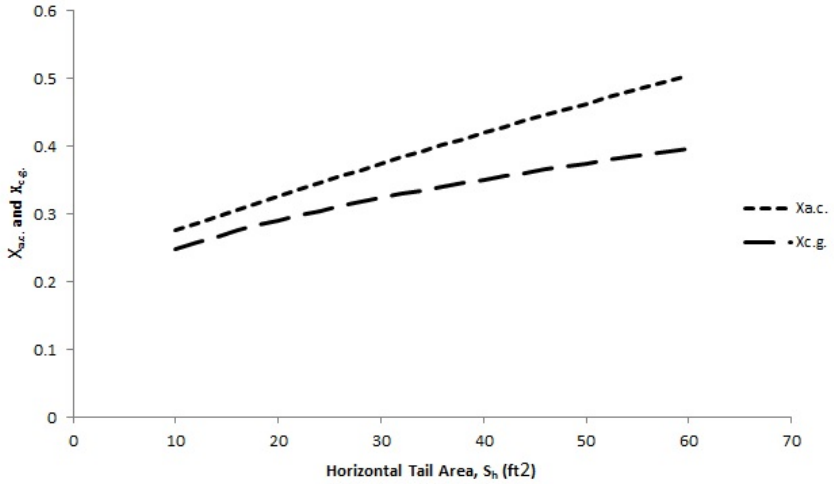

Figure 2 - 44 Refined Longitudinal X-Plot

The aerodynamic quantities are computed using the methods presented in Ref. 6****. The wing contributes only at high angles of attack and for preliminary estimation it is neglected. So, $C_{n\beta_w} = 0$. The contribution of the fuselage is found using the following formula:

$$C_{n_{\beta_f}} = -57.3 K_N K_{R_1} (S_{f_s} l_f / Sb) \tag{128}$$

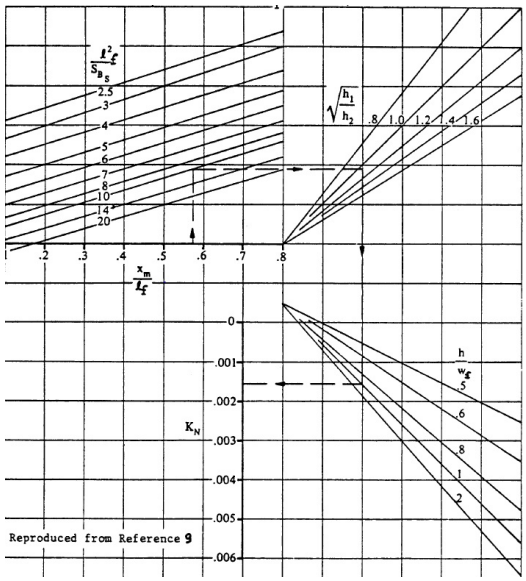

Figure 2 - 45 Factor Accounting for the Wing Fuselage Interference[17]

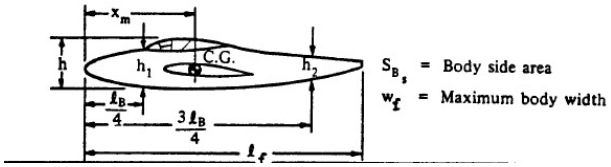

For reading **Fig. 2-29**, some quantities are needed to be known. The meaning and the representation of the quantities are provided in the Fig. above. Using appropriate values, the empirical factor $K_N$is determined. The value of S_{f_s} is obtained from subtracting the vertical tail area from S_{B_s}, where S_{B_s} is given in the above Eqn.. Sweeping through different vertical tail area different values of $C_{n\beta_f}$ can be obtained. The value of K_{R_1} is obtained from **Fig. A4**. At first the fuselage Reynold's number is calculated for a cruise condition. From the graph in **Fig. A4**, the value of K_{R_1} is computed. After this, the vertical tail contribution is found using **Eqn. (129)**. The geometric quantities described in **Eqn. (129)** are defined in **Fig. 2-46**.

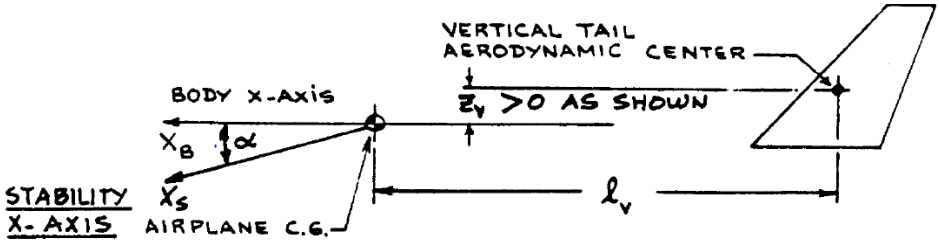

Figure 2 - 46Geometry for Locating the Vertical Tail [7]

$$C_{n_{\beta_v}} = -(C_{y_{\beta_v}})(l_v \cos\alpha + z_v \sin\alpha)/b \tag{129}$$

Assuming steady and level flight (in cruise) the above Eqn. can be reduced. $C_{y\beta_v}$ is obtained from the following Eqn.:

$$C_{y_{\beta_v}} = -k_v (C_{L_{\alpha_v}})(1 + d\sigma/d\beta)\eta_v (S_v/S) \tag{130}$$

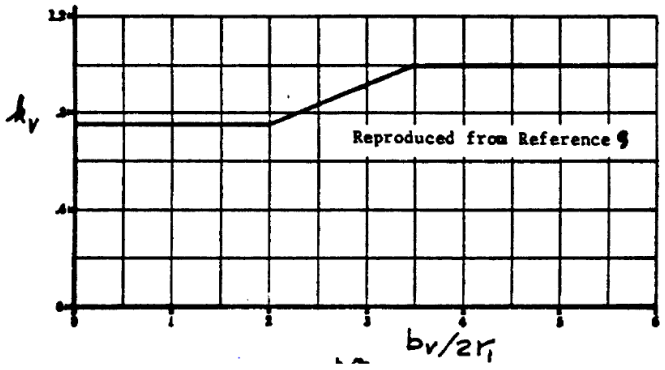

Figure 2 - 47 Empirical Factor for Estimating Side-Factor[7]

K_v is obtained from **Fig. 2-47** and

$$\left(1 + \frac{d\sigma}{d\beta}\right)\eta_v = .724 + 3.06\left(\frac{\frac{S_v}{S}}{1 + cos\Delta}\right) + \frac{.4z_w}{z_f} + .009AR_w$$

Here, sweep angle $\Delta = 0$.

z_v is the z-axis distance from the *cg* to the vertical tail aerodynamic center and z_f is the vertical height of fuselage at the root chord. Both of these quantities are obtained from the CAD model of the aircraft. Sweeping through different vertical tail areas, corresponding $C_{y\beta_v}$ values are obtained. Finally using **Eqn. (129)** $C_{n\beta}$ leg is calculated and the directional X-plot is plotted in **Fig. 2 - 48**. The weight per ft^2 of the vertical tail is known from this weight analysis. Since the airplane needs to be inherently stable, the overall level of directional stability must be: $C_{n\beta} = .001\ per\ degree$. From **Fig. 2-48** it is observed that level of lateral stability is achieved when the vertical tail area is 23.5 ft^2. This means that the aircraft has a slightly bigger vertical tail area than required for providing a sufficient lateral directional stability. The above calculations show that the aircraft vertical tail configuration is fairly accurate providing a good lateral directional stability.

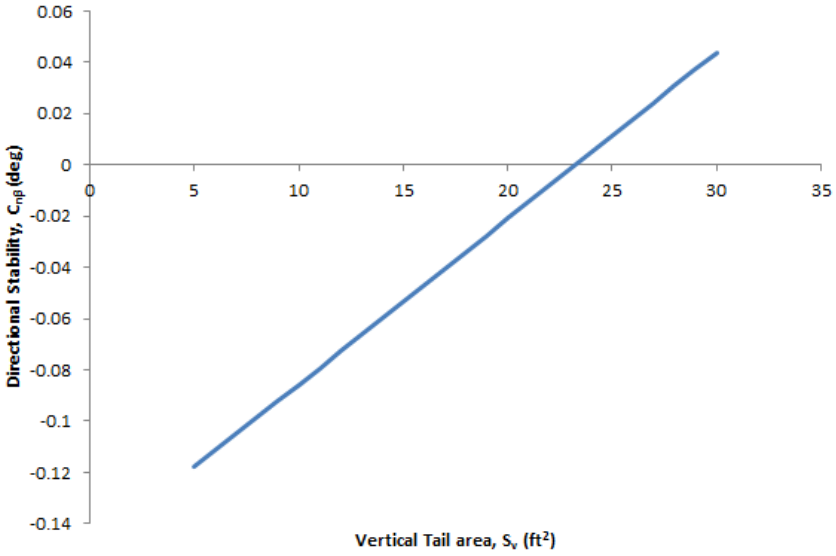

Figure 2 - 48 Lateral Directional X-Plot

Minimum control speed with one engine in operative: The critical engine-out yawing moment is first calculated from the following equation:

$$N_{t_{crit}} = T_{TO_e} y_t \tag{131}$$

Here, y_t is the corresponding lateral thrust moment arm of the most critical engine. For a propeller driven airplane the engine power (P_{TO}) is converted to corresponding T_{TO} using **Fig. 2-49**.

The drag induced yawing moment is then calculated using $N_D = .75N_{crit}$

Using the Fig.s and the Eqn.s, $N_{crit} = 1455\ lb.ft$ and $N_D = 1091.25\ lb.ft$.

Maximum allowable velocity for minimum control is obtained using $V_{mc} = 1.2V_S$. Where, V_S is the lowest stall speed of the aircraft. This usually is the landing stall speed.The rudder deflection required to hold the engine out condition at V_{mc}:

$$\delta_r = (N_D + Nt_{crit})/\bar{q}_{mc}SbC_{n\delta_r}$$

The value of control power derivative $C_{n\delta_r}$ is computed using the methods described in Roskam's Volume 6. The rudder deflection for variable horizontal tail area is tabulated in **Table 2-18**.

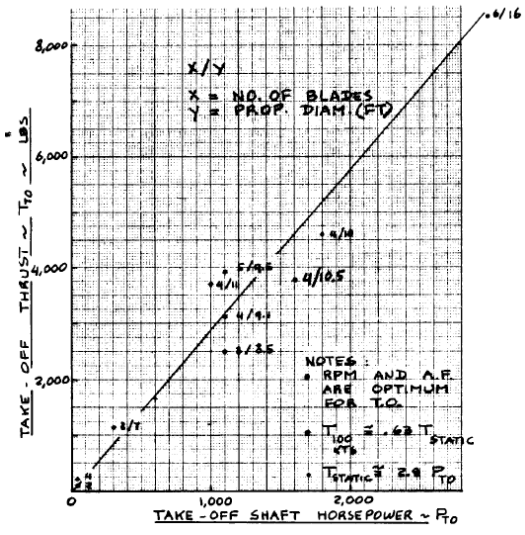

Figure 2 - 49 Effect of Shaft Horsepower on Take-off Thrust[1]

Table 2 - 18 Rudder Deflection at Different Vertical Tail Area

Vertical Tail area, S_v	Rudder deflection, δ_r	Vertical Tail area, S_v	Rudder deflection, δ_r	Vertical Tail area, S_v	Rudder deflection, δ_r
1	-382.681	11	-34.7892	21	-18.223
2	-191.34	12	-31.8901	22	-17.3946
3	-127.52	13	-29.437	23	-16.6383
4	-95.6702	14	-27.3344	24	-15.945
5	-76.5362	15	-25.5121	25	-15.307
6	-63.7802	16	-23.9176	26	-14.7185
7	-54.6687	17	-22.5106	27	-14.1734
8	-47.8352	18	-21.2601	28	-13.6672
9	-42.5201	19	-20.1411	29	-13.1959
10	-38.2681	20	-19.134	30	-12.756

According to Roskam Volume 2 the rudder deflection from the above Eqn. should not be more than 25^{o2}. From the preliminary sizing the vertical tail area is chosen to be around $27\ ft^2$. The rudder deflection at that specific surface area is $14.2°$ which is within the maximum value. However it is specified in the mission requirements that the $V_{mc} < V_s$. Thus, using reverse calculation at maximum rudder deflection $\delta_r = 25° = .436\ rads$, using $S_v = 26ft^2$ and the corresponding $C_{n\delta_r}$, the velocity at minimum control is obtained to be $V_{mc} = 55.24\frac{ft}{s} = 32.73kts$. This value is less than the stall speed and it satisfies the mission requirements.

Control Systems Layout

There are two types of flight control systems, the reversible flight control system and the irreversible flight control system. In a reversible flight control system, when the cockpit controls are moved, the aerodynamic surface controls move and vice versa. On the other hand, in an irreversible flight control system, when the cockpit controls are moved, the aerodynamic surfaces move and not vice versa. Typically reversible flight control systems are used in economical aircrafts and irreversible flight control systems are used in advanced aircrafts. For the conceptual aircraft, the flight control system chosen was a reversible one because of its simplicity, low cost and low maintenance. However, there are some design problems associated with this type of systems: friction, cable stretch, weight, handling qualities, flutter etc.

Reversible lateral flight control system: Fig. 2-50 shows several possible layouts for reversible lateral flight control systems. Since this aircraft is required to serve as a trainer two-inter-linked-stick controller is developed so that if one stick is moved, the other one mirrors it. This arrangement is dual cockpit arrangement. The structure is somewhat like that in **Fig. 2-50 E**. The aileron control systems are made up of a combination of torque tubes and cables represented in **Fig. 2-50 B.** The aircraft has a high wing, so the torque tube is extended up to the edge of the cockpit underneath the floor, and in between the baggage area wires and pulleys are used to elevate the system to the ceiling. Through the ceiling the wires are extended to the ailerons inside the wing using more pulleys. Since the airplane has tandem cockpit laterals controls are combined with longitudinal controls through a concentric tube-cable arrangement the details are presented in **Fig. 2-51**.

Most ailerons when deflected asymmetrically over the same angle, induce an adverse yawing moment onto the airplane. To counteract this adverse yawing moment, the ailerons are deflected 'differentially' which is shown in **Fig. 2-52.**

Reversible Longitudinal Flight Control System: Fig. 2-43 presents a number of layouts used in reversible longitudinal flight control systems. **Fig. 2-43 A** is acceptable only if the cables do not rub together. **Fig. 2-42 C** only

uses push rods and tend to be a little bit heavier. The system in **Fig. 2-43 B** is chosen since it employs a mixture of cables and push-rods. It removes the probability of cables grinding together and makes the thing lighter than the third model since it has cables in it. Also push-rod system tends to have less friction than cable systems. **Fig. 2-43 D** is redundant and is not kept in any consideration.

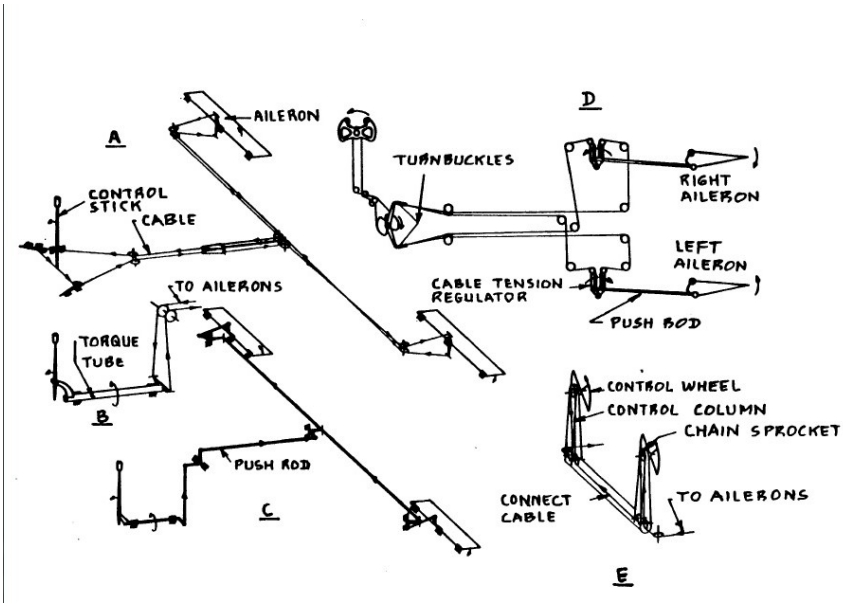

Figure 2 - 50 Example of Reversible Lateral Control

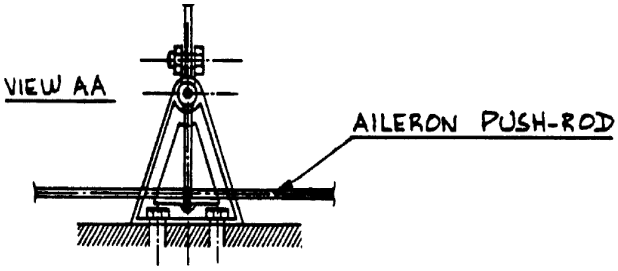

Figure 2 - 53 Combined Cockpit Controls

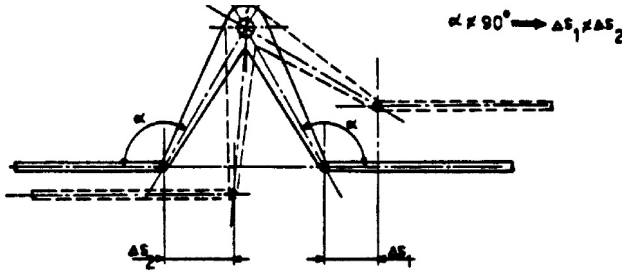

Figure 2 - 51 Differential Control Action

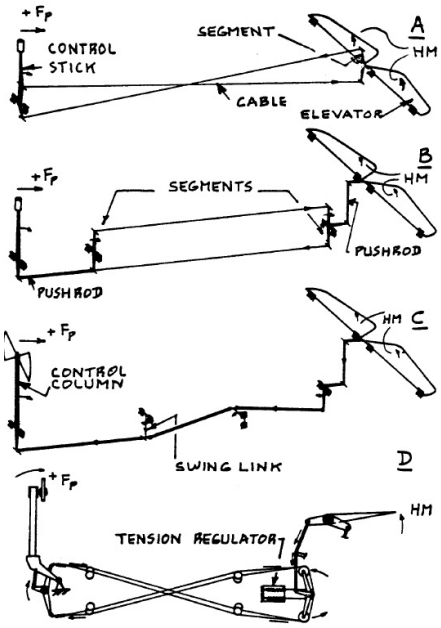

Figure 2 - 52 Reversible Longitudinal Control

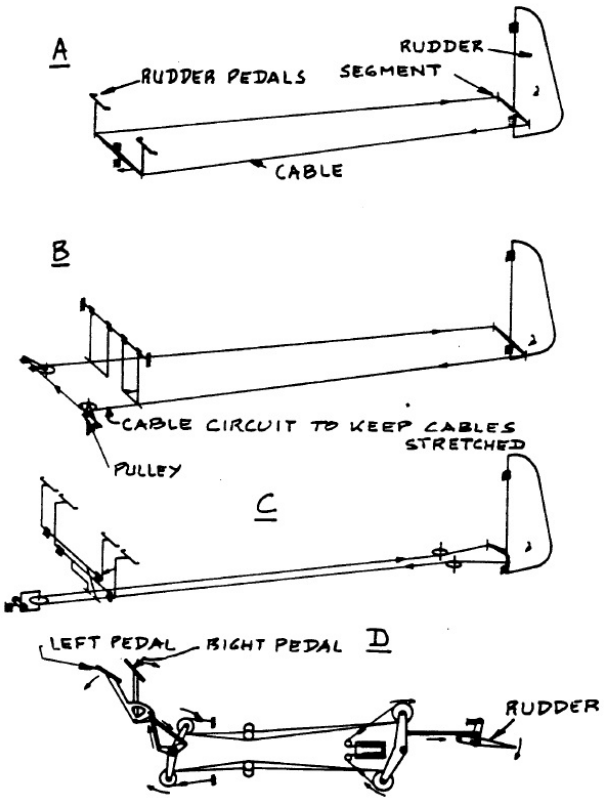

Figure 2 - 54 Reversible, Direction Control

Reversible Directional Flight Control System: The system of **Fig. 2-39 A** is found in many light airplanes. However, dual cockpit controls are needed for the conceptual aircraft so layouts of **Fig. 2-39 B** and **C** are preferable. **Fig. 2-39 D** is redundant and is not considered in the design. Because of its simplicity and added pulley to keep the cable circuit stretched, **Fig. 2-39 B** is chosen as the required rudder control system.

Important Design Aspects: In laying out reversible flight control system, the following important design aspects are needed to be kept in mind.

- Mechanical design requirement for cable and push-rod system
- Efficiency consideration
- Cable and push-rod control force levels
- Control surface types and hinge moments
- Aerodynamic balance requirements
- Mass balance requirements

While laying out the control systems, it is to be taken into account the amount of friction the system produces, the cable stretch or slack, the system elastic deformation and the kinematic feasibility. These are the subject matters of higher level and detailed studies

The detailed description of the entire control system layout is depicted in **Fig. 2-55**. In this figure the green

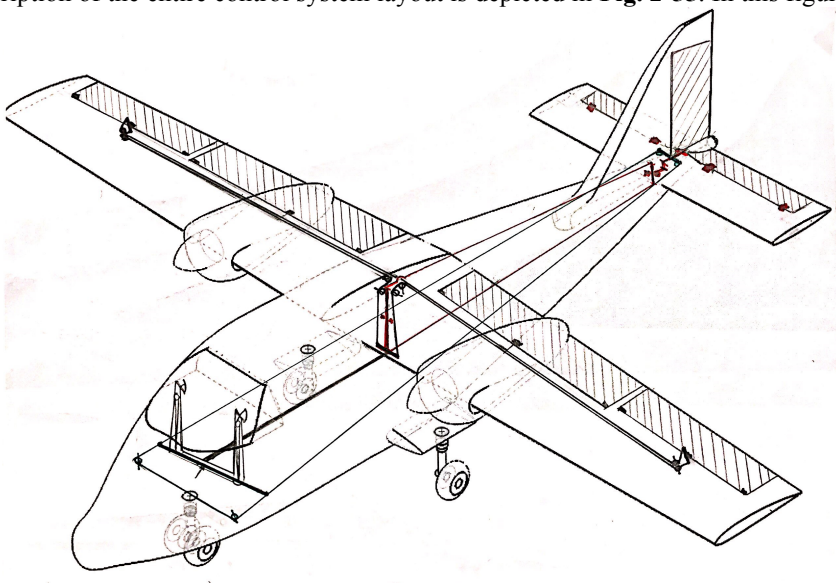

Figure 2 - 55 Combined Layout of the Control System

1st Drag Polar Determination

Drag polar is the relationship between the lift and drag of an aircraft. Determining this is essential to understand how the aircraft perform as a whole.

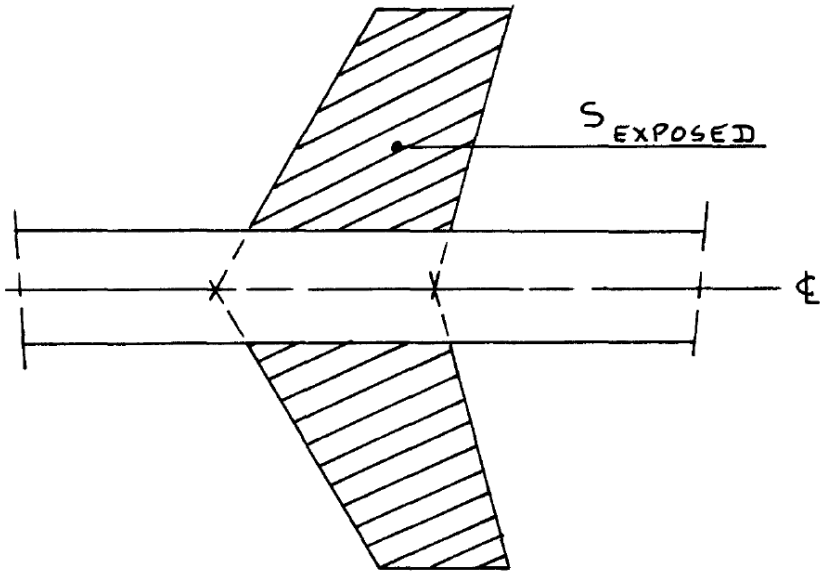

Figure 2 - 56 Definition of Area of Exposed Plan form

The first step in determining the drag polar is to find wetted area of the overall the aircraft, S_{wet}. This was done by breaking the aircraft down into components: Wing, horizontal tail, vertical tail, fuselage, and nacelles.

For a straight tapered plan form, the wetted areas for plan forms can be found using **Eqn. (132)**. The exposed area of the plan form, $S_{exp.plf}$ is defined by **Fig. 2-56**. τ is found using **Eqn. (133)**, which is the ratio of the thickness-chord ratio of the root and tip. λ is defined by **Eqn. (134)** which is the ratio of the chord of the tip and the chord of the root.

For the wing of this aircraft, the $S_{exposed.W}$ was found to be 152.3 ft^2 by using AutoCAD. λ was found to be .67, while τ was found to be 1. Using these values, the $S_{Wet.W}$ was found to be 313.74 ft^2.

For the horizontal tails of the aircraft, the same method of calculating the S_{wet} can be used. $S_{exposed.HT}$ was found to be 40.907 ft^2 by using AutoCAD. The horizontal tails also do not have a tapered or sweep so the chord and thickness is constant throughout. Because of this, τ and λ are equal to 1. Using these values and **Eqn. (132),** $S_{wet.HT}$ is equal to 82.104 ft^2.

For the vertical tails of the aircraft, the same method of calculating the S_{wet} can be used. $S_{exposedVT}$ is found to be equal to 24.433 ft^2 by using AutoCAD. There is a taper on the vertical tail. The chord of the tip, c_t, is equal to 1.338 ft, while the chord of the root, c_r, is equal to 7.3983 ft. The thickness ratio of both, however, is constant. This yield a τ value of 1 and a λ value of .1809. Using these values and **Eqn. (132)**, $S_{wet.VT}$ was found to be 50.332 ft^2.

The fuselage and nacelles are not plan forms, so the previous method cannot be used. For the fuselage, the perimeter method was used. For this method, the perimeter at each major section is found and then multiplied by the length of that section to get the surface area. These values are summed up and S_{wetF} can be found. A formulation of this can be seen in **Fig. 2 -56**. The S_{wetF} is found to be 333 ft^2.

For the nacelles, because it's built into the wings, SolidWork was used to find the wetted area of the nacelles. This value was found to be 41.78 ft^2 before subtracting out the area covered by the wing.

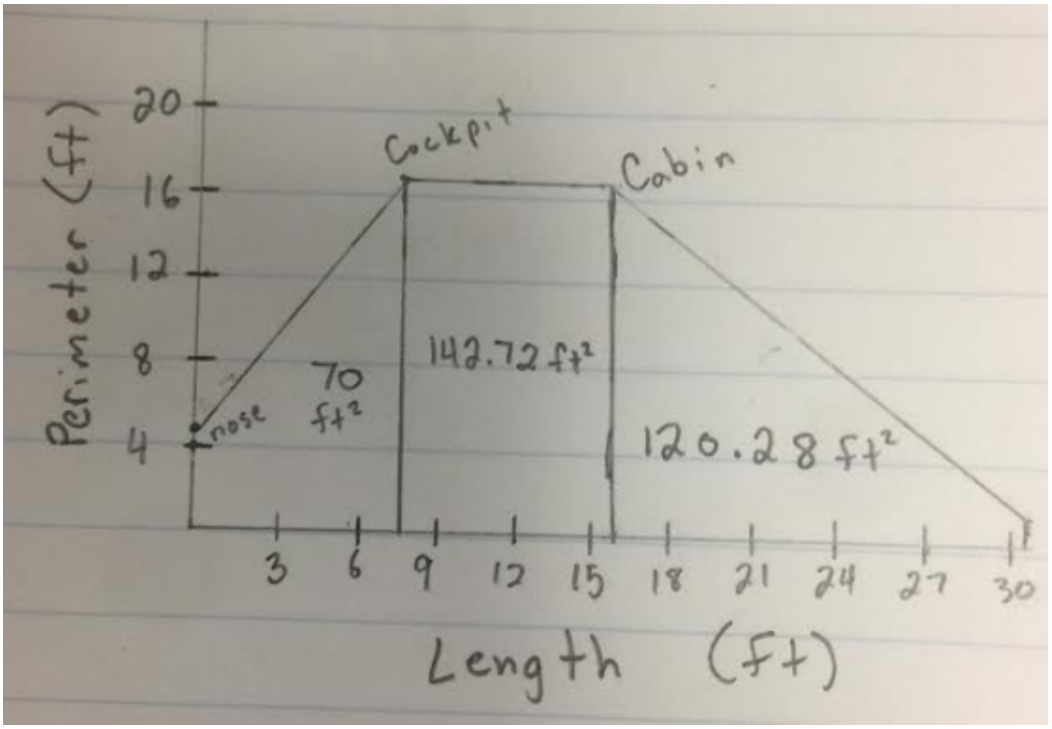

Figure 2 - 57 Perimeter Method for Calculation S_{wet} F

The previous values found for the wetted area are the gross wetted area. The total gross S_{wet} is 819.13 ft^2. To find the net S_{wet}, The first subtraction that is needed to be taken out of the gross wetted area is the surface area between the high wing and the fuselage. This area is found to be 22.83 ft^2. This value needs to be multiply by 2 because that section of the wing and the fuselage is being covered. This gives a value of 45.661 ft^2. The second subtraction of area that is needed to be done is the area between the horizontal tails and the fuselage sides. This value was found to be 5.089 ft^2. The next area that needs to be taken out is the area between the vertical tail and the top of the fuselage. This gives a value of 1.575 ft^2. The last area that needs to be taken out is the area between the nacelles and the wings because the nacelles area built into the wing. This area was found to be 21.261 ft^2. After applying all these values, the net S_{wet} is equal to 743 ft^2. Based on historical data, this value is a bit big for the take-off weight, but because this aircraft is using composite material, the actual weight is .9 times lighter than normal aircraft used in historical data.

$$S_{wet_{plf}} = 2S_{exp.plf}\{1 + 0.25(t/c)_r(1 + \tau\lambda)/(1 + \lambda)\} \tag{132}$$

$$\tau = (t/c)_r/(t/c)_t \tag{133}$$

$$\lambda = c_t/c_r \tag{134}$$

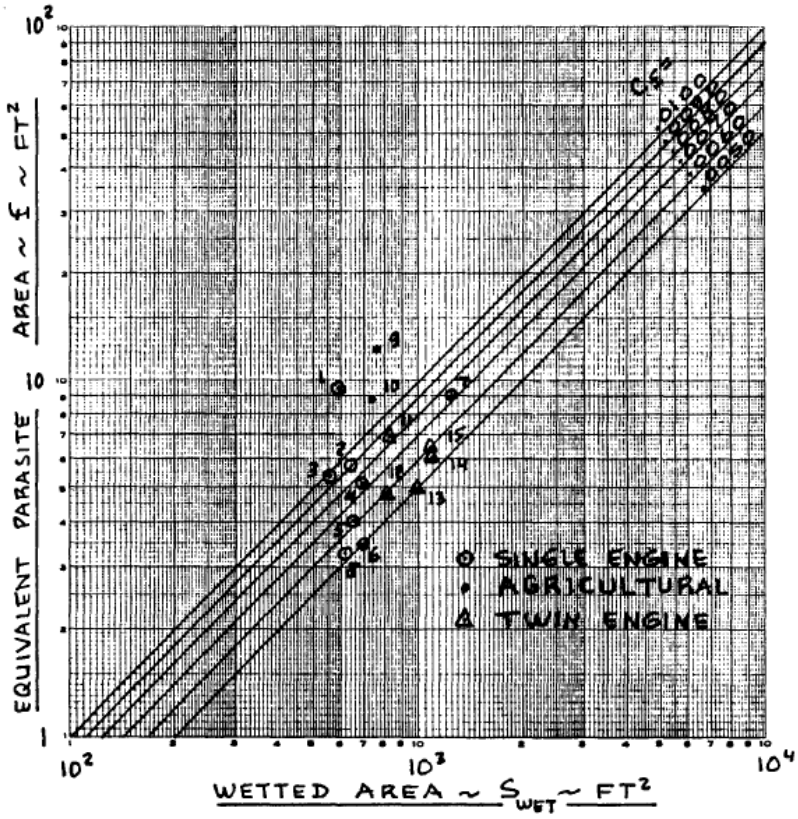

Figure 2 - 58 Effect of Equivalent Skin Friction of Parasite and Wetted Areas [reference (Figure 1 -11)]

The skin friction coefficient was estimated to be .007 based on the conventional configuration for a twin turbine driven propeller aircraft. With this and the total wetted area, **Fig. 2 -58** was used to find the equivalent parasite area, f, which is 5.5 ft^2. **Eqn. (135)** was then used to find the clean zero lift drag coefficient, C_{Do}. C_{Do} was found to be .0313. This value is bigger than the .0251 earlier found in the first estimation. This is because S_{wet} is bigger than previously estimated.

The flap drag increments and landing gear drag increment were found using Table 4. The Take-off flaps drag increment is .01 with an Oswald's efficiency factor, e value of .77; the landing flaps drag increment is .06 with an 'e' value of .73; the landing gear drag increment is .016 with no effect on the 'e' value.

Putting the zero lift drag coefficient, drag increments and Oswald's efficiency factor together, the drag polar can be calculated. **Eqn. (136)** was used to determine the drag polar for different configurations. A summary of the drag polar Equations are given in **Table 2-19**. Using these Equations, drag polar plots were generated as seen in **Fig. 2-59**. It can be seen that the addition of flaps and gear drives up C_L. The drag for the configuration of landing with flaps and gear down is greatest.

Table 2 - 19 Estimates for ΔC_D and 'e' with flaps and Gear

Configuration	ΔC_{D_o}	e
Clean	0	0.80 - 0.85
Take-off flaps	0.010 - 0.020	0.75 - 0.80
Landing Flaps	0.055 - 0.075	0.70 - 0.75
Landing Gear	0.015 - 0.025	no effect

Table 2 - 20 Airplane Drag Polars at different Configurations [Reference Table 1- 11]

Configuration	Drag Polars
Low Speed, Clean (e=.83)	Cd=.02595+.054787Cl^2
Take-off, Gear up (e=.77)	Cd=.03595+.05906*Cl^2
Take-off, Gear Down (e=.77)	Cd=.05195+.05906Cl^2
Landing, Gear up (e=.73)	Cd=.08595+.062292Cl^2
Landing, Gear down(e=.73)	Cd=.10195+.062292Cl^2

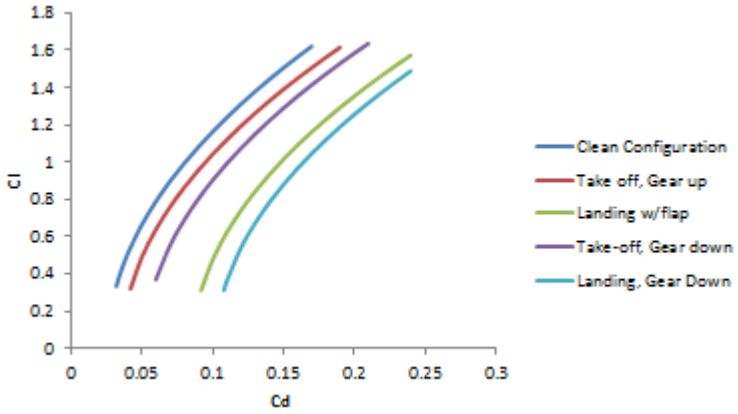

Figure 2 - 59 Drag Polar at Different Configurations

$$C_{D_o} = f/S \tag{135}$$

$$C_D = C_{Do} + \frac{C_L^2}{\pi A \,\mathrm{Re}} \tag{136}$$

2nd Drag Polar Determination

The overall drag can be calculated using the component drag method. To do this, the Reynolds Numbers were found for each component of the aircraft using **Eqn. (137)** at cruise: fuselage, wing, horizontal tail, vertical tail, nacelles. Using these Reynolds numbers, the coefficient of skin drag friction can be found using **Eqn. (138) Table 2-18** shows each component of the aircraft with its Reynolds Number and skin drag friction at cruise speed. With this value, the coefficient of drag based on wetted area can be found using **Eqn. (139)**. The ratio d/l is found by measuring the equivalent diameter of the fuselage while l is the length of the fuselage. Using these values, C_{DWet} of the fuselage was found to be .0028. Δf_e is equal to the area of the planform times the C_{DWet} as seen in **Eqn. (140)**, which is basically the flat plate drag. Δf_e of the fuselage was found to be .868.

A second method based on the frontal area of the fuselage was used to determine Δf_e of the fuselage to obtain a more accurate drag value for the fuselage **Eqn. (141)** was used to obtain the C_D needed to calculate Δf_e for the

fuselage. The C_D found for the frontal area of the airplane was .0469. This value was multiplied by the area of the frontal area which was 22.85 ft. This yield a Δf_e of 1.071. Because Δf_e of the fuselage was found using two different methods, the average was taken, which gave a value of .967. This value is estimated for a fuselage is assumed to be a perfect airfoil, but that is not a case. Additional drag has to be accounted for. There is a 10% additional drag for the interference of the wing and fuselage; 5% additional drag for the interference of vertical tail and the fuselage; 5% additional drag for the roughness and 3-D model; 5% additional drag for the doors, gaps, etc. This summed up to 25% additional drag to the fuselage which gives a Δf_e value of 1.212 for the fuselage.

$$Re = \frac{\rho V D}{\mu} \tag{137}$$

$$C_{Df} = \frac{.455}{(\log Re)^{2.58}} \tag{138}$$

$$C_{D_{wet}}/C_{F_B} = 1 + 1.5\,(d/l)^{3/2} + 7\,(d/l)^3 \tag{139}$$

$$\Delta f_e = S_{planform} * C_D \tag{140}$$

$$C_{D_{wet}}/C_{F_B} = 3(l/d) + 4.5\,(d/l)^{\frac{1}{2}} + 21(d/l)^2 \tag{141}$$

Table 2 - 21 Reynolds Number C_{DF}

Reynolds Number	Re	Coefficient of Skin friction Drag
		CFb or CdF
Fuselage	40367186.9	0.00242451
Wing	8121870.861	0.003106088
Horizontal Tail	4438715.572	0.003432367
Vertical Tail	5853409.358	0.00327734
Nacelles	4537740.804	0.003419635

For the wing profile drag, a different method was taken. The C_D of the wing was obtained using data tested for the NACA2412 because that was the airfoil used. Because laminar flow can't be assumed for this case, the fair curve method was used. **Fig. 2-60** shows how this was done. A C_D value of .008 was found. **Eqn. (140)** was used to find Δf_e, but this is the gross value has to take the wetted area into account. The Δf_e was multiplied by the ratio of the net wetted area of the wing and the gross area of the wing. This yields a Δf_e value of 1.2543 for the wing. Just like the fuselage, additional drag has to be accounted for because the wing is not a perfect airfoil. 10% additional drag for the interference of the wing and fuselage; 5% additional drag for the roughness and 3-D model; 5 % for the control surface, gaps, etc. Summing up all these values, the total Δf_e of the wing was

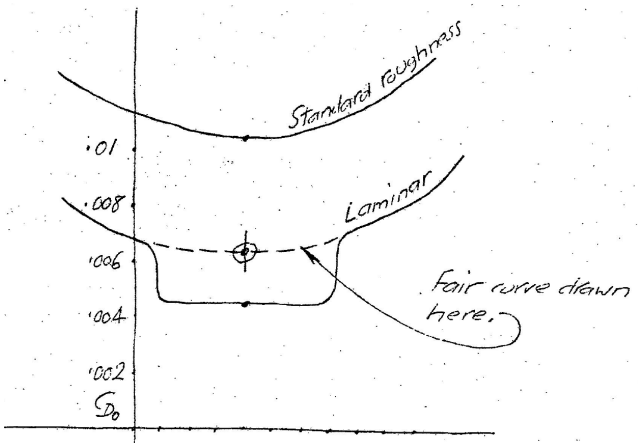

Figure 2 - 60 Fair Method to Obtain CD of Plan form

found to be 1.443. Value of Δf_e for the horizontal tail was found using the same method as the wings. NACA0012 airfoil was used for the horizontal tail. Using the fair curve method and **Fig. 2-44**, a C_D value was found to be .008. **Eqn. (140)** was used to find the value of Δf_e, but it the net wetted area was also accounted for. A total of 20% additional drag was added to the final value of Δf_e: 10% for horizontal and vertical tail inference; 5% for roughness and 3D- model; 5% for the control surface, gaps, etc. The total Δf_e value of the horizontal tail is then equal to .429.

$\Delta f_e$for the vertical tail was found using the same method as the horizontal tail and wings. NACA0012 airfoil was used for the vertical tail, so C_D value is .008. **Eqn. (140)** and accounting the net wetted area was used to findΔf_e. A total of 15% additional drag was added to the value of Δf_e: 5% for the interference of the fuselage and vertical tails; 5% for the roughness and 3-D model; 5% for the control surfaces, gaps, etc. The total Δf_e for the vertical tail is then equal to .2445.

Δf_e of the nacelles was found using the frontal method. **Eqn. (142)** was used to find the C_D of the nacelles, using the C_{FB} value found from **Table 2-21**. This provides a C_D value of .066 which was multiplied by the frontal area of 3.76 ft^2 to obtainΔf_e. An additional 20% drag was added to Δf_e of the nacelles: 10% for the interference with the wings; 5% for the roughness and 3-D model; 5% for control surface, gaps, etc. The total Δf_evalue of the nacelles was found to be .294.

The summed of Δf_e for all the components of the aircraft is equal to 3.622. This value, however does not account for protuberances, trim and momentum drag. An additional 10% drag for protuberances was accounted; an additional Δf_e of .30 was accounted for the trim; an additional Δf_e of .04 was accounted for the momentum. The total Δf_e of the aircraft at cruise speed was found to be 4.324. This value was divided by the wing area to obtain a C_{D_0} value of .0241. To find the overall drag of the aircraft at any speed, Δf_e just needs to be multiply by the dynamic pressure. For cruise at 7500 ft, the overall drag of the aircraft was found to be 325 lbs. **Table 2-22** provides the summary of Δf_e for each component of the aircraft.

The zero lift drag coefficient for takeoff and landing was then calculated for. The drag additional sections such as gears and flaps were found. The Δf_e of gears are used for both takeoff and landing drag, but the Δf_e caused by the flaps will only be used for landing because that's the only time flaps are deployed.Δf_e can be seen in **Table 2-23**. The drag polar equations for the different configuration along with their equations can be seen in **Fig. 2-61**.

$$C_D/C_{F_B} = 3(1/d) + 4.5(d/l)^{\frac{1}{2}} + 21(d/l)^2 \quad (142)$$

Table 2 - 22 Drag Contribution

	Δf_e
Fuselage	1.212006717
Wings	1.442599048
Horizontal Tail	0.429019774
Vertical Tail	0.244491321
Nacelles	0.293909614
Protuberances	0.362202647
Trim	0.3
Momentum	0.04
Total	4.32422912

Table 2- 23 Drag Contribution of Gears

	δf_e
main gear oleos, etc.	0.7
main gear wheels	0.32
nose gear oleos, etc.	0.185
nose gear wheels	0.157
main gear doors	0.023620895
nose gear doors	0.014969688
wing fairing	0.005446997

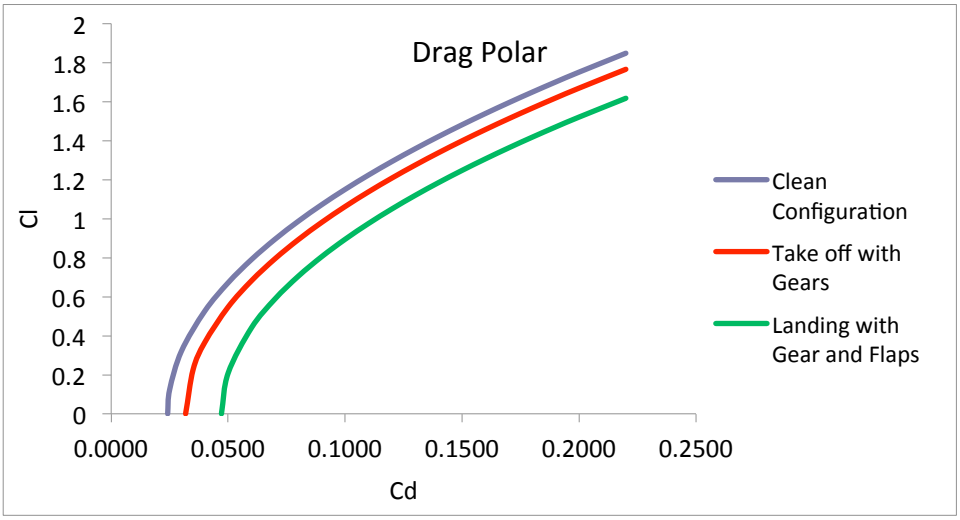

Figure 2 - 61 Drag Polar

For Clean Configuration: $Cdo = .0241 + .05732CL^2$
For Take-off with Gears: $Cdo = .0319 + .603CL^2$
For Landing With Gears and Flaps: $Cdo = .0471 + .0661CL^2$

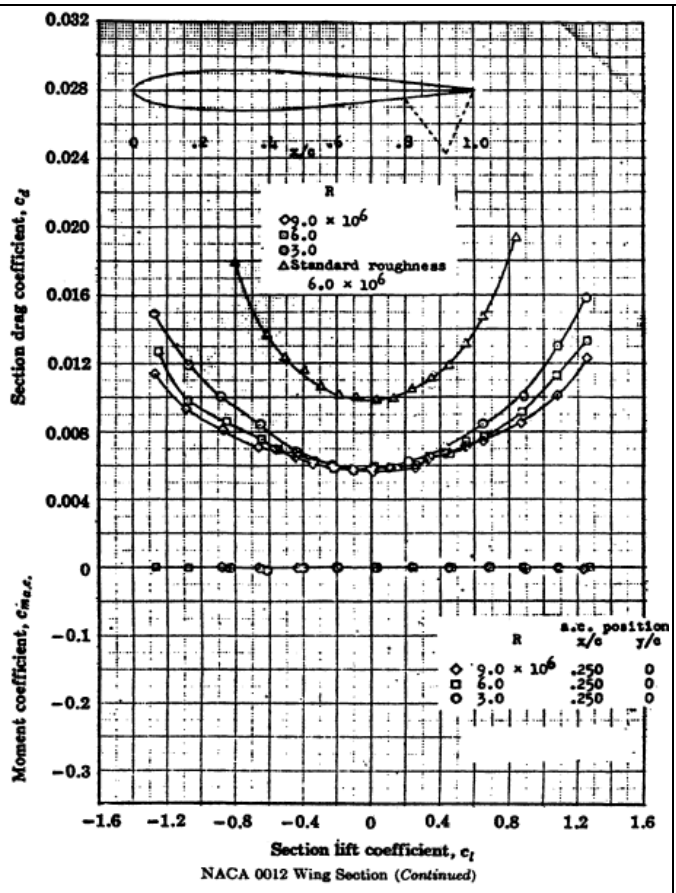

Figure 2 - 62 NACA 0012 Wing Section[4]

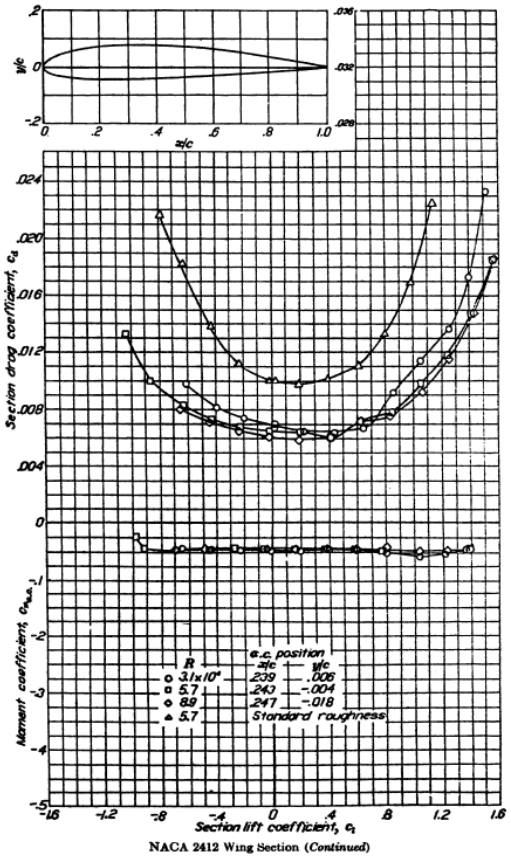

Figure 2 - 63 NACA 2412 Wing Section[4]

Span Loading

Span loading is the breakdown of how Cl varies throughout the wing. This was done by finding the sectional wing lift coefficient of the wing by using data based on taper and Aspect Ratio. The semi span location was broken down into 9 points. At each of these points, the La and Lb were found, the basic and additional loading coefficients, respectively. Once these values were found, the chord at each spanwise was calculated. The coefficient of La was found by multiplying La by the ratio of the wing area and wing span, and then dividing by the chord at the spanwise. This can be model in Eq. (143). Cl_b was found using Equation (144), where ε is the twist angle. The sectional clmax was assumed to be constant throughout the wing at 1.65 for the NACA 2412 airfoil. Subtracting from this the c_{lb} and dividing it by the c_{la} provides us with information needed for the overall aircraft C_{Lmax}. This was found by taking all these values at different spanwise, and finding out the minimum value at different spanwise. This was found to be C_{Lmax}=1.528. The C_{LmaxTO} was found to be also 1.528 because flaps were not used for takeoff. For C_{LmaxL}, however, a single slotted flap was used at 30 degrees to achieve the desired $C_{LmaxL.}$The ΔC_{Lmax} found for the flaps was .328 using values from **Fig. 2-64** and **2-65**. The span loading plot show Cl is varying throughout the wing. **Figure 2-66** provides the span loading of the wing

$$c_{L_{a1}} = \frac{S}{cb} L_a \tag{143}$$

$$c_{L_a} = \frac{\epsilon a_o S}{cb} L_b \tag{144}$$

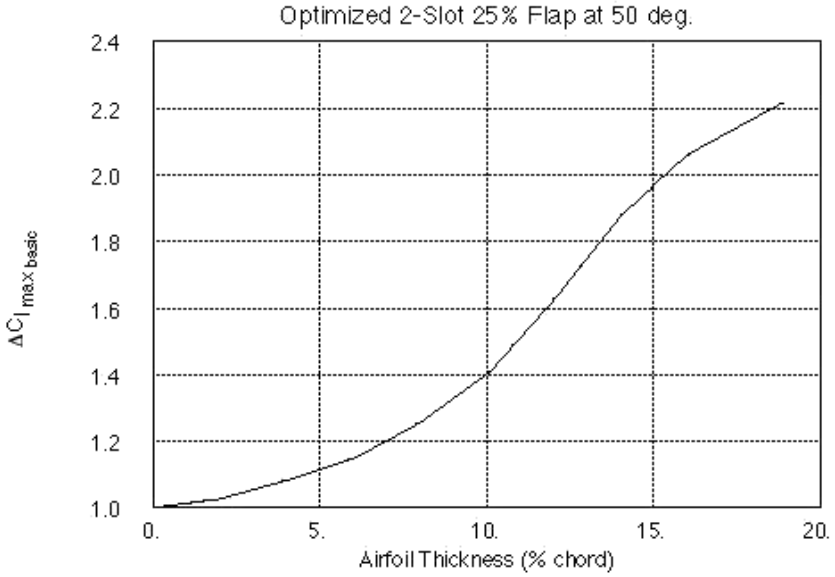

Figure 2 - 64 C_{Lmax} Increments Due to Flaps

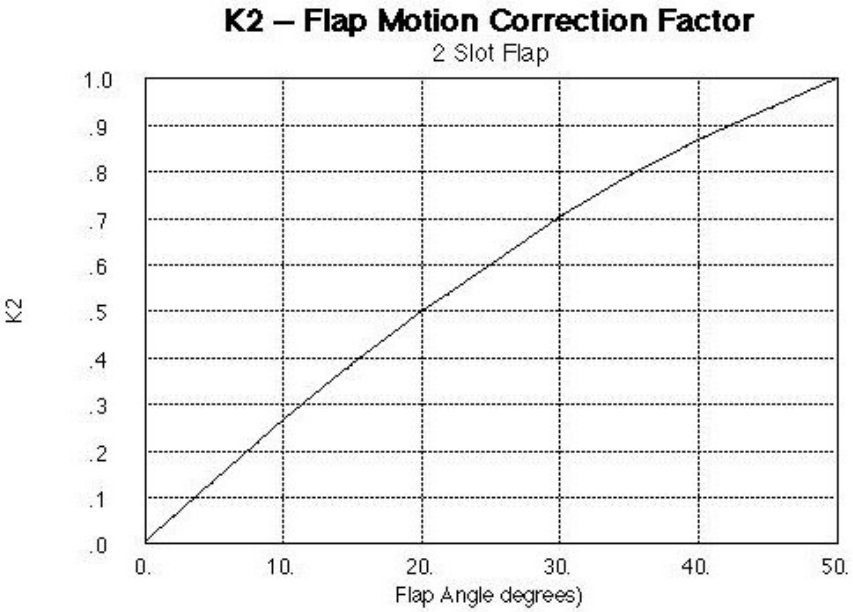

Figure 2 - 65 Flap Motion Correction Factor

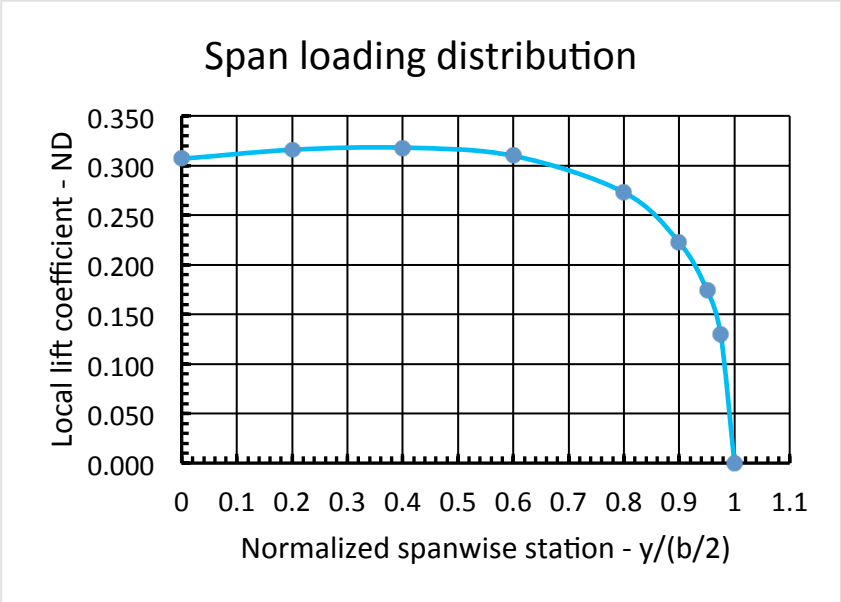

Figure 2 - 66 Spanwise Loading Plot

The angle of attack of the wing corresponding to any value of the wing lift coefficient is found using Equation (146), where *a* was found using Equation (145). *f* was found through Fig. 2-50 for an aspect ratio of 7 and a taper of .67 to be 1.002886. J was found to be -.422246 using Figure 2-51. Using these values α_s is found to be 1.643 degrees for cruise.

$$a = f\frac{a_s}{1+(57.3a_s/\pi A)} \tag{145}$$

$$\alpha_s = \frac{C_L}{a} + \alpha_{l_{0_s}} + J\epsilon \tag{146}$$

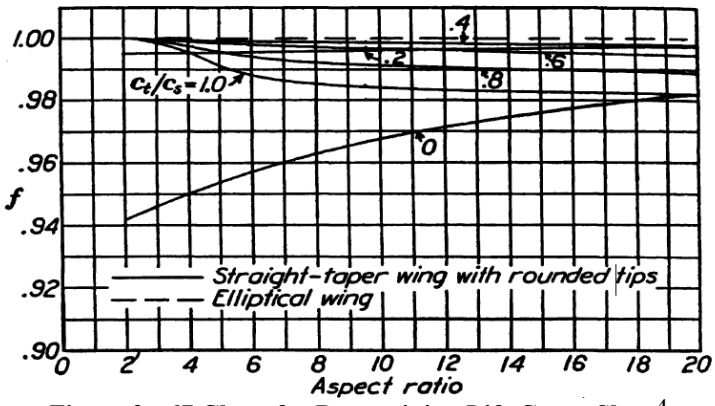

Figure 2 - 67 Chart for Determining Lift-Curve Slope[4]

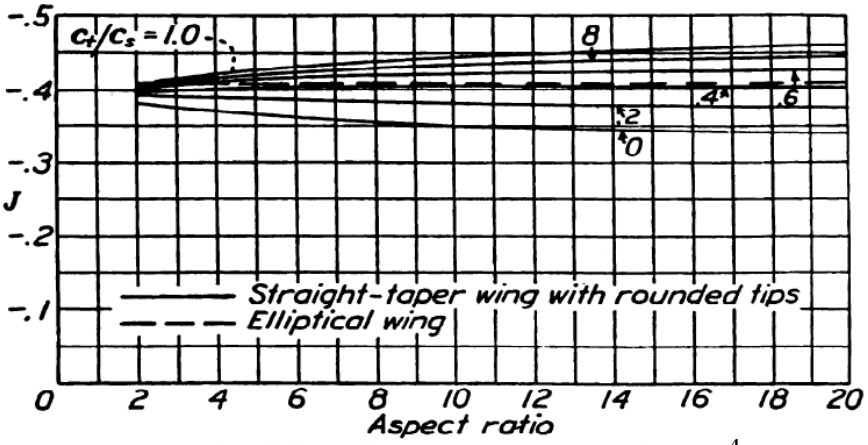

Figure 2 - 68 Chart for Determining Angle of Attack[4]

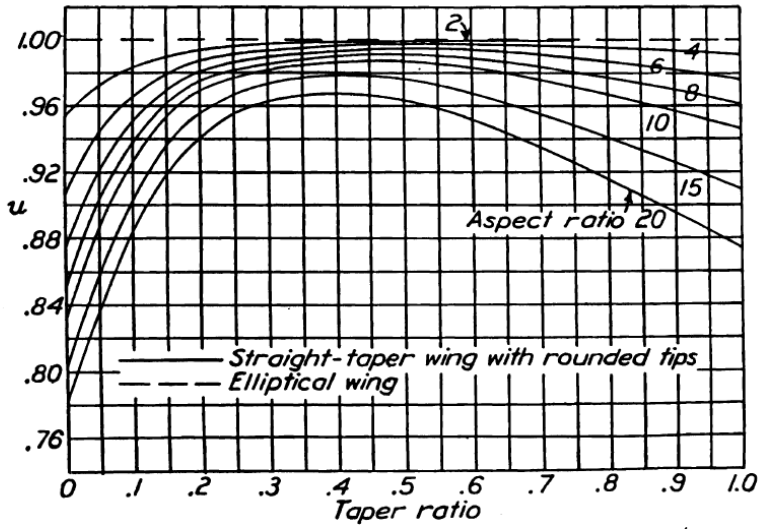

Figure 2 - 69 Chart for Determining Induced-Drag Factor[4]

Performance Analysis

In the process of preliminary design for an aircraft it is necessary evaluate the configuration of the aircraft and see if it meets all of the mission requirements so we can then make the necessary changes to the configuration until all of the mission requirements are met. There are also airworthiness regulations that are described by FAR requirements that must be considered. Although FAR regulations are considered for most cases in testing mission requirements, this section will focus mainly on the evaluation of those specific mission requirements for our preliminary aircraft design before going more in depth with performance analysis of other parts of the mission profile. To start our analysis we must split the mission into segments to evaluate the conditions of each section separately. A general representation of our mission profile is provided is **Fig. 2-70**.

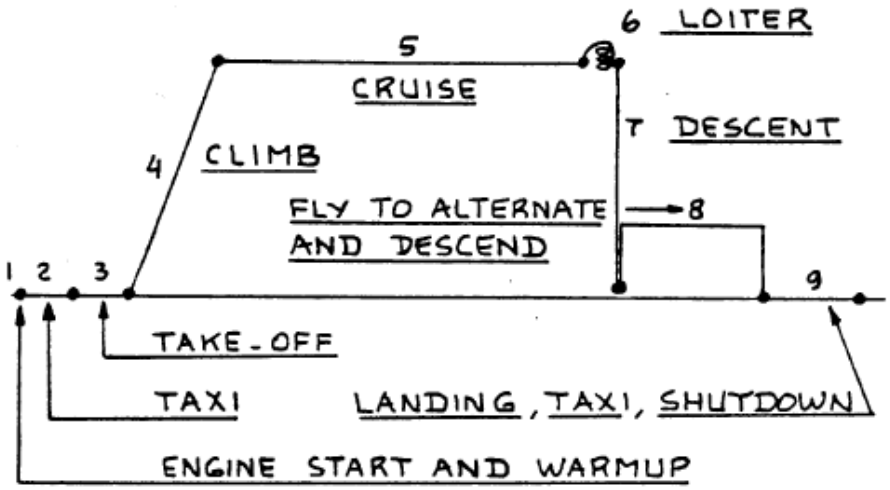

Figure 2 - 70 General Layout for Aircraft Mission Profile[2] [Reference Figure 1-1]

In this first run at performance analysis we will not be looking at every mission profile segment in detail but rather those segments whose conditions apply to the specific mission requirements we are given. Based on the mission requirements we are evaluating there will be four main segments that will be used for analysis of our aircrafts performance in certain required tasks. These mission profile parts to be used in this section are as follows: Takeoff, Climb, Cruise and Landing.

1. Takeoff

For the takeoff portion of the mission profile the takeoff distance required will be the main focus of the performance check. Our mission requirement states that the takeoff distance must be no more than a distance of 1,500 ft. In order to calculate the takeoff distance we can use the following Eqn. if we assume that the landing distance is less than or equal to the takeoff distance.

$$S_{TO} = f_{TO}h_{TO}[\left(\frac{1}{\gamma_{LOF}}\right) + ((\frac{V_3}{V_{STO}})^2\left(\frac{W}{S}\right)\left(\left(\frac{T}{W}\right) - \mu'\right)^{-1} + 1.414)/(h_{TO}\rho g C_{Lmax_{to}}(1 + 1.414\gamma_{LOF}))] \quad (143)$$

Where,

$$T = 4.6P_{TO}((\sigma N D_P^2)/P_{TO})^{1/3} \quad (144)$$

$$\mu' = \mu_g + .72(\frac{C_{D_o}}{C_{L_{max}}}) \quad (145)$$

$$\gamma_{LOF} = .9(\frac{T}{W})_{TO} - (\frac{.3}{\frac{1}{A^2}}) \quad (146)$$

These Equations have many terms that change with altitude so for these calculations we will be using an altitude of the Denver airport since our aircraft will need to land in Denver. This altitude that will be used for calculations is 5,335ft and the corresponding air density is .0652 lb/ft^2. For these calculations we will also use the case of engines at max power for the thrust portion of the Eqn.. Apart from these values that can be calculated for our specific aircraft there are a few terms given by FAR 23 requirements. The definition of the FAR 23 requirements are shown in **Fig. 2-56** from Roskam part VII.

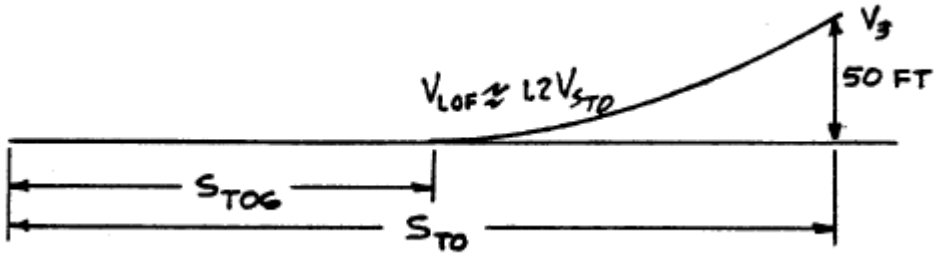

Figure 2 - 71 Definition of FAR 23 Requirements[1]

For our case the of our aircraft the values included in the takeoff distance Eqn. of f_{To} which depends on the obstacle height, h_{TO} which is the obstacle height, and ($V_3/V_{s,TO}$) which is the ratio of the speed at the obstacle height to the stall velocity at takeoff conditions are all provided by Roskam for FAR 23 requirements. These values are given to be 1, 50ft, and 1.3 respectively. With these values and the values obtained by our configuration and the atmospheric conditions at takeoff altitude, we obtain our value for the necessary takeoff distance that we can then compare to the stated mission requirement. The design must be altered if the computed value has a 5% discrepancy to the required takeoff length. The results of calculations for our aircraft yield a necessary take off distance of 1194.33 ft, this distance is smaller than the required 1,500 ft so we can claim that this mission requirement is met.

2. Climb

For the mission segment of climb there will be two mission requirements to be checked. The first will be the service ceiling which is the altitude at which the rate of climb of the aircraft first drops to 100 ft/min, the mission requirements state that the service ceiling must be above 15,000ft. The second mission requirement states that the rate of climb of the aircraft with one engine inoperative at sea level must be no less than 250 ft/min.

To find the service ceiling of our aircraft we must first vary the rate of climb of the aircraft with altitude to see what altitude corresponds to a value for rate of climb of 100 ft/min. From Roskam volume VII the following Eqn. is provided for calculating rate of climb for propeller driven aircraft:

$$\mathrm{ROC} = 33000\left(\frac{\eta_p}{\frac{W}{P}} - ((W/S)^{1/2}/(19\left(\frac{C_L^{3/2}}{C_D}\right)\sigma^{1/2}\right) \tag{147}$$

Many of the terms in this Eqn. vary with altitude so each will have to be considered when making a linear curve of rate of climb versus altitude. If we assume steady climbing flight though we can use a more simple relation using the difference between the power available and the power required:

$$\mathrm{ROC} = (P_{available} - P_{required})/W \tag{148}$$

This relation makes evaluation of rate of climb changing with altitude much easier. As we increase altitude the power available will increase while the power required will increase, both of these changes are due mostly to the change in air density as you increase altitude. From these changes and the above relation we can see that as would be expected the rate of climb decreases with altitude. These two terms can be defined as shown below to get values at several different altitudes.

$$P_{Req} = \sqrt{\frac{2W^3}{(\rho S(\frac{C_L^{3/2}}{C_D})}} \tag{149}$$

And,

$$P_{avail} = \eta_p P \tag{150}$$

Where P in the power available relation is shaft horsepower. In order to find the point at which the rate of climb drops to 100ft/min we construct a curve for the rate of climb vs altitude, this is shown in **Fig. 2-55**.

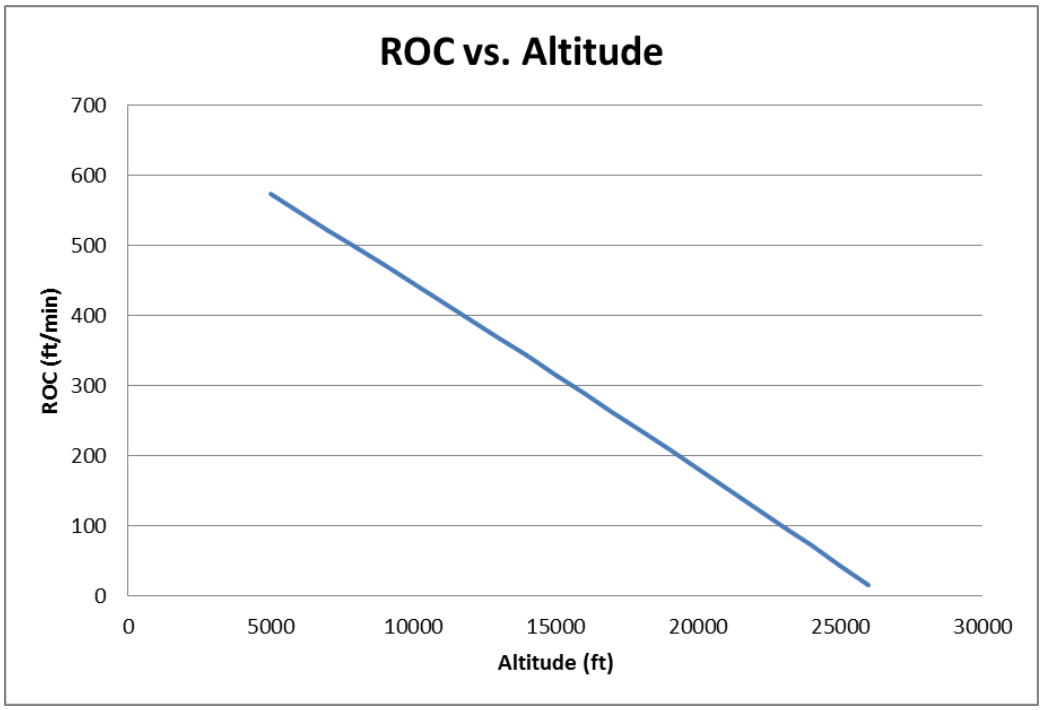

Figure 2 - 72 Rate of Climb vs. Altitude

From the linear curve shown in **Fig. 2-72** we can obtain our value of altitude for which the rate of climb is 100 ft/min. In analyzing the plot we see that the rate of climb value of 100 ft/min corresponds to an altitude of just about 23000 ft. This is the service ceiling for our aircraft and as the value is higher than the needed altitude of 15000 ft., our mission requirement is met.

The next step in evaluating the climb of this aircraft design is to check the rate of climb with only one engine operating and compare with our needed value of 250 ft/min. In doing this we will assume that the inoperative engine is feathered and so does not create much additional drag. So repeating calculations but using sea level conditions and half power (because of the one engine inoperative) we can get our value for OEI case of rate of climb. In performing

these calculations a value of 291.86 ft/min is obtained as the rate of climb for this case. Comparing this to the mission requirement our value of 291.86 is greater than the minimum value 250 ft/min required, therefore we can conclude that this mission requirement is also met.

3. Cruise

The conditions for the mission segment of cruise will be used to evaluate two more of the stated mission requirements. These requirements are that the cruise velocity at 75% power must be above 140 kts. and that the total range should be at least 725nm. To find the cruise speed at our cruise conditions we can use Loftin's formula for cruise velocity shown below.

$$V_{CR} = [\left(\frac{\frac{W}{S}}{\frac{W}{P}}\right)((\sigma C_{Do})/\eta_P)]^{1/3} \tag{151}$$

or the alternate version of:

$$V_{CR} = [(1100HP\eta_P)/(\rho S(1.1)C_{Do})]^{1/3} \tag{152}$$

Using this relation the velocity is given in unit mile per hour and must be then converted to knots in order to compare to the stated mission requirement. For the calculation of our cruise speed we must consider the case of engines running at 75% power and atmospheric conditions at an altitude of 7,500 ft. For this case the value of cruise velocity obtained from calculations is 133.829 kts., this value is slightly less than our required minimum of 140 kts.. Therefore our configuration does not meet this particular requirement yet and the design must be altered with this in mind. The direction in which the cruise velocity acts with respect to the other forces acting on an aircraft for steady symmetric flight is shown in **Figure 2 -73.**

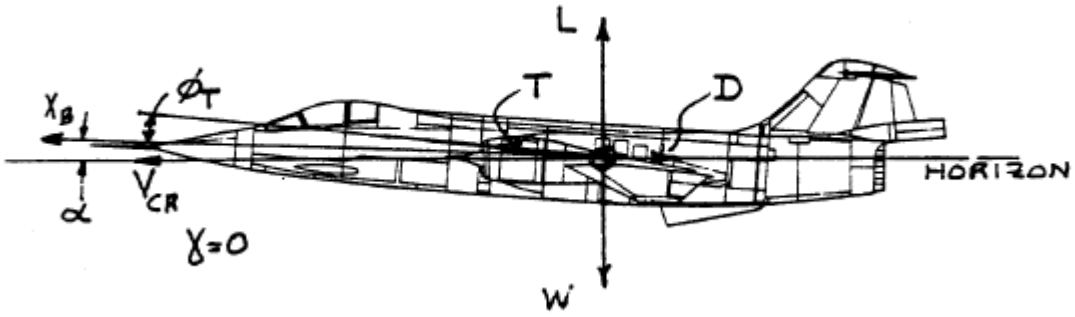

Figure 2 - 73 Forces Acting on Aircraft for Steady Symmetric Flight[2]

The next step is the evaluation of the range of our airplane given our aircraft geometry and flight conditions with the amount of fuel we are allowed to carry. The amount of fuel for the aircraft is taken from the available weight of the fuel of 335 lbs. which corresponds to 55.7 gallons of fuel. The range of the aircraft configuration being analyzed can be found from Equations provided by Roskam for propeller driven aircraft at constant cruise velocity. So the Eqn. for range of our particular configuration is given to be:

$$R = 326\left(\frac{\eta_p}{C_p}\right)\left(\frac{L}{D}\right)\ln\left(\frac{W_i}{W_e}\right) \tag{153}$$

Where, W_i and W_e are the initial and ending weights respectively so only differing by the weight of fuel [Reference Eqn. (5) & Table 1- 2]. Using the relation shown, range is given in nautical miles. In order for this range Eqn. for constant cruise velocity to be valid we must make the assumption that the values η_p, C_p, and L/D remain relatively the same regardless of type of cruise. This assumption is usually valid so the given Eqn. will be the relation used to calculate our aircrafts range and compare to the mission requirement of a minimum range of 750nm. Using the shown Breguet range Eqn. to calculate the range we obtain a value of 1046.5nm. this value is greater than our required 750nm so we can say that the mission requirement for range is met.

4. Landing

The landing portion of the mission profile is the last segment to be evaluated in analyzing the performance of our aircraft. There are regulations given for landing velocities and distances, the definitions of the FAR 23 requirements are shown in **Fig. 2-59**.

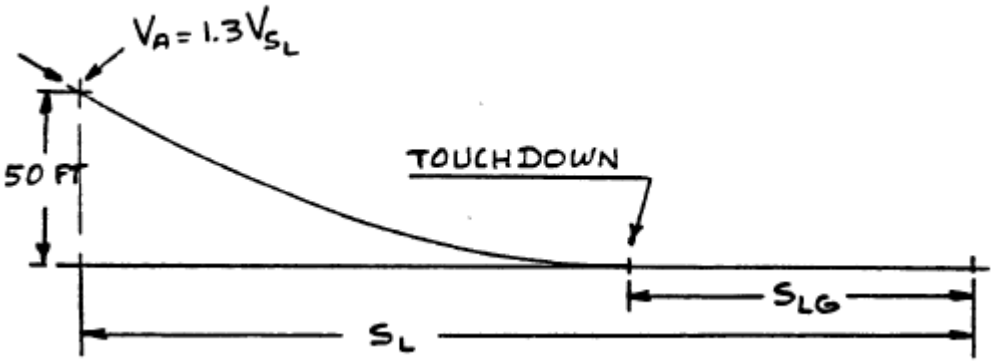

Figure 2 - 74 Definition FAR 23 Landing Requirements[2]

This will help in evaluating different aspects of landing in the future but in the evaluation of the preliminary design we will only focus on the mission requirements for the moment. The mission requirement that relates to landing conditions is the requirement of a stall speed of less than 48kts.. The stall speed during landing is assumed to be the lowest value of stall speed so this case serves as the best constraint. Since we are considering the case of landing for the stall speed calculation, we assume that the thrust will be zero. With this assumption the stall speed is given as [also see **Eqn. (21)**]:

$$V_S = \left(\frac{2W}{\rho C_{Lmax} S}\right)^{1/2} \tag{154}$$

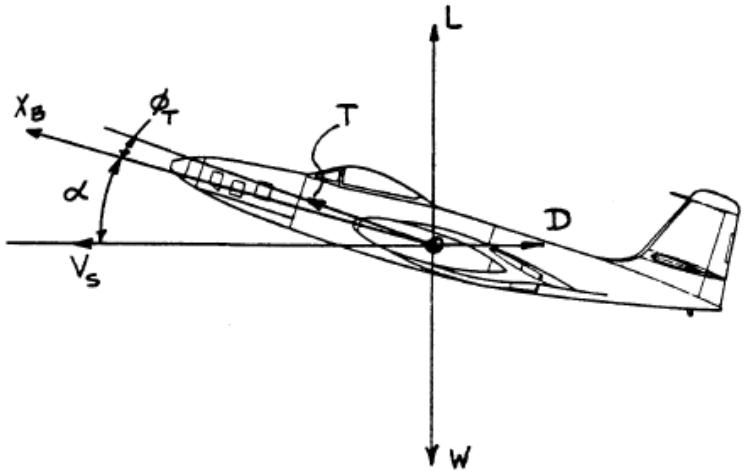

Figure 2 - 75 Forces on an Aircraft in 1-g Stall[2]

Fig. 2-75 above shown the direction in which V_s acts in reference to the forces acting on the aircraft. The 1-g stall speed shown in the Fig. and calculated using the listed Eqn. is usually conservative by about six percent compared to the stall speed determined from certification flight tests.

For calculation of the stall speed at landing we will be using the density and maximum lift coefficient corresponding to our landing altitude. For finding the minimum stall speed we use conditions for sea level because this will yield the lowest stall speed due to the higher density at sea level. In using these conditions to calculate the stall speed we obtain a value of a 47.64 kts.. This value is barely less than the required stall speed maximum value of 48 kts. stated in the mission requirements so this mission requirement is met for our preliminary design.

5. *Flight Envelope*

The flight envelope of the aircraft or otherwise known as a V-n diagram is a graph that shows the aircraft limit load factor with respect to velocity. The V-n diagram is the border of the flight regime that is shaped by the aircraft aerodynamics, propulsion, structure, and dynamics. This area of the flight envelope is basically a constraint for pilots because if the aircraft is flown outside the flight envelope then there is a good chance there will be a problem like the plane will stall or the load will be too much for the structure to handle. The V-n diagram has two separate parts overlapping each other, one case of load factors when not considering gust and another one where the gust contribution to the load on the aircraft is considered. A V-n diagram usually consists of two curves and a couple linear segments. The V-n diagram based on our aircraft data is shown in **Fig. 2-76.**

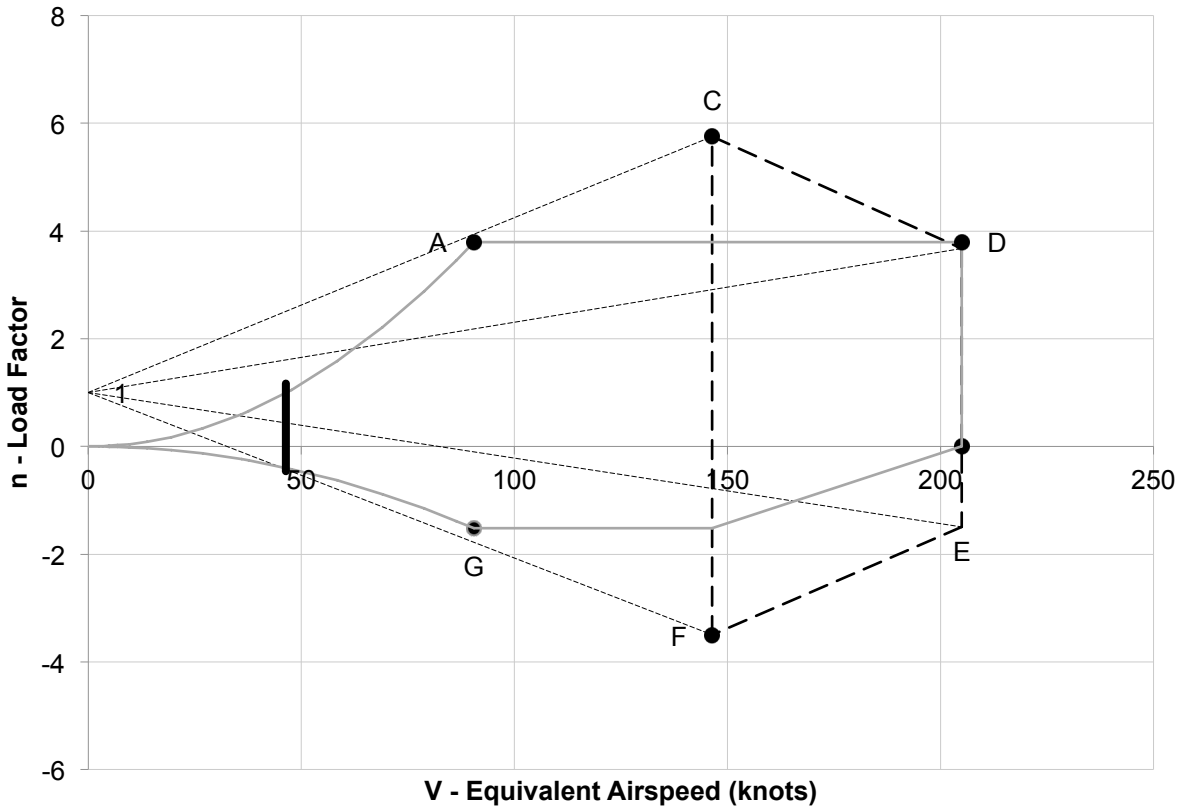

Figure 2 - 76 Flight Envelope (V-n) Diagram

The curves on the left side of the plot are representative of the aerodynamic limit on load factor that is constrained by stall. The top segment of the diagram is a curve that is based on a variation of the Eqn. for stall speed that is changed into the form shown below.

$$n_{max} = (V^2 \rho S C_{Lmax})/(2mg) \tag{155}$$

Any point above the curve made by this Eqn. is the stall area and is the upper constraint for aircraft maneuverability. This curve is cut off by the very top load factor constraint which for our case is 3.8; this is the horizontal line at the top of the diagram. The far right vertical line constraint is the speed that should never be exceeded in this aircraft, we take this to be the dive speed and from FAR 23 requirements the regulation is the dive speed is more than 140% of the cruise speed.

The dotted lines shown in **Fig. 2-76** are the gust contributions to the V-n diagram. From the FAR 23 requirements, aircraft must withstand 50 ft/s of gust up to 20000 ft, after that gust velocity decreases to 25 ft/s. Also an aircraft must safely fly at maneuver speed when gust velocity reaches 66 ft/s. To obtain the gust induced load factor as function of gust speed we use the following Eqn.:

$$\mathrm{n} = 1 + (k_g V_g V_E \mathrm{a}\rho\mathrm{S})/(2\mathrm{W}) \tag{156}$$

where,

$$\mathrm{k_g} = (.88\mu_g)/(5.3 + \mu_g) \tag{157}$$

And

$$\mu_g = (2m)/(\rho C_{bar} a S) \tag{158}$$

From these relations we obtain our gust contribution to the flight envelope or V-n diagram and can plot it in its entirety as previously shown. From this diagram we now have a visual representation of the parameters at which our aircraft should operate and where it should not in order to maintain safety.

Carpet Plots

Once the synthesis code is created which allows us to get every value we may need from simply putting in the geometry of our aircraft design, we can use this code to construct a carpet plot for our aircraft and determine our most desirable geometry and necessary engine horsepower. A carpet plot is a way to see which geometries can be used for the aircraft that will allow it to complete its required mission. For the construction of a carpet plot we evaluate the aircraft at each segment of the mission profile for different geometries and wing loadings. The main segments of the mission we will be evaluating are those of climb, cruise, and decent because these segments make up the most of the total mission range and so also use the most amount of fuel. At each of these segments we calculate the fuel consumed for that section so we can get the total amount of fuel we need to use in order to complete the mission. For each point on the carpet plot we pick a taper ratio and aspect ratio to use for calculations as almost all characteristics of the aircraft will change with the geometry of the wing and then check to see if it is possible to complete the mission. For every geometry, we evaluate we find the fuel necessary and from that we can find the lowest possible takeoff weight by combining the weight of the airplane from that geometry and the weight of the total fuel required to fly the mission. This value of the minimum takeoff weight is found because this will be used as the Y-axis of the carpet plot so we can compare different geometries and see which ones require the least amount of weight which translates to the lowest cost. While creating the carpet plots we must also check and make sure that the geometry will meet our basic mission requirements such as minimum stall speed and minimum cruise speed. After initial calculations and performance check we know that it is not possible to meet our cruise speed requirement of 140 knots no matter what geometry is used as long as we use the Rotax engine with a maximum of 100 hp. Because of this we use the supercharged version of this engine which has a maximum horsepower of 132 hp. With the use of this engine we meet the cruise speed requirement for almost every geometry we would want to consider and so the new constraint of the carpet plot is that of the minimum stall velocity. With this in mind we can now construct the carpet plots for different wing loadings to see what kind of geometries would be most desirable for our mission. The final product of our carpet plots for several wing loadings and varying taper and aspect ratios is shown in **Fig. 2-62**.

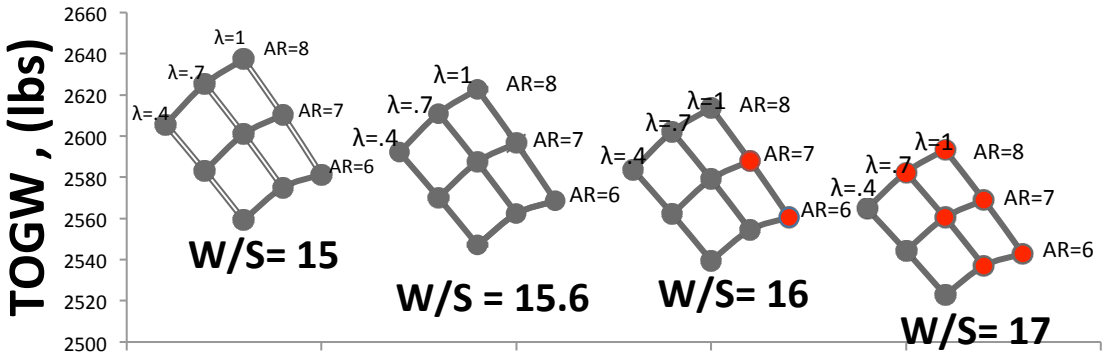

Figure 2 - 77 Carpet Plots of Aircraft for Varying Wing Loadings

The carpet plots above show what type of geometries are possible for several wing loadings. The points that are marked in red are the geometries for which the aircraft cannot meet the minimum stall speed requirement but can still complete the mission otherwise. From this we can not only see which values of taper and aspect ratio that we are able to choose to complete our mission, but also how they affect the takeoff weight and the margin for which they meet or do not meet the main constraining mission requirement of landing stall velocity. When picking our final geometry we must also take into consideration the structure of the aircraft and how these theoretical geometries will affect the structure and location of the center of gravity. From the carpet plots shown and keeping in mind how it will affect the other aspects of the aircraft we ended up picking a point that is quite typical for many aircraft and will not mess with the structural integrity of our aircraft and will not shift our center of gravity so much that it will affect our stability. The point we decided to use is for a wing loading of 15.6 and the geometry wing can be defined as having a taper ratio of .67 and an aspect ratio of 7. This point is not right on the line or too close to the points at which we do not meet the requirements so it may not be the very best geometry in terms of weight but we know we meet all requirements by a decent margin.

3D Model

Once the sizing of the design was set a three dimensional modal was the next step to take in building the aircraft. Three dimensional models to scale are a good way to calculate the performance of the aircraft to an accurate scale. The scale aircraft can be input into a wind tunnel for testing of drag and performance, even the wing itself its boundary layer performance. Furthermore, to design the three dimensional model to scale the software of SOLIDWORKS was use. The first step in creating the 3D model was to make sure it was to scale ant that was simply done by placing the 2D scale model views into SOLIDWORKS and tracing the outer layers. This was the fastest method known to create a good representation of the actual aircraft. The first step was to build the Fuselage and it was done by lofting the top and side view and a rectangular wing was also lofted before implementing the taper ratio and can be seen in **Figure 2 - 78.**

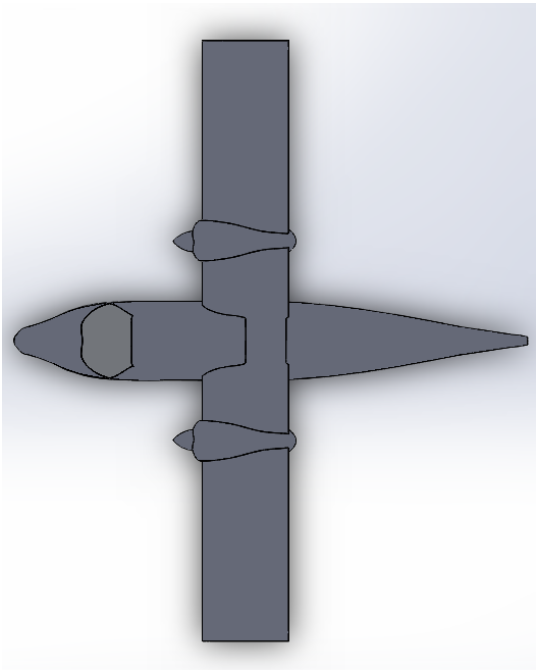

Figure 2 - 78 Model Fuselage and Main Wings Top View

Moreover, gears, nacelles, propellers, windshield, and empennage was made as a part and matted into each other to complete the entire aircraft construction and can be seen in **Figure 2 - 79.**

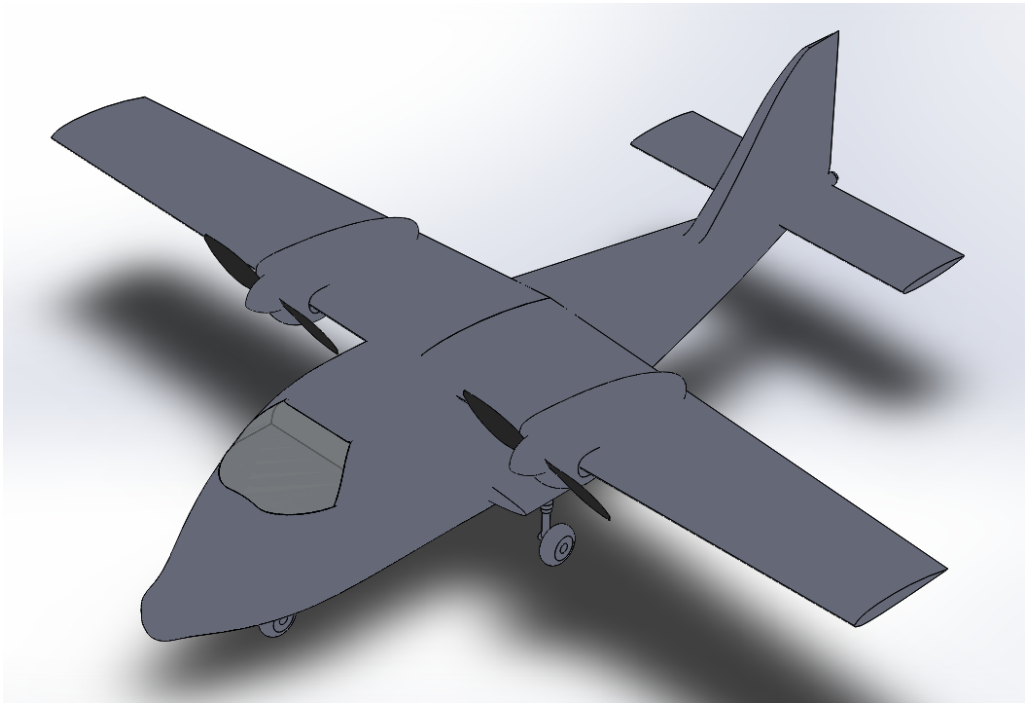

Figure 2 - 79 Full Aircraft Isometric View

The gears where constructed with historical data. Furthermore, the wheel was decided to be 6.5 x 10 by looking at other model aircraft that where similar in size and weight of the I.A.D aircraft design. This gear can be seen in **Figure 2 -80.**

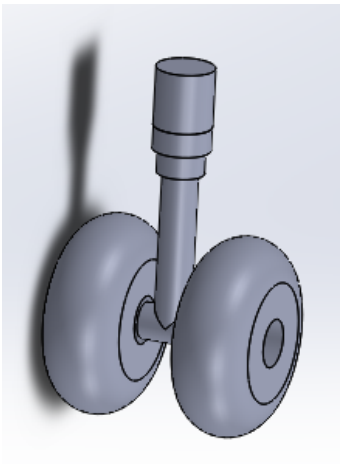

Figure 2 - 80 Gear Model Preliminary 3D Structure

Interior Structure of Aircraft

After completing the 3D model the interior structure was needed to be constructed. Using Roskam 3 and historical data beams, spars, ribs, where drawn into the isometric view of the I.A.D model. As seen on **Figure 2 -70** there is less ribs by the end of the wing because there is no need for much structure at the tip of the wing which decreases weight in total. Larger ribs where design between the fuselage and the nacelle to be able to support the engine. Moreover, the engine was also drawn with the propeller mechanism design. Also, struts and structure was added to the fuselage to support it by looking at historical data and making educated decision in drawing it. Finally, the empennage was constructed also by looking at historical data form Roskam volume 3 and deciding how much structure the empennage needed.

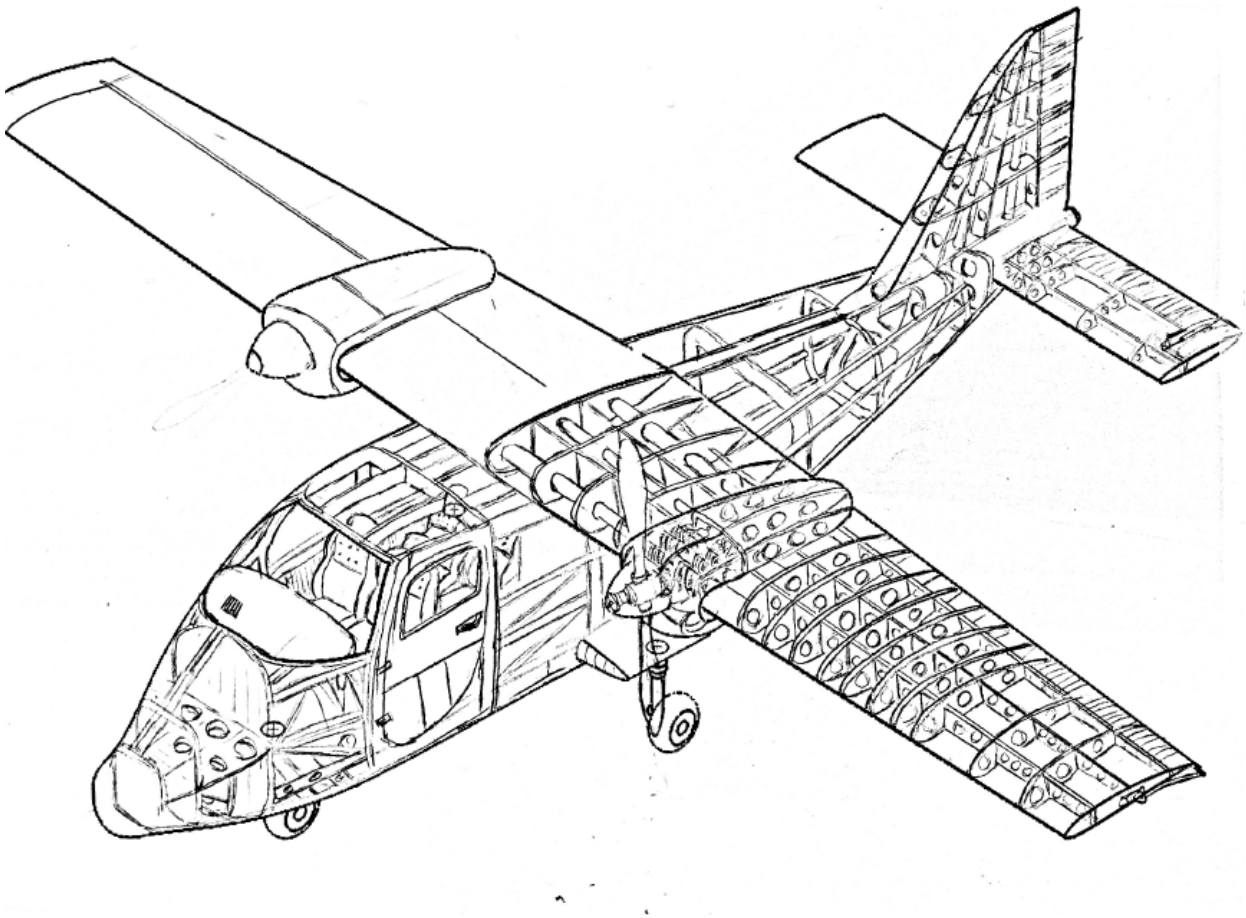

Figure 2 - 81 Conceptual Interior Structure of Aircraft

Final Design Performance

Once we have our final geometry we then repeat the performance analysis from the preliminary design so that we can make sure that this final design will meet all the requirements that we need it to. In going through these calculations we get new values for things such as the required takeoff distance and the service ceiling for our design. The calculated values for all mission requirements are shown in **Table 2 - 21**.

Table 2 - 24 – Calculated values corresponding to mission requirements for final design.

TakeOff Distance				
1380.691	ft.	≤	1500	ft.
Cruise Speed				
146.4685	kts	≥	140	knots
Dry tank Range				
893.7308	nm	≥	725	nm
Landing Stall				
46.43625	kts	≤	48	knots
ROC OEI				
263.7242	fpm	≥	250	ft/min
Service ceiling				
≈23000	ft.	≥	15000	ft.

From the above table we see that all of the mission requirements are met by our final design and so we can say that the aircraft we have designed could be expected to perform well in all areas of the mission that it would be tasked with completing.

Center of Gravity Envelope (Potato plot)

After having the forward and aft c.g. range obtained from **Fig. 2-14** the center of gravity envelope is constructed. The c.g. location with the empty weight is then plotted. Then the shift in the c.g. location with the added payload is calculated. The c.g. locations having total weight and only fuel weight is then plotted in the graph. The graph is depicted in **Fig. 2-82.**

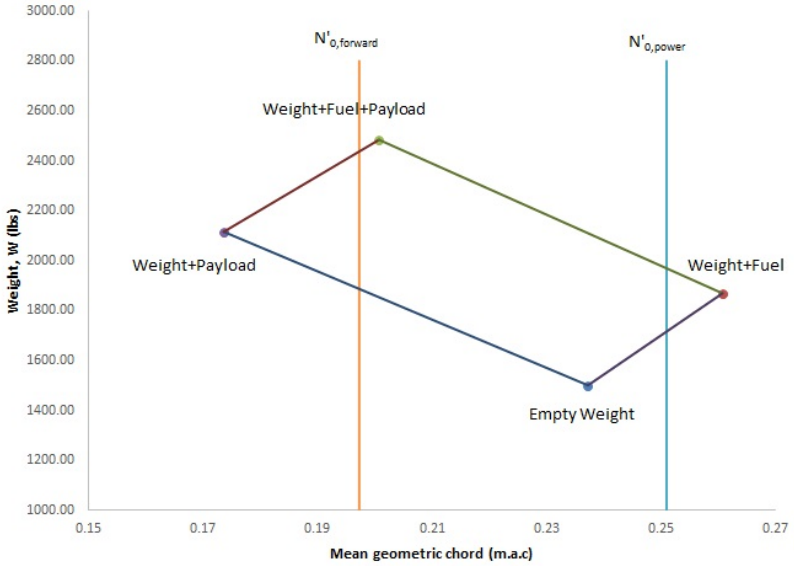

Figure 2 - 82 Potato Plot (C.G. Envelope)

It is seen from the above figure that the empty weight and the total weight locations are within the allowable c.g. shifting range. However, the weight with payload and the weight with fuel positions are outside of the c.g. shifting range. This indicates that our current configuration is unable to meet the required c.g. envelope to keep the aircraft statically stable in all flight conditions. It is also noticed from the above figure that the c.g shifts aft when fuel is added, this is because the fuel tank position is located aft of the center of gravity of the aircraft at all flying conditions. The proposed solution to move the aft most point (Weight+Fuel) inside the range is to increase the weight of the fuselage at the back. Other solutions would be to increase the empennage sizing or to increase the fuselage length. The latter solution would increase the drag on the aircraft and might affefct the performance, so the first solution is kept as the primary option.

To move the forward most point (Weight+Payload) behind the proposed solution is to move the position of the cockpit aft of the current position. It depends on how much change of the position is needed, and it might be only a couple of inches.

IV. Conclusion

This report has briefly presented the content comprised in Dr. Jan Roskam's Airplane Design Volume 1 and 2 and the procedures used to design a General Aviation Twin Engine Aircraft to be mainly utilized as a trainer aircraft. Being this the preliminary design, more iterations must occur in order to meet both costumer/design requirements and FAR requirements. Summarized here are some of the items to consider for next iteration. The horizontal tail area was increased to meet the stability requirements which moved the neutral points aft of the preliminary location. The ground effect was taken into the neutral point calculation which proved to be a stricter restriction on the forward c.g. limit. The stick free neutral points were also calculated which put new restrictions on the aft c.g limit. The forward and the aft c.g. limits were used to develop the c.g. envelopes. It is seen that the current aircraft configuration fails to meet the c.g. envelope entirely. Iterations and changes in the preliminary design parameters have to be met to move on forward from this point. The proposed solutions are to increase the fuselage weight at the back and to move the cockpit aft of the current location until the c.g. range is satisfied.

Appendix Tables

Table A1. Jonathan's Empty Weight Preliminary Code

Empty Weight Preliminary

Inputs (lbs)

Number of Passangers	2	410	W_Take Off (lbs) 2740
Number of Crew Members	1	205	
Weight limitations		Fuel + Payload	Landing Distance (ft) 2500
Useful Load Limit (lbs)	950		

Given (assumed from Historical Data)

Avg Weight/Person (lbs)	175	Propelent Efficiency	0.82	V_cr (Cruise Vel) (kts)	140
Avg Baggage/Person (lbs)	30	Cp	0.5	R_cr, Range (nm)	725
Total Payload (lbs)	410	L/D	11	h_cr (Cruis alt) (ft)	5000
				V_stall Lndg (kts)	48

Phases	Fuel Fractions	Historical
1 (Engine Start/ Warm Up)	W_1/W_to	0.992
2 (Taxi)	W_2/W_1	0.996
3 (Take Off)	W_3/W_2	0.996
4 (Climb To Cruise)	W_4/W_3	0.99
5 (Cruise)	W_5/W_4	0.884
6 (Loiter)	W_6/W_5	1
7 (Descend)	W_7/W_6	0.992
8 (Land/Taxi/ Shut Down)	W_8/W_7	0.992
Mff	**W_8/W_to**	**0.848**

FUEL WEIGHT Paramers	
W_Take Off (lbs)	2740.000
W_Trapped Fuel/Oil (lbs)	137
W_Operating Empty_(lbs)	1912.195
W_Operating Empty_tentative (lbs)	1912.206
W_Empty (lbs)	1570.195
W_Empty_tentative (lbs)	1570.206
Diff (lbs)	0.011
W Availble for fuel (lbs)	335
available Gallons of Fuel (Gal.)	55.7
W_F_used (lbs)	417.794
W_F_reserve (lbs)	0
W_FUEL Total (lbs)	417.794

should we subtract W_crew? W_TO = 3561.5 lbs

HISTORICAL DATA (for Twin Engines)		
A (Slope)	0.113	CL_max 1.4
B (Intercept)	1.0403	CL_max T.O. 1.6
C (We+D)/Wto)	0.7975	CL_max Ldng. 1.8
D (PayLoad+Crew)	615	*SIZING TO CLIMB REQ.*
F (lbs)	9414.9	*fig. S_wet vs. W_to*
Y = Payload Weigth	410	c 0.8635
d(C)/d(y)	0	d 0.5632
d(D)/d(y)	1	
Press Ratio, 'δ'	0.832	
Temp Ratio, 'θ'	0.966	
Dens Ratio, 'σ'	0.862	

Partial Derivatives (SENSITIVITY GRADIENTS)

Airplane Growth					
d(Wto)/R	d(Wto)/dy	d(Wto)/d(W_pL)	d(Wto)/d(cp)	d(Wto)/d(L/D)	d(Wto)/d(eta_prop)	d(Wto)/d(E)
1.60	4.05	4.05	2321.3	-105.51	-1415.42	1.82

Table A2. Typical Values for Landing Weight to Takeoff Weight Ratio

Airplane Type	W_L/W_{TO} Minimum	Average	Maximum
1. Homebuilts	0.96	1.0	1.0
2. Single Engine Propeller Driven	0.95	0.997	1.0
3. Twin Engine Propeller Driven	0.88	0.99	1.0
4. Agricultural	0.7	0.94	1.0
5. Business Jets	0.69	0.88	0.96
6. Regional TBP	0.92	0.98	1.0
7. Transport Jets	0.65	0.84	1.0
8. Military Trainers	0.87	0.99	1.1
9. Fighters (jets)	0.78	insufficient	1.0
(tbp's)	0.57	data	1.0
10. Mil. Patrol, Bomb and Transports (jets)	0.68	0.76	0.83
(tbp's)	0.77	0.84	1.0
11. Flying Boats, Amphibious and Float Airplanes			
(land)	0.79	insufficient	0.95
(water)	0.98	data	1.0
12. Supersonic Cruise Airplanes	0.63	0.75	0.88

Table A3. Correlation Coefficients for Parasite Area vs. Wetted Area

Equivalent Skin Friction Coefficient, c_f	a	b
0.0090	-2.0458	1.0000
0.0080	-2.0969	1.0000
0.0070	-2.1549	1.0000
0.0060	-2.2218	1.0000
0.0050	-2.3010	1.0000
0.0040	-2.3979	1.0000
0.0030	-2.5229	1.0000
0.0020	-2.6990	1.0000

$$log_{10}(f) = a + b\, log_{10}(S_{wet}) \tag{30}$$

Table A4. Regression Line Coefficients for Takeoff Weight Versus Wetted Area

Airplane Type	c	d
1. Homebuilts	1.2362	0.4319
2. Single Engine Propeller Driven	1.0892	0.5147
3. Twin Engine Propeller Driven	0.8635	0.5632
4. Agricultural	1.0447	0.5326
5. Business Jets	0.2263	0.6977
6. Regional Turboprops	-0.0866	0.8099
7. Transport Jets	0.0199	0.7531
8. Military Trainers*	0.8565	0.5423
9. Fighters*	-0.1289	0.7506
10. Mil. Patrol, Bomb and Transport	0.1628	0.7316
11. Flying Boats, Amph. and Float	0.6295	0.6708
12. Supersonic Cruise Airplanes	-1.1868	0.9609

$$log_{10}(S_{wet}) = c + d\ log_{10}(W_{TO}) \tag{31}$$

Table A5. First estimates for ΔC_{D_0} and 'e' With Flaps and Gear Down

Configuration	ΔC_{D_0}	e
Clean	0	0.80 - 0.85
Take-off flaps	0.010 - 0.020	0.75 - 0.80
Landing Flaps	0.055 - 0.075	0.70 - 0.75
Landing Gear	0.015 - 0.025	no effect

Table A6. Group Weight Data for Twin Engine Propeller Driven Airplanes None Dimensional Data

NON - DIMENSIONAL DATA FOR A/C TYPE (LBS.)										
	BEECH				CESSNA				ROCKWELL	
	65 QA*	E-18S	G-50 TB*	95 TA*	310C	404-3	414A	TP-441	690B	
FLIGHT DESIGN GROSS Weight, GW, lbs.	7368	9700	7150	4000	4830	8400	6785	9925	10205	AVERAGE (LBS.) 7596
Structure/GW	0.292	0.282	0.282	0.303	0.265	0.268	0.292	0.260	0.296	0.282
Power Plan/GW	0.219	0.235	0.224	0.218	0.259	0.194	0.206	0.128	0.164	0.205
Fixed Equipment/GW	0.123	0.128	0.114	0.122	0.103	0.134	0.167	0.194	0.187	0.141
Empty Weight/GW	0.638	0.651	0.624	0.649	0.628	0.596	0.665	0.582	0.647	
Wing Group/GW	0.091	0.090	0.092	0.115	0.094	0.102	0.094	0.088	0.098	0.096
Empennage Group/GW	0.021	0.019	0.022	0.020	0.024	0.022	0.024	0.023	0.020	0.022
Fuselage Group/GW	0.082	0.079	0.069	0.069	0.066	0.073	0.100	0.088	0.135	0.084
Nacelle Group/GW	0.039	0.034	0.037	0.045	0.027	0.034	0.029	0.026	-	0.034
Land. Gear Group/GW	0.060	0.060	0.063	0.055	0.054	0.038	0.045	0.035	0.043	0.051
Take off Gross lbs. Wto	7368	9700	7150	4000	4830	8400	6785	9925	10205	7270
Empty Weight lbs. W_E	4701	6318	4459	2595	3032	5006	4511	5781	6605	4779
	Surface Areas, ft^2									
Wing ,S	277	361	277	194	175	242	226	254	266	252
Horiz. Tail, Sh	79.3	71.6	79.3	42.4	54.3	63.4	60.7	63.4	58.4	64
Vert. Tail, Sv	30.8	33.6	30.8	23.3	25.9	43.5	41.2	43.5	44.8	35
Empennage Area, Semp	110	105	110	66	80	107	102	107	103	99
Wing Group/S , psf	2.4	2.4	2.4	2.4	2.6	3.6	2.8	3.4	3.8	3
Empennage/Semp , psf	1.4	1.7	1.4	1.2	1.5	1.7	1.6	2.2	2.0	2
Ultimate Load, g's	6.60		7.10		5.70	3.75	3.75	3.75	3.75	4

Appendix Figures

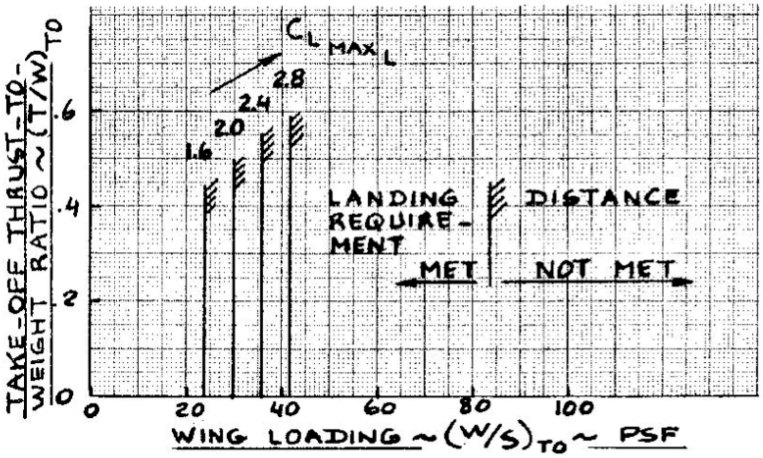

Fig. A1. Allowable Wing Loadings to Meet a Landing Distance Requirement

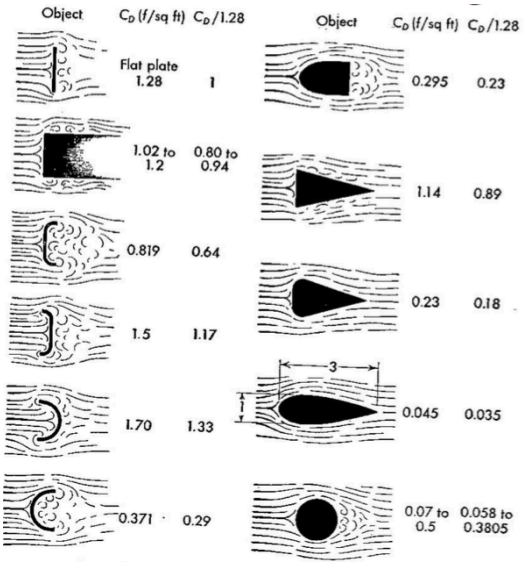

Fig. A2. Relative Drag of Various Objects a Low Mach Numbers

Table 8.3b) Twin Engine Propeller Driven Airplanes: Vertical Tail, Rudder and Aileron Data

Type	Wing Area S ft^2	Wing Span b ft	Vert. Tail Area S_v ft^2	S_r/S_v	x_v ft	$\bar{V}_v$	Rudder Chord root/tip fr.c_v	S_a/S	Ail. Span Loc. in/out fr.b/2	Ail. Chord in/out fr.c_w
CESSNA										
310R	179	36.9	26.1	0.45	15.9	0.063	.48/.41	0.064	.60/.90	.30/.29
402B	196	39.9	37.9	0.47	16.5	0.080	.48/.40	0.058	.64/.91	.29/.27
414A	226	44.1	41.3	0.38	17.0	0.071	.49/.37	0.061	.62/.87	.30/.28
T303	189	39.0	23.2	0.44	16.5	0.052	.46/.39	0.087	.64/.97	.31/.30
ConquestI	225	44.1	41.3	0.38	17.1	0.071	.47/.34	0.060	.61/.86	0.29
PIPER										
PA-31P	229	40.7	30.1	0.38	17.2	0.056	.37/.40	0.056	.59/.97	.24/.29
PA44-180T	184	38.6	21.5	0.37	14.4	0.044	.30/.30	0.077	.45/.90	.19/.18
Chieftain	229	40.7	29.5	0.40	17.3	0.055	.40/.38	0.060	.66/.98	.24/.30
Cheyen. I	219	42.7	26.5	0.40	16.5	0.045	.37/.42	0.057	.62/.93	.24/.29
Cheye.III	293	47.7	43.6	0.46	20.8	0.065	0.33	0.046	.66/.94	.23/.26
BEECH										
Duchess	181	38.0	25.6	0.29	14.2	0.053	.34/.42	0.059	.67/.97	0.28
Duke B60	213	39.3	28.8	0.43	17.4	0.060	.44/.46	0.054	.50/.84	.24/.26
Lear Fan										
2100	163	39.3	44.4	0.17	14.0	0.097	.32/.34	0.044	.72/.98	.31/.24
Rockwell										
Comdr 700	200	42.5	39.9	0.38	20.5	0.096	.37/.38	0.087	.58/.99	.28/.24
Piaggio										
P166-DL3	286	48.2	30.7	0.43	18.3	0.041	.38/.43	0.073	.61/.94	.19/.22
EMB-121	296	46.4	42.6	0.45	17.8	0.055	.42/.41	0.052	.71/.97	0.22

Fig. A3. Vertical Tail Rudder and Aileron Data.

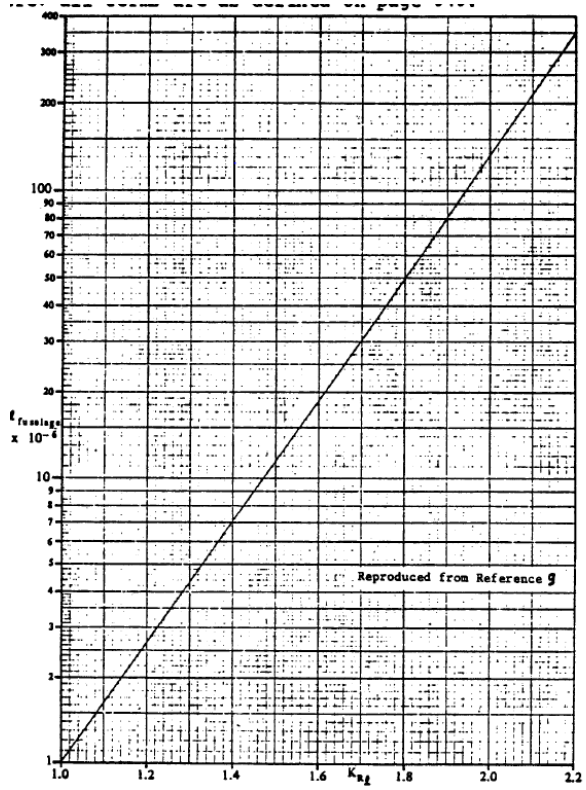

Fig. A4. Fuselage Reynold's number calculation

Appendix Codes

Engine CG

```
prompt={'Engine Weight:','Propeller Weight:'};
title='Engine Data';
data1=inputdlg(prompt,title);
xe = 1.84055;
ye = 1.88;
ze = 1.29411;
We = str2num(data1{1});
Wp = str2num(data1{2});
xcge = xe/1.7834296;
xcg = ((We*(xcge+1)+Wp*1)/(We+Wp))-1
ycge = ye/1.86364;
ycgp = ye/2;
ycg = (We*ycge+Wp*ycgp)/(We+Wp)
zcge = ze/1.58753;
zcgp = ze/1.04195;
zcg = (We*zcge+Wp*zcgp)/(We+Wp)
```

Fuel Consumption

```
prompt={'Engine Power percent:'};
title='Engine Data';
data1=inputdlg(prompt,title);
Eng_Pow = str2num(data1{1});
Eng_RPM = .0124*(Eng_Pow^3)-2.3492*(Eng_Pow^2)+186.01*Eng_Pow-1704.7
fuel_consumption_l = (9*10^-8)*(Eng_RPM^2.2588);
fuel_consumption_gal_per_hour = fuel_consumption_l*.26417
fuel_consumption_lb_per_hour = fuel_consumption_gal_per_hour*6
```

Fuel Tank Size

```
%Boundary Conditions
prompt={'Distance from leading edge to main beam(in):','Distance from leading
edge to secondary beam(in)','thickness of main beam(in):','thickness of
secondary beam(in):','Tank maximum fuel load(gal):'};
title='Fuel Tank Geometry';
data1=inputdlg(prompt,title);
primary_beam_length = str2num(data1{1});
secondary_beam_length = str2num(data1{2});
primary_beam_thickness = str2num(data1{3});
secondary_beam_thickness = str2num(data1{4});
fuel_tank_volume_gal = str2num(data1{5});
```

```
% a reduction factor for later material calculations
reduction_factor = .8;
primary_beam_length = ((1-reduction_factor)+1)*primary_beam_length;
secondary_beam_length = reduction_factor*secondary_beam_length;
primary_beam_thickness = reduction_factor*primary_beam_thickness;
secondary_beam_thickness = reduction_factor*secondary_beam_thickness;

%length Equations
Distance_from_beam_to_beam = secondary_beam_length-primary_beam_length;
y2_minus_y1 = secondary_beam_thickness-primary_beam_thickness;
m1 = (y2_minus_y1/Distance_from_beam_to_beam);
xf = 0:1:Distance_from_beam_to_beam;
Top_fuel_tank_slope = m1*(xf - primary_beam_length)+primary_beam_thickness;

%length and Height Geometry
fuel_tank_2D_geometry_in_square =
secondary_beam_thickness*(Distance_from_beam_to_beam)+.5*(Distance_from_beam_
to_beam)*(-y2_minus_y1);

%fuel tank Boundary Condition
fuel_tank_volume_in_cubed = fuel_tank_volume_gal*231

%Width of Fuel Tank
Geometry_width_inches =
fuel_tank_volume_in_cubed/fuel_tank_2D_geometry_in_square;

%change in airfoil thickness across wing
decreasing_airfoil_thickness = questdlg('Does the airfoil thickness decrease
with length along wing?','thickness change along wing','Yes','No','No');
switch decreasing_airfoil_thickness
    case 'Yes'
        airfoil_change = 1;
    case 'No'
        airfoil_change = 0;
end

%Airfoil thickness change with wing length
if airfoil_change == 1
    prompt={'thickness of primary beam midway through wing(in)','thickness of
primary beam near wing tip(in)','thickness of secondary beam midway through
wing(in)','thickness of secondary beam near wing tip(in)'};
title='change in thickness across wing';
data2=inputdlg(prompt,title);
primary_beam_thickness_mid = str2num(data2{1});
primary_beam_thickness_wing_tip = str2num(data2{2});
secondary_beam_thickness_mid = str2num(data2{3});
secondary_beam_thickness_wing_tip = str2num(data2{4});
primary_beam_thickness_mid = reduction_factor*primary_beam_thickness_mid;
```

```
primary_beam_thickness_wing_tip =
reduction_factor*primary_beam_thickness_wing_tip;
secondary_beam_thickness_mid = reduction_factor*secondary_beam_thickness_mid;
secondary_beam_thickness_wing_tip =
reduction_factor*secondary_beam_thickness_wing_tip;
%Width of Fuel Tank

geometry_thickness_Equations_1 =
.5*primary_beam_thickness+.5*primary_beam_thickness_mid
geometry_thickness_Equations_2 =
.5*secondary_beam_thickness+.5*secondary_beam_thickness_mid
Geometry_width_inches_varying_airfoil_thickness_1 =
fuel_tank_volume_in_cubed/(Distance_from_beam_to_beam*geometry_thickness_Equa
tions_1);
Geometry_width_inches_varying_airfoil_thickness_2 =
fuel_tank_volume_in_cubed/(Distance_from_beam_to_beam*geometry_thickness_Equa
tions_2);

if Geometry_width_inches_varying_airfoil_thickness_2 >
Geometry_width_inches_varying_airfoil_thickness_1;
    Geometry_width_inches_varying_airfoil_thickness =
Geometry_width_inches_varying_airfoil_thickness_2;
else
    Geometry_width_inches_varying_airfoil_thickness =
Geometry_width_inches_varying_airfoil_thickness_1;
end
else
end


%Change in angle across fuel tank calculator
prompt={'Fuel tank angle ( degrees)'};
title='Fuel tank angle for a gravity fuel flow';
data1=inputdlg(prompt,title);
fuel_tank_angle_degrees = str2num(data1{1});
fuel_tank_angle_radians = (3.1415/180)*fuel_tank_angle_degrees;
new_required_height_primary_thickness =
Geometry_width_inches*sin(fuel_tank_angle_radians)+primary_beam_thickness*cos
(fuel_tank_angle_radians);
new_required_height_secondary_thickness =
Geometry_width_inches*sin(fuel_tank_angle_radians)+secondary_beam_thickness*c
os(fuel_tank_angle_radians);
if new_required_height_primary_thickness >
.15*primary_beam_thickness+primary_beam_thickness;
    disp('Lower angle value required for Primary Beam')
elseif new_required_height_secondary_thickness
>.15*secondary_beam_thickness+secondary_beam_thickness;
    disp('Lower angle value required for Secondary Beam')
else
    disp('Angle is viable for fuel tank')
```

```
end


disp('so the geometry can be broken up into 2 parts, one being a rectangle
and one being a triangle and put together from there')

disp('with the rectangle length and height to be (in)')
rectangle_length = Distance_from_beam_to_beam
rectangle_height = secondary_beam_thickness

disp('with the triangle length and height to be (in)')
triangle_length = Distance_from_beam_to_beam
triangle_height = -y2_minus_y1

disp('with the rectangle and triangle 2D geometry being')
fuel_tank_2D_geometry_in_square

disp('And the width being')
if airfoil_change == 1
    Geometry_width_inches_varying_airfoil_thickness
else
Geometry_width_inches
end
```

Flight Envelope Matlab

```
h = 0:1000:20000;
w = 2700;
s = 175.5;
b = 35.05;
prompt={'e0:','Cd0L:','thrust per engine:','Max Coefficient of lift'};
title='FLight Envelope';
data1=inputdlg(prompt,title);
e0 = str2num(data1{1});
cd0l = str2num(data1{2});
tsl = 2*str2num(data1{3});
clmax = str2num(data1{4});
w = 2700;
s = 175.5;
b = 35.05;
rho=[.002377,.002308,.002241,.002175,.002111,.002048,.001987,.001927,.001868,
.001811,.001755,.001701,.001648,.001596,.001545,.001496,.001448,.001401,.0013
55,.00131,.001267];
%Preliminary calculations
AR=b^2/s; k=1/(pi*AR*e0);
%
% calculate the lift coefficients for high and low speed T=D flight from
% the Eqn.: KCL^2 - T/W CL + CD0L = 0
for ii=1:length(h);
t(ii)=tsl*rho(ii)/rho(1);
```

```
cl1=(t(ii)/w+sqrt((t(ii)/w)^2-4*k*cd0l))/(2*k);
cl2=(t(ii)/w-sqrt((t(ii)/w)^2-4*k*cd0l))/(2*k);
v1(ii)= sqrt(w/(0.5*rho(ii)*s*cl1));
v2(ii)= sqrt(w/(0.5*rho(ii)*s*cl2));
vstall(ii)=sqrt(w/(0.5*rho(ii)*s*clmax));
end
fid=fopen('F:\1 College\7th year\fall 2016\Senior Design 1\Power plant and
propeller\Propeller Efficiency\flight envelope data.txt','wt');
fprintf(fid,' Altitude Vstall Vmin Vmax \n');
for m= 1:length(h)-1
hr(m) = h(m); v1r(m) = v1(m); v2r(m)=v2(m); vstallr(m)=vstall(m)
fprintf(fid,'%8.0f %8.4f %8.4f %8.4f \n',...
hr(m),vstallr(m),v1r(m),v2r(m));
end
fclose(fid);
Fig.(6); hold;
plot(v1r,hr); plot(v2r,hr); plot(vstallr, hr);
xlabel('Airspeed');
ylabel('Altitude');
axis([0, 200, 5000, 20000]);
hold
```

Thrust Available MatLab Code

```
clear all
h = 5000:250:7500;
v=40:10:300;
%
%Enter aircraft properties
w = 2700;
s = 175.5;
b = 35.05;
e0 = .8;
cd0l = .0280;
tsl = 200*2;
clmax = 1.6;
%
%Enter densities of interest
rho=[.0020482,.002033,.002017,.002002,.001987,.001972,.001957,.001942,.001927
,.001912,.001898];
%
%Preliminary calculations
AR=b^2/s; k=1/(pi*AR*e0);
%
%Calculate thrust and drag - Use indices ii for altitude, and jj for
%airspeed
for ii = 1:length(h);
for jj = 1:length(v);
d0(ii,jj)=cd0l*0.5*rho(ii)*v(jj)^2*s;
di(ii,jj)=k*w^2/(0.5*rho(ii)*v(jj)^2*s);
```

```
dtot(ii,jj)=d0(ii,jj)+di(ii,jj);
t(ii,jj)=tsl*rho(ii)/rho(1);
end
vstall(ii)=sqrt(w/(0.5*rho(ii)*s*clmax));
end
for k=1:length(h);
Fig.(k);hold;
plot(v,dtot(k,:));
plot(v,t(k,:));
xlabel('airspeed (ft/sec)');
ylabel('Thrust, Drag (lbs)')
title('Thrust, Drag vs Airspeed');
grid on; hold;
end
fid=fopen('F:\1 College\7th year\fall 2016\Senior Design 1\Power plant and
propeller\Propeller Efficiency\thrust drag curve data.txt','wt');
for m=1:11
fprintf(fid,'\n');
fprintf(fid,'altitude=%8.00f  ft,\n', h(m));
fprintf(fid,' Airspeed Thrust Drag \n');
for n= 1:1:length(v)
fprintf(fid,'%8.0f %8.4f %8.4f\n',v(n),t(m,n),dtot(m,n));
end
end
```

Acknowledgments

I.A.D. authors thank Dr. Smith for his guidance, exceptional instruction and inspiration to practice lifelong learning and to the Mechanical and Aerospace Engineering Program at the University of Texas at Arlington that has allowed for the acquisition of knowledge necessary to be successful in the industry.

References

Books

[1]Roskam, Jan., *Airplane Design Part I: Preliminary Sizing of Airplanes*, Roskam Aviation and Engineering Corporation, Ottawa, Kansas, 1985, Chaps. 2, 3.

[2]Roskam, Jan., *Airplane Design Part II: Preliminary Configuration Design and Integration of the Propulsion System.,* Roskam Aviation and Engineering Corporation, Ottawa, Kansas, 1985, Chaps. 1-14.

[3]Nicolai, Leland M., Carichner, Grant E., *Fundamentals of Aircraft and Airship Design Volume I: Aircraft Design.*, American Institute of Aeronautics and Astronautics, Inc., Reston, VA, 2010, Chaps. 20.

[4]Abbot, Ira H., Von Doenhoff, Albert E., *Theory of Wing Sections: Including a Summary of Airfoil Data.*, Dover Publications, Inc., New York, NY, 1959, Pp. 465-466, 479-480.

[5]Courtland, Perkins D., Hage, Robert E., *Airplane Performance Stability and Control.*, John Wiley & Sons., New York, NY, 1959, Chap. 5.

[6]Oates, G. C. (ed.), *Aerothermodynamics of Gas Turbine and Rocket Propulsion*, AIAA Education Series, AIAA, New York, 1984, pp. 19, 136.

[7]Roskam, Jan., *Airplane Design Part VI: Preliminary Calculation of Aerodynamic Thrust and Power Characteristics.,* Roskam Aviation and Engineering Corporation, Ottawa, Kansas, 1985, Chaps. 1-14.

[8]Perkins, C. D., Hage, R. E. *Airplane Performance, Stability and Control.,* John Wiley & Sons., New York, NY, 1949, Ch. 5.

Electronic Publications

[9]Atkins, C. P., and Scantelbury, J. D., "The Activity Coefficient of Sodium Chloride in a Simulated Pore Solution Environment," *Journal of Corrosion Science and Engineering* [online journal], Vol. 1, No. 1, Paper 2, URL: http://www.cp/umist.ac.uk/JCSE/vol1/vol1.html [cited 13 April 1998].

[10]Vickers, A., "10-110 mm/hr Hypodermic Gravity Design A," *Rainfall Simulation Database* [online database], URL: http://www.geog.le.ac.uk/bgrg/lab.htm [cited 15 March 1998].

Propulsion

[1] [7]Aero Propulsion Technologies, "Rotax Service," 1 June 2000. [Online]. Available: http://www.rotaxservice.com/rotax_engines/rotax_912ULSs.htm. [Accessed 20 October 2016].

[2] [8]Mt- Propeller, "Propeller Overview," 16 February 2015. [Online]. Available: http://www.mt-propeller.com/en/entw/pro_hydr.htm. [Accessed 20 October 2016].

[3] [9]MIT, "Performance of Propellers," 1 August 2016. [Online]. Available: http://web.mit.edu/16.unified/www/FALL/thermodynamics/notes/node86.html. [Accessed 20 October 2016].

[4] [10]MIT, "Aircraft Performance," 1 January 2016. [Online]. Available: https://ocw.mit.edu/ans7870/16/16.unified/propulsionS04/UnifiedPropulsion4/UnifiedPropulsion4.htm. [Accessed 20 October 2016].

[5] [11]J. Roskam, Airplane Design Part I: Preliminary Sizing of Airplanes, Ottawa: Roskam Aviation, 1985.

[6] [12]Aviation Bull, "Light sport aircraft engine comparison," 1 January 2010. [Online]. Available: http://www.aviationbull.com/light-sport-aircraft-engine-comparison. [Accessed 20 October 2016].